

The impact of chromosome positioning in nuclear functions

Francesca Di Giovanni

TESI DOCTORAL UPF / 2016

THESIS SUPERVISORS

Dr. Manuel Mendoza

Dr. Marc A. Marti-Renom
(Gene Regulation, Stem Cell and Cancer, CRG)

CELL AND DEVELOPMENTAL BIOLOGY, CRG



Acknowledgments

Finishing this thesis would not have been possible for me without the support and encouragement of many people.

First, I would like to express my gratitude to my two PhD supervisors.

I thank Manuel Mendoza, he taught me to be intellectually independent and I am very grateful to him for this training. Manuel, I leave your lab with an increased strength to tackle new tasks.

Marc Marti-Renom, thank you for your scientific input and for giving me the moral support I needed to get this work done. I will never forget it.

Besides my supervisors, I would like to thank the rest of my thesis committee: Isabelle Vernos, Toni Gabaldón and Kerstin Bystricky for their guidance and encouragement through this process.

A special thanks goes to Marco Di Stefano, not only for his important scientific contribution to this work but also for being a great friend. Grazie Marco, non ce l'avrei fatta senza di te.

My thanks go to all my lab-mates, past and present, for the stimulating discussions and for all the fun we had together inside and outside the lab. I will miss you. I wish you all the best of luck.

I would like to thank all my dear friends who made these years very special for me.

Petra, it was a pleasure to share the passion for the same scientific topics with you. Besides that, in you I've found a very good friend.

Thank you for always showing up when I need support.

Andrea, sei un grandissimo amico e lo sarai sempre. Grazie per tutti i sorrisi che mi hai strappato durante questi anni, non sai quanto mi hanno aiutato. Ti voglio bene.

Nicola, thank you for all the support you gave me, but specially for your morning smiles. You spread positivity around you.

Michael, thank you for the fun and for your constant enthusiasm.

Nuno, I already miss the morning coffee with you, I hope to meet you again somewhere.

Gracias Trini, tú has sido siempre lista para ayudarme con cualquier cosa, hasta el último minuto. Esto es algo especial que nunca voy a olvidar.

Mimma e Alessia, sono contenta di aver fatto questa esperienza anche perché mi ha dato l'opportunità di incontrare due amiche speciali come voi. Grazie.

Finally, I would like to express my deepest gratitude to my family.

Mamma, Papà e Ale, grazie per aver creduto in me, avermi dato la forza per andare avanti e ricordato sempre chi sono. Carlo, ti includo nella famiglia perché per me sei un fratello. Grazie mille per esserci sempre stato.

Yannick, tu sei l'unica persona che può capire davvero quanto fosse importante per me finire questa tesi. La tua presenza mi ha aiutato

tanto, giorno dopo giorno, fino a farmi arrivare qui, oggi. Non vedo l'ora di affrontare le prossime esperienze della vita con te. Grazie amore.

Summary

Chromatin is not randomly organized inside the eukaryotic nucleus in interphase. In budding yeast gene expression of some specific loci is affected by their positioning in the nucleus. Replication firing of early origins is also correlated to the position of the respective ARSs (Autonomously Replicating Sequences) in the nucleus. However, the relationship between nuclear positioning and DNA processes is not yet fully understood.

To study the importance of chromosome positioning in nuclear processes and cell physiology, we use budding yeast strains carrying fused chromosomes, which are expected to dramatically change the chromosomes configuration in interphase. By combining microscopy and computational modeling we show that the chromosomes arrangement in strains carrying fused chromosomes is greatly modified. Despite the reorganization of chromosomes in the nucleus, our functional experiments show that transcriptional activity, replication timing and response to stress conditions are not affected. The results, thus, indicate that the function of the genome is mostly independent of chromosome positioning in the budding yeast nucleus

Resumen

La cromatina no está distribuida de manera aleatoria dentro del núcleo eucariota en interfase. En la levadura *Saccharomyces cerevisiae* la expresión de algunos genes específicos depende de su posición en el núcleo. El inicio de los orígenes de replicación está también correlacionado a la posición de las respectivas ARSs (Autonomously Replicating Sequences) en el núcleo. Sin embargo, la relación entre posición nuclear y los procesos del ADN no está completamente aclarado.

Para estudiar la importancia de la posición de los cromosomas en las actividades nucleares y en la fisiología celular, hemos utilizado cepas de *S. cerevisiae* con fusiones cromosómicas, en las que la conformación cromosómica típica de la levadura cambia drásticamente. Mediante la combinación de la microscopía y de los modelos computacionales mostramos que la organización cromosómica en las cepas que llevan cromosomas fusionados está ampliamente modificada. Aunque la organización de los cromosomas está modificada, nuestros experimentos funcionales muestran que la actividad transcripcional, el tiempo de replicación y la respuesta a condiciones de estrés no se muestran alterados. Por consiguiente, los resultados indican que la función del genoma es principalmente independiente de la posición de los cromosomas en el núcleo de la levadura *Saccharomyces cerevisiae*.

Preface

A common feature of eukaryotic genome is represented by a non-random positioning of chromosomal regions relative to each other and to nuclear landmarks.

Several studies performed in budding yeast showed that the chromosomal positioning in the nuclear space is correlated to the levels of transcriptional activity and replication timing. However, these studies were focused on specific loci or were done in absence of chromatin binding factors responsible for nuclear conformation.

Whether or not the chromosomal positioning plays a general and essential role for nuclear processes is not yet clear. Our work contributes to explain this question. We show that budding yeast strains carrying highly altered chromosomal arrangement do not show changes in gene transcription and replication timing compared to wild type. This work suggests that in budding yeast nuclear positioning is not essential for the nuclear processes in optimal conditions.

Table of Contents

Acknowledgements	i
Summary.....	v
Resumen.....	vi
Preface.....	vii
Table of Contents	ix
1. Introduction.....	1
1.1 The nucleus organization	2
1.1.1 The DNA fiber	2
1.1.2 Euchromatin and heterochromatin	5
1.1.3 Chromosome territories.....	8
1.1.4 Chromosome domains.....	11
1.2 The importance of nuclear architecture.....	16
1.2.1 Genome organization and differentiation.....	16
1.2.2 Genome organization and conservation	18
1.2.3 Genome organization and diseases	19
1.3 The organization of budding yeast nucleus.....	21
1.3.1 The “Rabl like” configuration.....	21
1.3.2 Mechanisms of DNA anchoring to NE	24
1.4 Nuclear organization and function in yeast	27
1.4.1 Telomere silencing	27
1.4.2 Inducible gene expression at Nuclear Envelope	30
1.4.3 Replication and nuclear organization in yeast	33
1.5 Modeling budding yeast nucleus	35
2. Objectives.....	39

3. Materials and Methods.....	41
3.1 Cell growth	41
3.1.1 Growth media	41
3.1.2 Automated growth experiments	42
3.1.3 Analysis of yeast cell growth	43
3.2 Yeast strains	43
3.2.1 Yeast transformation	44
3.3 RNA isolation and sequencing (RNA-Seq).....	45
3.3.1 RNA isolation.....	45
3.3.2 Sequencing and bioinformatics analysis	45
3.4 IF-FISH	46
3.4.1 FISH probe	46
3.4.2 IF-FISH	47
3.5 Microscopy and images analysis	49
3.6 BrdU-IP-Seq.....	49
3.6.1 BrdU-IP	49
3.6.2 BrdU-IP analysis	50
3.7 Polymer modeling.....	51
4. Results	55
4.1 Fused chromosomes strains	55
4.1.1 Generation of fused chromosome strains.....	55
4.1.2 Growth analysis of fused chromosome strains.....	59
4.2 Genome organization analysis of fused chromosome strains ..	62
4.2.1 Polymer modeling to predict chromosomal rearrangements ..	62
4.2.2 Microscopy analysis of loci positioning and validations of modeling	67
4.3 Transcriptional analysis of fused chromosome strains.....	70
4.3.1 Subtelomeric and peripheral genes are less expressed both in wild type and fused chromosomes strains	70

4.3.2 No differences in expression at loci displaced from their original position	75
4.4 Analysis of replication timing in fused chromosomes	78
4.4.1 Analysis of early origins in wild type and fused chromosomes strains	78
4.4.2 Modeling reproduces clustering of early replicating origins .	82
4.5 Analysis of stress response in strains carrying translocations .	85
5. Discussion	95
5.1 The yeast genome arrangement is mostly governed by simple physical rules.....	95
5.2 The impact of chromosome fusion in transcription	98
5.3 Chromosome positioning and replication timing	103
6. Conclusions.....	107
7. Future Directions	109
8. Bibliography	113

1. Introduction

The genetic information of eukaryotic cells is stored in long linear DNA molecules, sequestered in a membrane-enclosed compartment called nucleus. In the cell nucleus, DNA associates with proteins, which allow its folding and packing in higher order chromatin fibers, chromatin domains and chromosomes.

Chromosomes are not randomly distributed in the nucleus and several correlations between nuclear organization and nuclear processes have been found. For instance, the chromatin located in nuclear interior is more transcriptionally expressed compared to the more compacted and peripheral one. Moreover, chromatin regions functionally related tend to preferentially interact with each other.

These observations raised the possibility that the spatial organization of the genome can somehow regulate its functions. But does chromosome organization play a role in nuclear processes, or it is simply a result of these functions? In this dissertation I will show how I addressed this question using budding yeast strains as model system. The use of strains carrying big chromosome translocations, allowed me to study the effect of a highly altered genome organization in different functions, like transcription, replication timing and response to stress conditions.

1.1 The nucleus organization

1.1.1 The DNA fiber

The three dimensional (3D) structure of the DNA polymer was discovered in the '50s thanks to experiments carried out by Watson, Crick and Franklin with X-ray diffraction [1, 2]. Their results showed that DNA is organized in a double stranded helix. The nucleotides, the monomers forming the DNA polymer, are composed by a nitrogenous base, a five-carbon sugar (2- deoxyribose) and phosphate groups. They are linked together by covalent bounds between the phosphate groups and the sugar forming the backbone of the DNA chain. The formation of the double helix is due to hydrogen bounds between a double ring base (the purines) and a single ring base (pyrimidine). There are two purines, adenine (A) and guanine (G), and two pyrimidines, thymine (T) and cytosine (C), and A always pairs with T, and G with C.

The length of the DNA chain is huge if we compare it with the size of the nucleus in which it is stored. For example, in humans, DNA is composed by 6×10^9 nucleotides distributes in 2 copies of 23 chromosomes. If all aligned together and completely extended, chromosomes would reach a length of 2 meters. Considering that the cell nucleus is in average only $\sim 6 \mu\text{m}$ in diameter the cells need to face a challenging work: highly pack the DNA in a way that it can fit in the nucleus but at the same time being accessible to proteins responsible for several important processes like gene expression, DNA replication and repair.

The first level of DNA folding is due to its association with proteins generating what it is called “chromatin”. Two classes of proteins bind the DNA with roughly the same contribution: histone proteins and non-histone proteins. The DNA binding to histones forms a structure called nucleosome, which was first discovered in 1974 [3]. It consists in a core of eight positively charged histones (two molecules each of histones H2A, H2B, H3, and H4) around which 147 base pairs of DNA are wound. Between two nucleosomes there is a linker DNA of 10-80 bp length, to which another histone protein can bound (H1). This structure forms a 10 nm width fiber and is also called “beads on a string” structure because of its appearance on electron micrographs. The histones forming the nucleosome have an N-terminal amino acid tail, which is not part of the core but extends out of it. These histone tails can be subjected to different kinds of post-translational modifications like acetylation phosphorylation, ubiquitination and sumoylation. These modifications have also a role in a further DNA compaction as it will be explained in the next subsection.

This 10 nm fiber correspond to a level of compaction of 6 fold, that is far to be enough to pack the DNA inside the nucleus. The observation of reconstituted chromatin by X-ray crystallography and high-resolution electron microscopy allowed to see a 30 nm fiber generated by the formation of complexes of four nucleosomes [4-7](**figure 1.1**). However, the existence of a 30 nm fiber is highly debated [8].

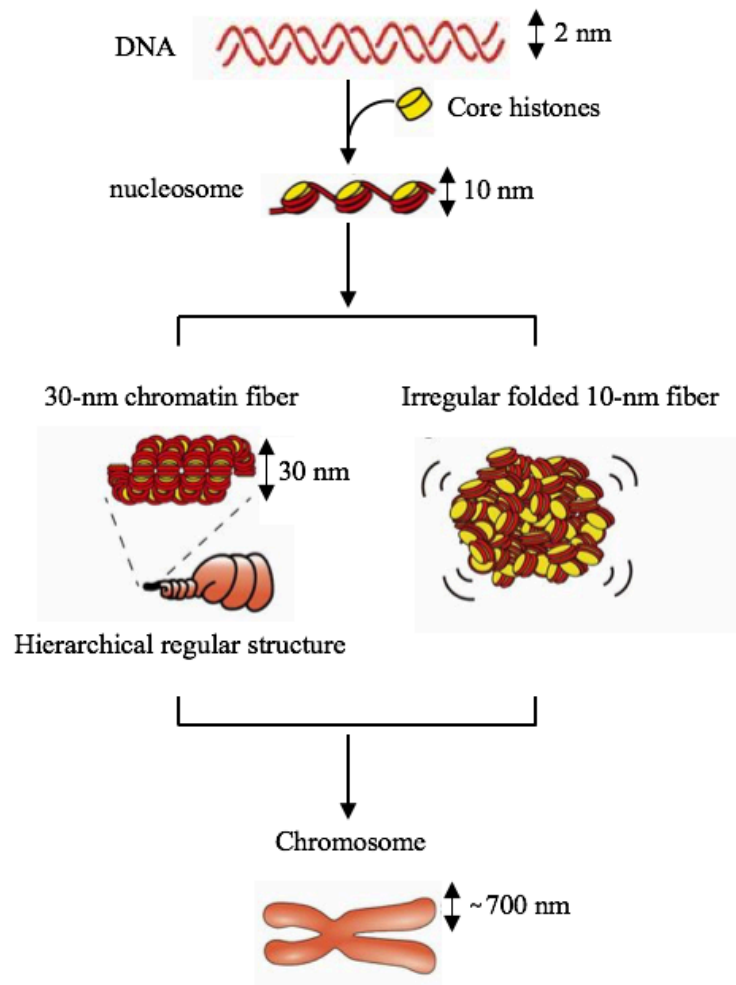


Figure 1.1 The DNA molecule is wrapped around a core histone octamer forming a nucleosome with a diameter of 11. Left: The nucleosome folds into a 30-nm chromatin fiber which organises into the higher order organization of interphase. In the right panel it is shown an alternative hypothesis which consists in irregularly folded nucleosome fibers. Adapted from [8].

Cryo-electron microscopy of HeLa cells chromosomes, and super-resolution light imaging of chromatin in embryonic and somatic cells show that the chromosome packing is much less regular, with a 10

nm fiber folding into irregular globules [10,11] (**figure 1.1**)

Finally, inside the nucleus chromatin does not look homogenously compacted but appears in different levels of folding, depending on the position that occupies in the nucleus and in correlation with different nuclear activities.

1.1.2 Euchromatin and heterochromatin

The chromatin inside the nucleus is not uniformly dense, and the first evidence was shown by the German geneticist Heitz, who observed by light microscopy two chromatin types in the nucleus of Bryophytes (mosses): heterochromatin and euchromatin [12]. The first one was distinguished from the second one because did not appear to undergo decondensation after mitosis. His observations were then confirmed some years later by different studies of electron microscopy [13].

Heitz also speculated that euchromatin could be the actively transcribed part of the DNA and the heterochromatin the inactive one. His hypothesis was then confirmed in the '60s when the purification of heterochromatic and euchromatic fractions from mammalian lymphocyte nuclei allowed to quantify the transcriptional activity present in both fractions. Most of the RNA synthesis was deriving from the eukaryotic fraction, despite it was the least represented of the two types (20% of the total chromatin) [13].

Today we know that there are two main types of heterochromatin

(figure 1.2). The constitutive one is composed mainly by repetitive sequences, hypoacetylated and contains histone H3 methylated at lysine 9 (meH3K9) to which is bound the protein HP1. This interaction is thought to contribute to the propagation and maintenance of heterochromatin [14,15]. The facultative heterochromatin, instead, is found in single copy genes, it is cell type and developmental stages specific and it is often enriched in methylation of H3K27 [16].

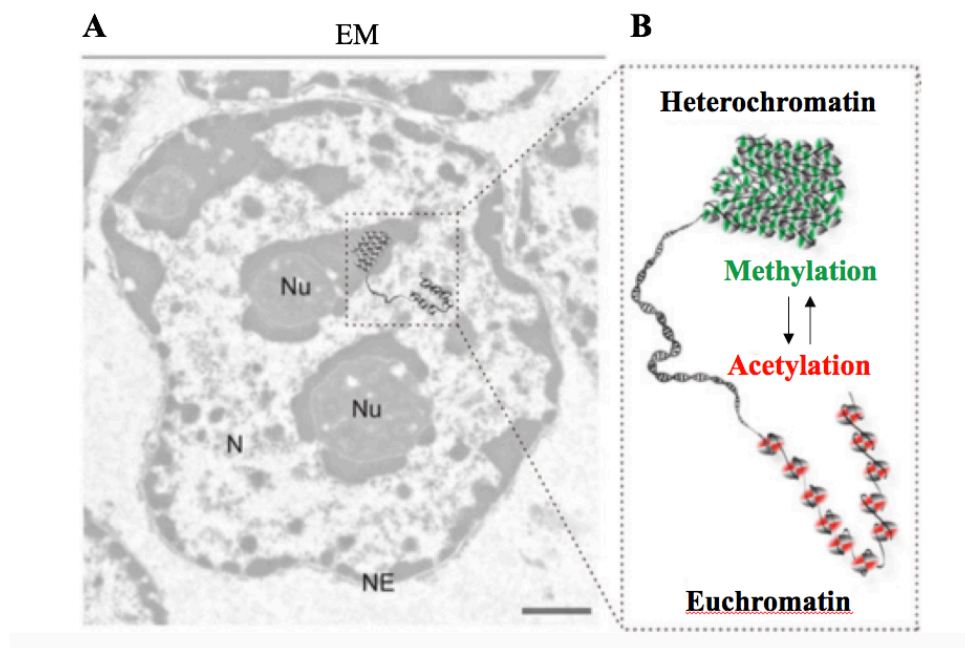


Figure 1.2 (A) An example of electron microscopy (EM) picture of a mouse liver cell nucleus (N nucleus, Nu nucleolus, NE nuclear envelope). Heterochromatin appears more electron dense compared to the more open state of euchromatin. (B) Heterochromatin and euchromatin are distinguished by their molecular features (histone and DNA modifications). Adapted from [17].

Both types of heterochromatin are localized in specific regions of the nucleus. In particular, in the nuclear periphery (excluding the nuclear pores) and in the periphery of the nucleolus, which is the nuclear

body where rDNA transcription, rRNA processing and ribosome biogenesis take place. Heterochromatin, finally, is also found in the interior of the nucleus, like the irregular mass of heterochromatic aggregates in mouse nuclei (chromocenters).

The fact that denser chromatin is less transcriptional active led to the hypothesis that this closed conformation had a regulatory role in transcription activation, by making DNA inaccessible to activation factors.

But this theory is in contrast with the finding of Nicolas Sadoni and colleagues obtained by visualizing with confocal microscopy the distribution of histone H2B fused with green fluorescent protein (GFP) in interphasic HeLa cells nuclei. This experiment showed that the poor transcribed heterochromatin results only 1.4 fold more compacted than the high transcribed and diffuse chromatin (euchromatin) [18]. Moreover, the compactness of the heterochromatin does not prevent the accessibility of macromolecules [19].

In addition, it was shown that the degree of chromatin condensation is linked more to gene density rather than transcription activity. Such gene density theory was first proposed in 1999, when it was observed that the position of human chromosomes 18, and 19 was radially differently distributed in lymphoblasts and fibroblasts [20]. The chromosome 18, a gene-poor chromosome was found to be localized at the nuclear periphery while the very gene rich chromosome 19, in the interior of the nucleus [20,21]. These findings were confirmed in different mammalian species like in Old World monkeys [10] and

in primates [23] and it appears to be also evolutionary conserved, being also found in birds [24].

However, many studies done in *D. melanogaster* and mammalian cells, show that the association of euchromatic genes with heterochromatin (epigenetically and cytologically identified), is correlated with their transcriptional repression, while the dissociation from heterochromatin coincides with activation [24-33].

In conclusion, the simple initial idea of a homogeneously compacted and inactive heterochromatin compared to a more open and active euchromatin does not always hold true. Although there is a difference in the degree of condensation between different chromatin regions, its functional significance is still unclear.

1.1.3 Chromosome territories

At the beginning of the 20th century Carl Rabl and Thomas Boveri first observed that chromosomes assume a specific localization in the nucleus after cell division. In particular, Boveri introduced for the first time the concept of “chromosome territories”. He postulated that the single chromosomes, which were clearly distinguishable in metaphase-anaphase because of the mitotic compaction, retain their individuality also in interphase, when they undergo relaxation [34,35].

The concept of chromosome territories (CT) was then recalled again during the '70s and '80s thanks to the visualization of single CT by

the fluorescent in situ hybridization (FISH) [36,37]. This technique relies in the fluorescent labeling of a DNA (or RNA) sequence (probe), which will then pair with its cellular homolog in fixed cells [38]. Probes can be of different lengths, allowing to visualize from very portions of DNA, like single genes, to larger ones like entire chromosomes (**figure 1.3**).

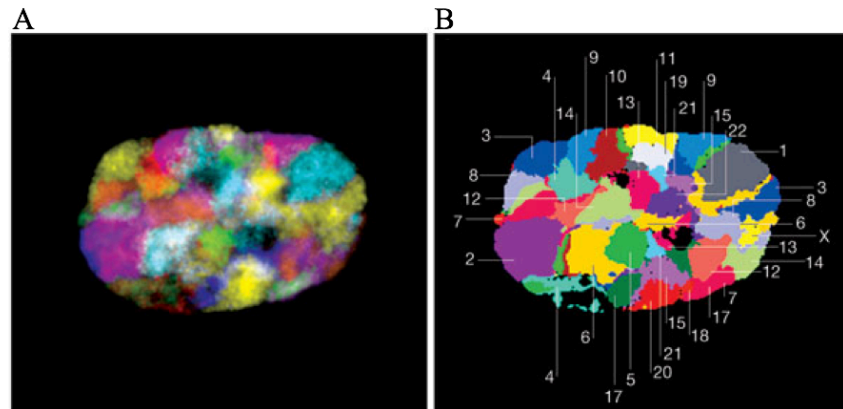


Figure 1.3 Chromosome territories visualization using fluorescence in situ hybridization. (A) All the chromosome territories of the human genome visualized simultaneously in a different colour with FISH. (B) Schematics showing each territory corresponding to a chromosome number. Adapted from [39].

Polymer physics models argue that the DNA polymer organizes in chromosome territories because of an intrinsic physical feature rather than being the result of a biological function [40]. In fact, being very long polymers, chromosomes would take more than the lifespan of most of the organisms to completely unfold and intermingle. Although it is true that chromosome occupy discrete territories, the borders of CTs can intermingle between each other, and this can explain the existence of chromosome translocations [41].

Results of FISH experiments conducted in human, mouse and

chicken cells showed not only the presence of chromosome territories but also that their distribution inside the nucleus is size and gene density dependent [42,43]. The CT distribution in the nucleus also changes during differentiation, so that each cell type has a specific chromosome territories distribution pattern [42].

The observation that each chromosome occupies a discrete territory in the nucleus has been confirmed by chromosome conformation capture experiments [44]. Chromosome conformation capture techniques consist in digestion and re-ligation of chromatin upon crosslinking, and high-throughput sequencing of the ligation products composed by different pairs of chromatin stretches. The probability of crosslinking and ligation between two restriction fragments is proportional to their proximity in the nuclear space. Enrichments of ligation products are then scored as contacts between genomic stretches. Hi-C, the chromosome conformation capture technique which interrogates the whole genome, has been performed in a variety of eukaryotic species such as yeast, *Caenorhabditis elegans*, *Drosophila*, and several other different metazoan species [45-48]. These experiments also permitted to detect interactions between different chromosomes (trans-interactions) even if much lower than interactions of fragments belonging to the same chromosome (cis-interactions) [45,46,49,50]. Interestingly the trans-interactions are usually gene rich and transcriptionally active and correspond to the regions that have been seen to loop outside of the chromosome territories [51].

These observations lead to the hypothesis that the looping out of the

territories was favoring transcription activation by allowing the exposure of genes to transcription factories [52-54]. But this theory is also not completely in accordance with later findings. First, by coupling DNA FISH and RNA FISH, it was demonstrated that genes sitting at the CT periphery, and therefore more likely to loop out of the territory, are already transcriptionally active and associated with transcription factories before looping out [55]. Second, it is still under debate whether transcriptional factories are physical assemblies that a gene have to reach to be transcribed or if active genes cluster together to create these structures [56].

In summary, chromosomes do not randomly organize in the nucleus but occupy cell type specific territories. Chromosome can though intermingle at the border between territories, where transcription is more active. The distribution of the territories depends on gene density, with chromosomes with higher gene density being in the interior while chromosomes with lower density tend to be at the periphery. Molecular biology techniques in the XXI century allowed to identify structural domains inside the territories. Their role in genome function is still not clear and it will be discussed in the next subsection.

1.1.4 Chromosome domains

Lamin Associating Domains (LADS)

From the beginning of the 2000 the arrival of different molecular biological techniques permitted to study chromosome organization at the sequence level on a genome-wide scale.

One of such techniques, called DamID, was based on the expression of trace levels of a fusion protein between a protein of interest and the DNA adenine methyltransferase Dam from *Escherichia coli*. If a chromatin region is close to the fusion protein, it gets methylated and can then be extracted, amplified and hybridized to microarrays or sequenced [57]. Thanks to DamID, large domains of chromatin, called LADs, have been discovered to be associated with proteins of the nuclear lamina [58]. The lamina is composed by lamins, intermediate filament proteins located closed to the INM (Inner Nuclear Membrane) by binding the nuclear envelope transmembrane proteins. Lamins can bind many different proteins, including chromatin components such as histones, or HP1 (heterochromatin protein 1), and interactions between the lamina and the chromatin can regulate the position of chromosomes in the nucleus and various other activities [59,60].

In mammalian cells, LADs occupy around 40% of the genome with a size that goes from 10 kb to 10 Mb. The fact that they are peripheral and low expressed reminds the high density regions seen by electron microscopy [61,62]. They are characterized by low transcription activity and also low gene density, confirming the FISH experiments done in the '90s. In addition, LADs are enriched of H3K9 and H3K27 methylation silent chromatin marks and lack of the active ones [58,63-65].

It is possible to distinguish two types of LADs. The constitutive ones, which are conserved between cell types and also between human and mouse [66,67], and the facultative LADs, which are the minority and

cell-type specific [66]. In particular, when a non-LAD domain, during ESCs-neuronal progenitor differentiation, becomes associated to nuclear lamina, the genes get repressed. But the change between a LAD domain to a non-LAD domain does not correlate with transcriptional activation [64].

Topologically Associating Domains (TADs)

Chromosome conformation capture techniques were designed to study the 3D organization of chromatin, by detecting chromatin-chromatin interactions [44,68]. Hi-C, which in particular interrogates the whole genome, confirmed both the presence of chromosomes territories seen by microscopy [46,47,69,70], and other features like telomeres and centromere clustering in yeast, *Drosophila* and *Arabidopsis* [47,70-75].

Hi-C experiments could also detect the so-called A and B compartments, corresponding to the two chromatin types seen first by microscopy by Heinz. A compartments correspond to a more open and transcriptionally active chromatin and have more inter-chromosomal interactions compared to the B compartments, which are more closed and less active. The compartments of the same type cluster together in the nucleus and they probably reflect the tendency of euchromatin and heterochromatin to segregate in the nuclear space [45-47,49,76,77].

But the resolution in Hi-C experiment can be much higher. Inside A and B compartments is possible to detect subdomains of megabase scale called Topologically Associated Domains (TADs), or the smaller sized Chromosomal Interaction Domains (CIDs) in

prokaryotes [47,75,78-80]. TADs have an average size of 1 Mb and are separated by boundaries and their presence has been confirmed by FISH experiments [78,79,81]. Across the boundaries between TADs, contacts are very infrequent compared to the contacts inside the TADs [78,79]. It is still not clear if TADs have a biological function and how they are formed. In flies and mammals the borders between TADs host highly transcribed genes. This suggests that the unfolding of the chromatin is due to transcription at the TAD borders. This phenomena is even more clear in bacteria where the insertion of a highly transcribed gene inside a CID in *Caulobacter* split it into two by generating a new boundary [80].

The boundaries between TADs are also enriched in binding sites of CTCF (architectural proteins CCCTC-binding factor) and TSS (Transcription Start Sites) [47,73,78]. It is not clear however if the CTCF binding, and the cohesin which is recruited by CTCF, are responsible for TADs boundaries. In fact, knockdown of CTCF leads to an increase of interactions between TADs, but not a loss of the boundaries [82]. Moreover, it is still not clear if Transcription Starting Sites (TSS), which are enriched in the boundaries, have a role in the formation of the TADs. TADs have been found in all the human and mouse cell types examined [78,79,81-84], and in *Drosophila* [47], even if the average size of the TADS is 100 kb. Several observations shown that TADs are not only structural but also transcriptionally functional regions. First of all, TADs borders are often seen to overlap with A and B compartment borders [78]. Although TADs borders are conserved in different cell types, depending on the differentiation type TADs can be part of A or B

compartment (**figure 1.4**). Moreover, TADs are associated with markers of gene activity like histone methylation or association with nuclear lamina [78,79,84].

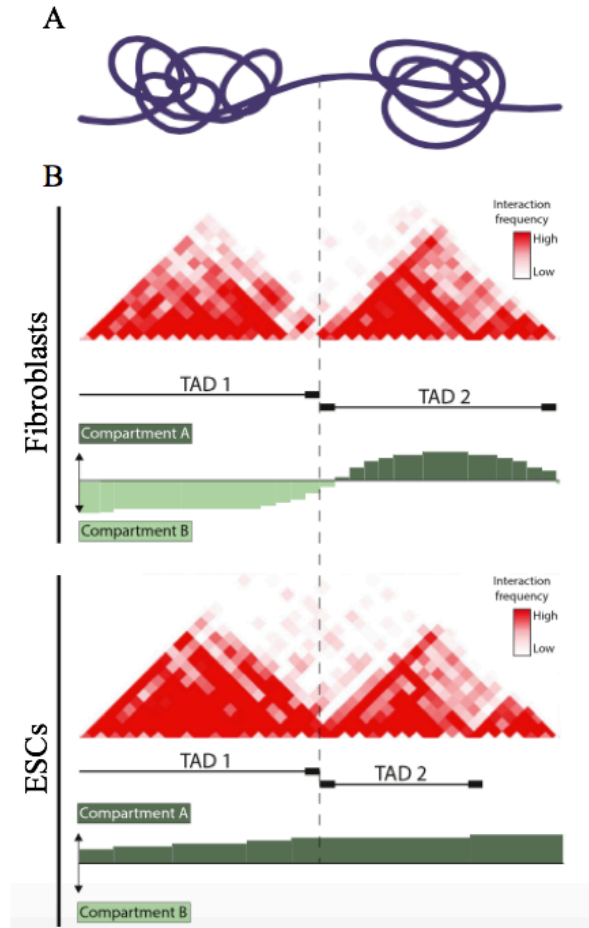


Figure 1.4 A) Representation of two consecutive TADs. (B) TADS in region chr11:115,470,000–116,770,000 of human genome. TADs structure and positioning of TAD boundary do not differ between two the cell types, fibroblasts and ESCs. However, in fibroblasts TAD1 is in the inactive compartment B, whereas it is instead in the active compartment A in ESCs. Adapted from [85]

In conclusion, despite the large amount of work conducted to study the different levels of chromatin structures, it remains still

controversial the role that these structural domains have in the functions, at least in gene transcription. In fact, it remains unclear if it is the level of transcription which shapes the chromatin, creating domains and territories, if they represent a structural consequence of nuclear functions, or if we have a contribution from both sides. The transcriptional state could contribute to the formation of topological domains, whose structure, in turn, might create a favorable environment to maintain the same functional state.

1.2 The importance of nuclear architecture

1.2.1 Genome organization and differentiation

Microscopy data have identified great changes in nuclear organization in cell differentiation during development. It is in fact known that in embryonic stem cells the level of heterochromatin is much lower compared to differentiated cells [86,87]. Moreover, it is also known that during cell differentiation, many genes reposition within the nucleus in correlation to changes in their transcriptional activity. Some genes move to the nuclear periphery to be silenced by interacting mostly with the nuclear lamina, while actively transcribed genes tend to cluster to nuclear pores [88-91]. Other genes when active are found to loop out from the core of their territory [92-95].

So, active genes are distributed either between territories or close to the nuclear pores, whereas inactive genes are inside in the interior of the territories or close to the nuclear lamina.

One possibility is that the transcriptional activation itself induces chromatin re-localization. But not all the promoters are able to induce such moving [91]. The fact that the changing of chromatin marks is sufficient to move the gene loci, leads to the theory that not the transcription itself but the transcription-dependent change in the chromatin structure is responsible for loci movement [90,96-98]. The effect of epigenetic state in chromatin location can be also found in LADs. When a LAD sequence is inserted in a non-LAD one, it autonomously relocates at the nuclear periphery [99,100]. It is still not clear the contribution of specific binding motifs and chromatin markers in LAD positioning at the nuclear periphery. However, it is known that targeting to the nuclear periphery depends either on deacetylases or on H3K9 and H3K27 methyltransferases. For example, it has been shown in *C. Elegans* that H3K9 methylation is a sufficient signal for perinuclear anchoring [101,102] and that histone acetylation impedes LADs formation [63,65].

The observation that co-regulated genes colocalize in single transcription factories (what is called “gene kissing”), brings to the hypothesis that the three dimensional position of genes in the nucleus might have an important role in transcriptional regulation [52,89].

While by microscopy large changes in territories and genes positioning are observed during differentiation, with chromosome conformation capture technique, loops and TADs seem conserved [103,105]. This discrepancy can be explained by the fact that while epigenetic marks are clearly changing during development, structural domains remains mainly unaltered. According to this, the epigenetic

state of a domain does not change the TAD borders, but changes the level of interaction within and between TADs. They can fall in two different compartment (A or B), depending on the cell type [105]. In fact, it has been observed that TADs with similar epigenetic marks tend to have preferential chromatin interactions among each other creating a compartmentalized genome [47,104].

1.2.2 Genome organization and conservation

Chromosome organization in territories has been observed in a large variety of Eukaryotic species from human to yeast, from birds to plants [24, 106-108]. However, some of them have a radial chromosome positioning, and others, like budding yeasts, a “Rabl like” configuration [109]. In higher primates positioning of specific territories are evolutionary conserved. A study in humans, New World monkeys and Old World monkeys demonstrates that positioning of primate chromosomes homologous to HSA18 and HSA19 is conserved, despite important chromosomes rearrangements between the species. It is not possible to say the same for mouse chromosomes, which are differently distributed compared to syntenic human chromosomes in human nuclei [110]. TADs, as well as CTCF binding sites at the TAD borders, are instead largely conserved in syntenic regions [78,104,111]. Another conserved characteristic of the nucleus is the positioning of origin firing. The early replicating ones are more likely found in the interior of the nucleus, while the late replicating, closer to the nuclear periphery. This is true for mammals, but also yeast, and chicken [24,25,112-

115].

1.2.3 Genome organization and diseases

Several diseases have been associated with changes in genome organization, either due to chromosome translocation or to the presence of mutated architectural chromatin proteins.

Local changes in chromatin structure could create fragile sites that are more likely to undergo breakage. Chromosome breakage can in turn lead to formation of chromosome translocations during interphase, consisting in the joining of two chromosomes bearing damaged DNA, like double-strand breaks (DSBs). The specific spatial arrangement of the genome in non-cancer cells might be important to determine which chromosomes are involved in cancer translocation. In fact, two chromosomes can undergo translocation only if they are in close proximity in the nuclear space and the frequency of cancer translocation correlates with the proximity of the chromosomes involved in the specific cell type [116]. For example, in chronic myeloid leukemia, the translocation of chromosomes 9 and 22, leads to the formation of a fusion protein between BCR and ABL genes, responsible for the disease. These genes are found in much higher proximity to each other in normal hematopoietic cells to the expected based on their random distribution [117-119].

Another example is given by the mouse lymphoma, in which it is often found a translocation between chromosomes 12 and 14, while translocations between chromosomes 5 and 6 are more likely to happen in mouse kidney cancer cells. Moreover, other studies

showed that a high degree of intermingling between chromosomes (looping out the chromosome territories) could affect the translocation frequency between the chromosomes [41].

Also mutations in genes coding for proteins associated to nuclear architecture may result in serious disease. For instance, mutations in genes coding for lamins or internal nuclear envelope proteins, which cause also the disassembly of the heterochromatin domains at the nuclear periphery, are responsible for several human degenerative diseases [120,121]. Also mutations in genes coding for cohesin and CTCF, that lead to changes in TADs organizations, are often seen in tumor, but it is still not clear the role of domains rearrangement in cancer formation [122].

1.3 The organization of budding yeast nucleus

1.3.1 The “Rabl-like” configuration

The budding yeast nucleus, as well as all the eukaryotes, is delimited by a double layer membrane, the nuclear envelope, which is continuous with the endoplasmic reticulum. In budding yeast, differently from the majority of eukaryotic organisms, the nuclear envelope persists intact also in mitosis, the cell cycle stage when the cell divides to form two daughter cells with the same genetic material. For this reason, in budding yeast mitosis is called “closed”.

The nuclear envelope regulates the molecules trafficking between cytoplasm and nucleus through about 200 nuclear pore complexes (NPCs). NPCs is composed by 456 nucleoporins of 30 different types assuming doughnut-shaped structure with eightfold symmetry around a central channel [123]. Flexible NPC protein filaments that are in the cytoplasm and nucleoplasm sides are the binding sites responsible for proteins transport and chromatin anchorage. The nuclear envelope in *S. cerevisiae* differs from the mammalian one also because it lacks lamins. But other proteins play the same role of lamins in chromosome anchorage; for example, Mps3, a member of the SUN family which is a shared component of the INM (Inner Nuclear Membrane) and of the spindle pole body (SPB) [124]; and Heh1 and Heh2, orthologs of the mammalian lamin associated protein MAN1 [125], and Esc1 (Enhancer of silent chromatin 1) which anchors silent chromatin to the INM [126]. Apart from

separating the nucleoplasm from the cytosol, the nuclear envelope creates also chromosomes subcompartments in the nucleus. Chromosomes are in fact organized in a so called “Rabl like” organization, because resembles the one observed by Carl Rabl in *Salamandra* larvae cells in the end of the 19th century [34]. This conformation depends on interactions between specific regions of chromosomes with structural components of the nuclear envelope. Three compartments are easily distinguished in the budding yeast nucleus: the cluster of centromeres close to the SPB; the nucleolus, which occupies around a third of the nuclear volume, bound to the nuclear envelope on the opposite site of the SPB; and the anchoring of the telomeres also at the inner membrane of the nuclear envelope (figure 1.5).

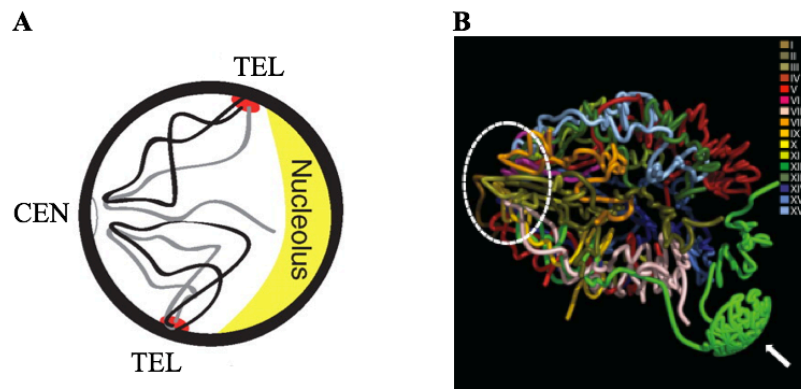


Figure 1.5 Rabl like configuration of budding yeast nucleus. (A) Schematics of yeast nucleus configuration. All centromeres are cluster close to the SPB, the nucleolus lies on the opposite pole of the SPB and the telomeres organize in few foci at the nuclear periphery. (B) Three-dimensional model of the yeast genome. Adapted from [72,127].

Each chromosome has one centromere, which in yeast corresponds to a short specific DNA sequence of 125 base pairs. In other

organisms instead, centromeres are not defined by a specific sequence but from epigenetic marks [128]. The centromeric chromatin is transcriptionally inactive and recruits the kinetochore, a protein complex which is responsible to attach the chromosomes to the spindle pole body (SPB), through the microtubules. In yeast, each centromere is attached to the SPB by one single microtubule, and they stay attached during the whole cell cycle.

The 32 budding yeast telomeres are also anchored to the NE but in different foci. Telomeres are composed by irregular tandem repeats of 250–300 base pairs (called TG1-3) which are at the two ends of each chromosomes [129]. They also have an overhang of the G-rich strand, which is 10–15bp in length and is the substrate of telomerase [130], a conserved ribonucleoprotein complex with reverse transcriptase activity important for preventing progressive erosion of chromosomes ends.

The first observation of the Rabl like configuration of yeast chromosomes was done by FISH [131]. Later on, several experiments using chromosome conformation capture technique gave new insight in chromosomes conformation and confirmed the Rabl like configuration [72]. The metacentric chromosomes, like chromosome III and VI have been shown to have the two telomeres juxtaposed, while chromosomes with different length seem to interact less likely. [44,107,132]. These findings have been confirmed by Duan et al, who performed genome-wide chromosome conformation capture experiment in budding yeast. They could also find chromosomal territories yeast. In fact, contacts among different chromosomes are

lower than the intrachromosomal ones. But the intrachromosomal contacts decrease in genomic regions far from the centromeres, suggesting that yeast chromosome arms are highly flexible, and chromosome territories are much less defined compared to mammalian cells.

The biggest substructure of budding yeast nucleus is the nucleolus. It is the site where rDNA is located and occupies roughly one third of the nucleus opposite the SPB [107,133]. The nucleolus is, thus, a physical and functional compartment. In fact, it is the site where RNA pol I-mediated rDNA transcription and ribosome subunits assemble. The rDNA is composed by in 100–200 tandem repeats. Each repeat unit is 9.1 kb in size and yields a 35S precursor rRNA, transcribed by RNA polymerase I and a 5S rRNA, transcribed by RNA polymerase III. The 5S unit is surrounded by two intergenic spacers, IGS1 and IGS2. Within this spacer there is a so-called polar replication fork barrier (RFB), a recombination enhancer (RE), a RNA polymerase I transcription initiation region (TIR) and an origin of replication (ARS, from autonomously replicating sequence).

1.3.2 Mechanisms of DNA anchoring to NE

There are two redundant mechanisms responsible of the telomeres tethering to the inner nuclear membrane, one requires the silencing factor Sir4, and the second the yKu70/yKu80 heterodimer [134, 135] (**figure 1.6**). Sir4 binds telomeric chromatin through its interaction with Rap1 (Repressor Activator protein 1) which binds the double-stranded telomeric repeat [136]. Sir4 binds to Rap1 together with Sir3

forming a stoichiometric complex with the NAD-dependent histone deacetylase Sir2 [137-139], that mediates the transcriptional repression at the subtelomeric regions [140,141]. Sir4 anchors the telomeric chromatin to the NE via its partitioning and anchoring domain (PAD), which binds the protein Esc1 that localizes in patches at the inner part of the NE and it is excluded from the nuclear pores complexes [126,142,143].

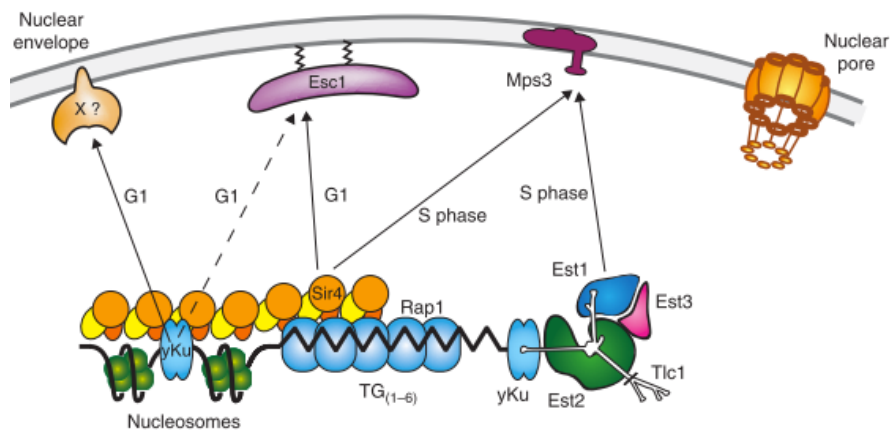


Figure 1.6 Mechanisms of telomere anchoring to the NE. Sir4, yKu80 and Mps3 bind the Esc1 C terminus. yKu80 binds also telomerase. Telomerase binds Mps3 in S phase through interaction with Est1. In G1 yKu binds the NE in a Esc1- and Mps3-independent manner. Adapted from [127].

Although Sir4 and yKu80 interact, in mutants in which yKu80 is not able to interact with Sir4, yKu80 retains its role in anchoring the chromatin to the NE [126,144]. This is mediated by the binding of yKu80 to telomerase [145]. Interestingly, the Sir4-independent tethering mechanism of telomeres to the NE mediated by yKu80, changes depending on the cell cycle stage of the cell. In S phase, when chromosomes are being replicated, the DNA end binding factor

yKu80 binds a stem-loop in the telomerase RNA Tlc1 and Est1 which forms a complex with Est2, the catalytic subunit of telomerase. Est1 in turn interacts with the acidic amino-terminal domain of the integral nuclear membrane protein Mps3 [124,145,146]. This anchoring process specific to S phase has also a role in preventing hyper-recombination among telomeres that could happen by unequal strand invasion during replication in S phase [145]. After S phase the yKu-telomerase-Mps3 anchoring is off, allowing the telomeres to be dislodged from the NE, probably facilitating so the sister chromosomes segregation during mitosis. Mps3 protein is also part of the Sir4-dependent mechanism of telomeres anchoring in S phase [147]. In G1 phase, when DNA still did not start replication, the anchoring role of yKu80 is independent from telomerase and requires yKu80 interaction with yKu70. It is still not clear however which is the binding partner at the NE, since is independent both from Mps3 and Esc1.

The anchoring of the rDNA at the nuclear envelope has been proposed as a mechanism to stabilize the rDNA repeats preventing their recombination. In fact, when rDNA is repaired for a double strand break, it gets transiently delocalized outside the nucleolus at the interior of the nucleus [148].

1.4 Nuclear organization and function in yeast

1.4.1 Telomere silencing

The expression of several RNA Pol II transcribed genes near a telomere are repressed, a phenomenon called TPE (telomere position effect), or telomere silencing, which is not gene nor telomere specific. TPE was discovered in budding yeast in the early '90s, when it was discovered that upon the integration of the *URA3* cassette marker right upstream the left telomere of chromosome VII, many cells expressing the marker were also resistant to a drug which kills cells expressing *URA2* (FOA). These cells carried a non-mutated copy of *URA3*, and moreover the FOA-resistant phenotype was reversible. It has been shown that the phenotype is actually due to the mRNA levels of *URA3*. In fact, when cells grow on medium lacking uracil they express 10 times more *URA3* mRNA than FOA-grown cells [149].

TPE is initiated at telomeres and it spreads several kilobases from the Rap1-bound telomeric repeats into subtelomeric nucleosomes. This spread is mediated by protein-protein interactions between Sir3 and Sir4 with the N-terminal tails of histones H3 and H4 [150,151] and the deletion of the amino terminal tails of histones H3 and H4 abolishes TPE [140,152,153].

The peripheral clustering of telomeres in few foci not only represents a physical compartment but also a functional one. In fact, the Sir4 protein, which is responsible together with yKu proteins of NE

anchoring, is also involved in the transcriptional repression of subtelomeric chromatin, providing a mechanism for self-organization of transcriptional repressive region. The amount of SIR proteins in the nucleus, Sir3 and Sir4 in particular, is highly regulated. Each SIR complex binds in equal molar ratio one Rap1 protein and one subtelomeric nucleosome [141]. Hence, the 3 to 8 foci of telomeres concentrate in their site between 30 and 40 SIR complexes. The histone deacetylase activity of Sir2 is also required for TPE, as acetylation, especially of histone H4K16, decreases Sir3/4–histone interactions [154]. Not only Sir2, but many others genes that modify histones or that regulate histone modifications also affect TPE. The fact that the limited amount of Sir proteins concentrates in these compartments limits the probability that this repressive complex localizes in different regions of the nucleus, avoiding so the eventual Sir-dependent repression of promoters of genes non located at the periphery [154]. This theory is supported by two studies, which reported that deleting yKu70 or Esc1, that is, disrupting so the telomere anchoring, genes in the internal loci get repressed and the subtelomeric ones get derepressed [155,156]. However, a third study showed no correlation between the location of a specific gene at the telomere clusters and its silencing efficiency [157].

Intriguingly, early studies suggested that TPE does not only requires the proximity to a telomeric sequence but also to be close to the telomere itself, as an 81-bp internal tract of telomeric DNA does not silence an adjacent gene [149]. However, another study showed that long (300 bp) internal tracts of telomeric DNA can repress

transcription [158].

In genome-wide transcriptional studies by Wyrick and colleagues it was found that 267 genes that are within 20 kb of a telomeres, produced 5 times fewer mRNA molecules (0.5/cell) compared to genes that are not telomere proximal. But the low transcriptional activity of this genes was not only dependent on Sir3. In fact, only the expression of 20 out of 267 was inhibited by Sir3, and they were all within 8 kb from a telomere [159].

Other evidences showed that Hda1 also deacetylates subtelomeric domains, causing the repression of genes between 10–25 kb from telomeres [160].

The telomeric proximity appears to be a nuclear compartment in which a specific set of genes is regulated. In fact, many genes close to the telomeres, which are hypothesized to be regulated either via Sir3 or via Hda1, are not expressed under standard growth conditions, they are for example involved in rapamycin resistance [161], stress responsiveness, and ability to grow in nonstandard carbon sources [160].

In conclusion, these studies, do not clearly show if the spatial position of genes is actually important for their transcriptional regulation, or if it is only their epigenetic state. To address this question we use performed a genome-wide analysis of RNA transcription in strains in which entire chromosomes, and hence also single gene loci, have been delocalized from their initial position, without generating any mutations in genes responsible for the tethering of telomeres to the

NE, and neither in genes responsible to regulate gene transcription.

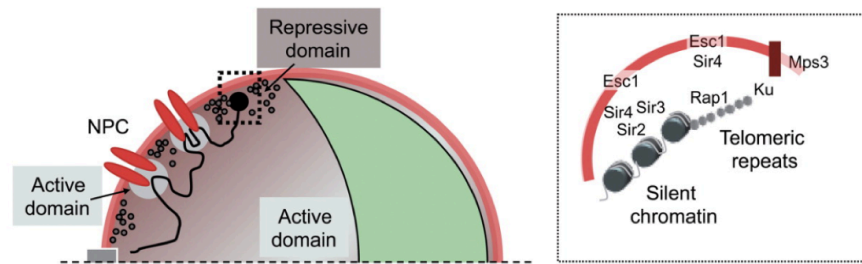


Figure 1.7 Left. Polymerase II transcription domains. PolII transcriptionally repressive domains, are found at the nuclear periphery, where silencing proteins are concentrated. In the nuclear interior and in the proximity of NPCs there are domains permissive for transcription. Right. Molecular determinants of transcriptional silencing acting at telomeric and subtelomeric regions .Adapted from [109].

1.4.2 Inducible gene expression at Nuclear Envelope

The nuclear envelope (NE) is not only a “repressive” region, instead it appears as a mosaic in which the regions close to the NPCs are actually associated with highly transcribed genes. The first evidence that associated the nuclear pore complex with gene transcription was given by Ishii and colleagues, who showed that the nucleoporin Nup2 prevents the spreading of heterochromatin to a reporter gene by bounding to its promoter [162]. By using the LacOp/GFP–lacI tagging method, several inducible genes, like *INO1*, *HXK1*, *GAL1*, *GAL2*, *HSP104*, were shown to be relocated from the nuclear interior to the nuclear periphery, in proximity to the NPC when activated [62,163]. The association to the NPC can be of importance for inducible genes because they are likely to require rapid and high level

expression and export, which can be facilitated by their proximity to the pores. Additionally, genome-wide chromatin immunoprecipitation studies [164,165] showed that a number of highly transcribed genes are interacting with components of the NPC and the nuclear transport machinery, although their stable interaction did not seem to be necessary for their activation [164]. It is not yet clear how specific genes get associated to the NPC, but the association depends both on the promoter and on the 3'UTR of the gene. For example, the activation of *HXK1* by targeting the viral transcriptional activator VP16 to its promoter leads to the movement of the loci in the interior instead of being target at the periphery. Moreover, two identical constructs, which included the same GFP reporter gene driven by the *GAL1* promoter but carrying different 3'UTRs show different localizations, but the same level of transcriptional activation in galactose. Different studies show also that transcription per se is not necessary for the anchorage of a gene to the NPC, but the initiation of transcription [166-168]. For example, the Nup2 interaction with the *GAL* locus needs the TATA box, the specific activator *GAL4* and its DNA binding site (UASg), but not the SAGA histone acetyltransferase nor active transcription. In fact, the mutant of the largest RNA polII subunit still recruits *GAL1* or *INO1* genes to the NPC.

Two more studies decoupled the expression levels with loci localization. It was shown that the disruption of the interactions of *GAL1* or *HSP104* genes with the NPC did not affect expression levels, suggesting that the localization of these genes could be a consequence rather than a cause of transcriptional activation

[166,169]. Other evidences instead, suggested that the NPC has a regulatory function in gene transcription. For example, the artificial targeting of components of the Nup84 nuclear pore subcomplex to the promoter of a reporter gene activates its transcription [170].

Another role of the NPC could be the to act as an epigenetic mark allowing past events to be remembered. In fact, the *GALI* gene remains associated with the NPC for at least six generations after its repression, and this association allows the gene to be activated faster. This “cellular memory” requires the incorporation of the histone variant H2AZ [168].

Hence, the nuclear envelope plays a dual role in transcriptional regulation: first, it creates a telomeric repressive compartment, and second, in the proximity of the NPC, it promotes transcription. The two functionally distinct compartments have been shown to not overlap, as by microscopy the positioning of subtelomeric domains is in-between nuclear pores [126].

The fact that repressive and active compartment at the nuclear periphery are close, can actually favor both the efficiency and the reversibility of gene induction. This can be especially important for subtelomeric genes, which are mainly involved in the usage of alternative carbon sources and need to be highly expressed only under specific growth conditions [171]. In fact, the artificial association of the *HXK1* subtelomeric gene with the nuclear periphery improves both its repression on glucose medium and its activation in the absence of glucose [172].

1.4.3 Replication and nuclear organization in yeast

Beside gene expression, DNA replication timing appears also to be influenced by chromosome positioning and topology.

Chromosome replication initiates at specific sites of the chromosomes, called origins of replication, which in budding yeast are sequence specific dependent [173]. There are around 500 Autonomously Replicating Sequences (ARS) in all the budding yeast genome, which are recognized and bound by replication factors and where replication starts. During S phase DNA duplication does not start from every ARS, and some of them tend to replicate in early S phase, and others in late S phase, named early firing and late firing origins respectively [174].

Interestingly, early origins tend to cluster together, and are localized mostly close to the centromeres and in the interior of the nucleus [175,176]. Late origins do not cluster together and tend to be at the periphery (**figure 1.8**). It has been shown that the early firing origins clustering is due to two different mechanisms. The clustering of origins which are not close to the centromeres depend on the two Forkhead transcription factors Fkh1 and Fkh2, either by binding to origins and homodimerize, or by binding to different origins [177,178]. This clustering is thought to favor the binding of the initiation replication factor Cdc45, whose amount is limited only to a fraction of origins at the time. So when the early replicating origins have started, Cdc45 gets released and available for the initiation of

replication of the late firing ones. The origins which are close to centromeres, in a range distance of 19 kb maximum, are early firing and the binding of Cdc45 is Fkh independent [179,180]. In Fkh1 and Fkh2 mutants in fact, Cdc45 amount at the centromeric origins is increased, probably due to the fact that more Cdc45 is available and centromeric proximal origins fire even earlier [180]. Probably the clustering mediated by centromeres play the same role of Fkh1 and Fkh2. Also yKu70, a protein responsible for tethering telomeres to the periphery, seems to play a role in origin firing timing. Strains with deleted yKu70 show an advance of replication timing as well as Sir3 deleted strain [181,182]. Also histone acetylation level is important in regulating the time of firing of early origin. Deletion of RPD3, which deacetylates histones, advances the non subtelomeric late firing origins [183,184]. But this does not cause the late firing origins to initiate replication as early as the early firing ones.

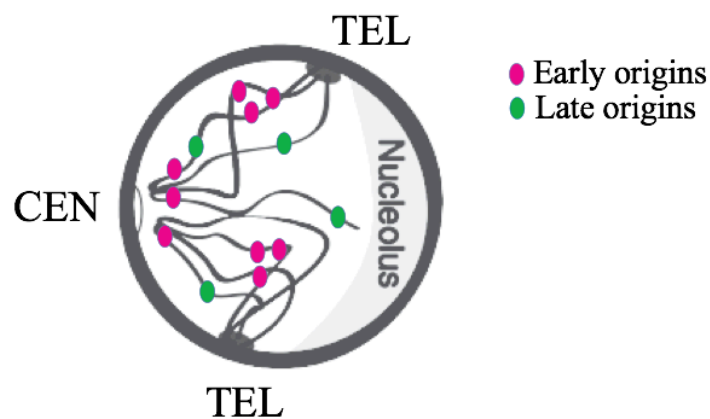


Figure 1.8 Schematics representing early and late origins location in the budding yeast nucleus. Early origins cluster together close to the SPB and in the nuclear interior. On the contrary, late origins are distributed far apart to each other in the nuclear space.

Altogether, these evidences suggest that local factors, like histone acetylation, as well as long-range organization of chromosomes cooperate together to determine replication timing in budding yeast.

1.5 Modeling budding yeast nucleus

Computational modeling of entire genomes or parts of chromosomes are often combined with experimental procedures to characterize the genome organization and how chromatin folds. It is useful, especially to study to what extent the genome folding is dependent on the physical properties of the DNA fiber, and hence to know how important are functional processes in genome organization. I will now summarize two examples of computational models of budding yeast genome architecture.

The first one is a “direct model”, meaning that it is actually based on the laws of polymer physics, relying on minimal physical assumptions and very few parameters. With this modeling Wong and colleagues investigated if a polymer model with a very few set of assumption could predict the architecture of the yeast genome [185]. They represent the 16 chromosomes as self-avoiding chains composed by jointed rigid segments (called Kuhn segments) with a length of 60 nm, a diameter of 20 nm and DNA content of 5 kb. The budding yeast nucleus is represented by a sphere with a 1 μm radius which encloses the 16 chains. The simulations of the chains motions were done following the Brownian dynamics and three constraints were added to the generic polymer model. First, the centromeres were

attached to a structure which mimics the SPB by an additional segment, to simulate the centromeric cluster close to the SPB. Then since the telomeres were known to be anchored to the INM (Inner Nuclear Membrane), a radial outward force was applied to keep the 32 end segments in the vicinity of the periphery of the sphere. Finally, a 1.5 Mb rDNA locus of chromosome 12 adjusting the diameter of the segments to 200 nm was modelled to reach the effective volume of the nucleolus in the opposite side of the SPB. The simulations were run till reaching the equilibrium and then the models were sampled at large time interval. Finally, they compared the predictions obtained using the models with the experimental data, such as the presence of nuclear territories, the distances between specific genomic loci and the contact frequencies obtained by chromosome conformation capture techniques. The results showed that the polymer models were able to recapitulate, with a high degree of agreement, the experimental data, suggesting that in budding yeast genome architecture can be a consequence of physical properties of the chromatin fiber, with the exception of the specific sequences (centromeres, telomeres and rDNA) [185].

Unlike to the “direct” modeling, the “inverse” ones reconstruct chromosome configurations from large data sets. An example is given by the work of Duan and colleagues, who reconstructed the budding yeast chromosome architecture using Hi-C data [72]. In this model the polymer chains were represented by beads with a DNA content of 10 kb. Then they transformed the Hi-C contact frequencies into distances between pairs of beads. This transformation as done first by plotting the average intrachromosomal contact frequencies as

function of genomic separation s , and then by assuming a DNA compaction in chromatin of 130 bp/nm. Next, they transformed the genomic separation s into spatial distances (estimated in [186]). In this way they could estimate all the intrachromosomal and interchromosomal distances. Several geometric constraints were then added to the modeling: the chains were enclosed in a 1 μ m radius sphere; assuming a folding of 30 nm fiber, two beads on the same chromosome could not be closer than 30 nm; and finally the rDNA and the centromeres were constrained on the opposite poles of the sphere. Since all the calculated distances among the beads could not be satisfied at the same time, they performed an optimization step, in which all the beads were moved till reaching the conformation that satisfied the best all the constraints imposed.

This model reproduced very accurately some of the features of the yeast genome, like the chromosome arms extended away from the SPB, and the 16 centromeres clustering together. But, since it is a static model, it cannot reproduce the cell to cell variability of nuclear positioning, which instead can be reproduced in the direct model described above.

2. Objectives

Chromosomes and genes are not randomly organized inside the nucleus. Chromosomes occupy discrete territories in the nuclear space which correlate with cell types and gene content. Gene loci positioning correlates with transcription level and replication timing. We thus wondered whether changes in chromosomal arrangement affect nuclear processes and physiological responses. To address this question we used as a tool budding yeast strains carrying chromosomal translocations generated by chromosome fusion.

The objective of the work presented here were to determine:

- How chromosome fusion affects nuclear organization.
- Whether changes in nuclear organization reflects in changes in gene transcription.
- The influence of chromosome rearrangement in replication timing.
- Whether chromosomal rearrangements affect cell physiology.

3. Materials and methods

3.1 Cell growth

3.1.1 Growth media

Yeast cells were normally grown on rich YP medium ((1% Yeast Extract (Becton Dickinson, #212720), 2% BactoPeptone (Becton Dickinson, # 211820)), supplemented with 2% sugar (Glucose (Sigma-Aldrich, #G7528), Galactose (Sigma-Aldrich, #48260) or Sucrose (Sigma-Aldrich, #S0389)). Rich medium was supplemented with 0.004% adenine (Sigma-Aldrich, #A9126).

For antibiotic selection rich medium was supplemented with the following compound: 100mg/L nourseothricin (ClonNAT, Werner Bioagents, 51000).

For selection of auxotrophic markers cells were grown on synthetic minimal medium, lacking the amino acid of choice. Complete synthetic minimal medium was composed of 0.67% Yeast Nitrogen Base w/o ammonium sulfate (Becton Dickinson, #291920), 0.004% adenine (Sigma-Aldrich, #A9126), 0.002% uracil (Sigma-Aldrich, #U0750), 0.002% tryptophan (Sigma-Aldrich, #T0254), 0.002% histidine (Sigma-Aldrich, #53319), 0.003% lysine (Sigma-Aldrich, #62840), 0.003% leucine (Sigma-Aldrich, #61820) and 0.002% methionine (Sigma-Aldrich, #M9625). Solid medium contained 2%

agar (Becton Dickinson, #214510). Agar, Peptone and yeast extract were mixed with water and autoclaved, all other components were filter sterilized. To stock strains, cells were scraped directly from 2-3 days old rich solid medium and resuspended in 30% glycerol/70% liquid rich medium. Stocks were kept at -80 °C.

3.1.2 Automated growth experiments

Automated cell growth experiments were performed essentially as described [187].

Yeast cells were grown in a pre-growth cultivation overnight in YP medium (1% Yeast Extract (Becton Dickinson, #212720), 2% BactoPeptone (Becton Dickinson, # 211820)), supplemented with 2% sugar (Glucose (Sigma-Aldrich, #G7528) and 0.004% Adenine (Sigma-Aldrich, #A9126).

Growth experiments were performed in a 96 well Falcon flat bottom microwell plate in at 30°C in a TECAN Infinite M200 plate reader with 120µl medium per well. An optical density (OD) measurement at 600nm was made every 10 minutes to follow cell growth. The plates were shaken linearly every second minute for one minute. The start OD₆₀₀ is in the linear range around 0.1. Measurements were taken for 48hrs, if the stationary phase had already been reached, otherwise for longer, till cultures reach the stationary phase. The different growth conditions used in the experiments are: 2% Glucose, 2% Galactose, heat (42°C), 400 µg/ml Paraquat (superoxide), 1.25M NaCl, 30 µg/ml 5FU, pH3, pH7.5, Tunicamycin 1.5 µg/ml, 0.01% MMS, 0.7M CaCl₂, 225mM LiCl, 5mM Arsenite, 15% Methanol, 15

mg/ml Hydroxyurea, Glycerol, 2.5mM DTT, 0.1 µg/ml Cycloheximide, 20 µg/ml Doxorubicin, H₂O₂, 50 µg/ml Benomyl.

3.1.3 Analysis of yeast cell growth

ODs, taken every 10 minutes, are divided by the initial OD (calculated by averaging the first five ODs) and transformed into a growth curve by applying natural logarithm. A smoothing procedure is applied to the corrected ODs by averaging each point with its eight closest neighbours. Since growth rate is given by the slope of the log transformed ODs, maximal growth rate is identified as the maximum value of the curve. The doubling time is calculated as $[\ln(2)/\text{maximal growth rate}]$. The maximum yield was determined by measuring the optical densities (OD_{600nm}) as a function of time (min), and plotted as raw OD curves.

3.2 Yeast strains

Saccharomyces cerevisiae strains are derivatives of S288c background. The strains carrying the TetO and LacI arrays on chromosome IV were derived from a previously described strain [188] of a BF264-15 15D background [189]. All haploid strains carrying the TetO and LacI arrays used in this study have genomic contributions corresponding to 1/2 S288c, 1/4 W303 and 1/4 BF264-15D. Fused chromosome strains were generated by transformation as described [190,191]. As fused chromosomes were generated by transformation, they are always isogenic to the corresponding mutant

strain with normal karyotype, except for the subtelomeric genes that were lost during chromosome fusion.

Cells used in BrdU experiments were transformed to render them competent for the incorporation of BrdU. Cells were transformed with the plasmid p306-BrdU-Inc [192] linearized with *StuI* and selected in synthetic minimal medium lacking Uracil.

Cells used for live cell imaging were transformed to generate a Nup60-mCherry fusion protein to visualize the nuclear envelope. The template plasmid to generate a fluorescent mCherry fusion protein was provided by Karsten Weiss (University of California, Berkeley).

3.2.1 Yeast transformation

Transformations of PCR products or linearized plasmids were generated essentially as described in [193]. Yeast cells were inoculated overnight in liquid medium and diluted to an optical density of OD₆₀₀=0.1 in 10ml rich medium in the morning. Cells were harvested when the cultures reached an optical density of OD₆₀₀=0.6 by centrifugation at 400g for 5min at room temperature in a 15ml tube. Cells were washed in 1ml transformation buffer (100mM Li acetate, 10mM Tris, 1mM EDTA, pH 8) and resuspended in 72µl transformation buffer. 8µl of freshly denatured, chilled salmon sperm DNA (10mg/ml salmon sperm DNA (Sigma-Aldrich, #D1626); 10min denatured at 95 °C, cooled on ice) were added to the cells. 1-10µl of PCR product or plasmid were added to the cells,

followed by 500µl of PEG buffer (as transformation buffer, but containing 40% PEG-3350 (Sigma-Aldrich, #P4338) and incubated on a rotating wheel for 30min. After addition of 65µl of DMSO (Sigma-Aldrich, #D2650) cells were heat-shocked for 15min at 42 °C. Cells were harvested by centrifugation at 400g for 2min, resuspended in 100µl medium and plated. Selection for auxotrophic markers was carried out directly on synthetic minimal medium lacking the amino acid of choice. For selection of antibiotic resistances, cells were first plated on rich medium and replicated onto plates containing the antibiotic after 1-2 days. Genomic DNA of transformants was isolated for analysis by PCR essentially as described [194].

3.3 RNA isolation and sequencing (RNA-Seq)

3.3.1 RNA isolation

Cells were harvested by centrifugation and total RNA was extracted from fresh pellets using a RiboPure Yeast Kit (Ambion). RNA concentrations were determined using a NanoDrop 1000 (Thermo Scientific), while quality and integrity was checked using a Bioanalyzer 2100 (Agilent Technologies) at the CRG Ultrasequencing Unit.

3.3.2 Sequencing and bioinformatics analysis

The isolated RNA was sequenced at the CRG Ultrasequencing Unit facility on a HiSeq2000 (Illumina).

For each biological replicate, paired-end reads of 50 bp were aligned to the reference *S. cerevisiae* genome (R64-1-1) using STAR [195] with parameters `--outFilterMultimapNmax 1 --alignIntronMin 10 --alignIntronMax 10 --alignMatesGapMax 5000`. Next, the resulting uniquely mapped reads were filtered for PCR and optical duplicates using Picard (<https://github.com/broadinstitute/picard>). The coverage per nucleotide was then computed using the BedTools [196]. Next, the coverage per nucleotide was used to compute the average coverage per region of 3.2kb, which correspond to the size of a single particle of the produced 3D computer models. The differential expression analysis was carried out using DESeq2 to test whether particles had a Log2 fold-change significantly higher than 0.58 in absolute value ($p\text{-value} < 0.05$), which corresponds to an expression fold-change of 1.5.

3.4 IF-FISH

3.4.1 FISH Probe

Genomic DNA was isolated from log phase culture by Phenol:Chloroform:Isoamyl alcohol (Sigma-Aldrich, #P2069) extraction, and treated with RNase as described [197]. Genomic DNA extracted has been used as template to amplify a 6 kb PCR fragment from the subtelomere of the right arm of chromosome IV. The primers designed to amplify the fragment are:

5'-atcttccttacacataaactgtcaaaggaagtaaccagg-3';

5'-gtaacatacaaaactcaacgcctactaagattaatacatca-3'.

The 6kb fragment was then labeled with Alexa Fluor® 488 dye by a

nick translation reaction using the kit FISH Tag™ DNA Multicolor Kit (Invitrogen).

3.4.2 IF-FISH

IF (Immunofluorescence)

FISH-IF was performed as described [198].

After an overnight culture $1-2^{10}$ cells/ml were treated with 10 mM DTT in 0.1 M EDTA/KOH, pH 8.0, to make them competent for spheroblasting. Cells were then treated with 0.4 mg/ml Zymolyase 100T (Seikagatu Biobusiness, #120493) for 15 min at 30°C in YPDA medium containing 1.1 M sorbitol (YPDA-S). This treatment allowed the cells not to be completely converted into spheroplasts, but partially retained their cell walls, to help stabilize their three-dimensional structure. Partially spheroblasted cells were fixed for 20 min by incubation at room temperature with 3.7% paraformaldehyde in YPD-S. Cells were recovered by centrifugation (1000g for 5 min), washed three times in YPD-S, resuspended in YPDA, spotted on Teflon slides, and left to air-dry for 5 min. Slides were immersed in methanol (6 min) and in acetone (30 s) at 20°C. Slides were then rinsed in a phosphate-buffered saline containing 0.1% Triton X-100 (PBS-T) and 1% ovalbumin. Slides were incubated overnight at 4°C (or for 1 h at 37°C) with the primary antibody Anti-Nuclear Pore Complex Proteins antibody [Mab414] - ChIP Grade (ab24609) diluted 1:2 in PBS-T. Slides were then washed in PBS-T and incubated with the preabsorbed secondary antibody Cy™5

AffiniPure Goat Anti-Mouse IgG (H+L) diluted to 0.025 mg/ml in PBS-T at 37°C for 1 h.

FISH (Fluorescent In Situ Hybridization)

After immunofluorescence (IF), slides were fixed again in PBS containing 3.7% freshly paraformaldehyde for 20 min and incubated overnight in 4x SSC, 0.1% Tween 20, 20 µg/ml of RNase A at room temperature. The slides were then washed in water, sequentially immersed for 1 min in 70, 80, 90, and 100% ethanol at 20°C, and air-dried. Slides were then denaturated at 72°C with of 70% formamide and 2 SSC, slides were again immersed for 1 min sequentially in 70, 80, 90, and 100% ethanol at 20°C and air-dried. The hybridization solution (50% formamide, 10% dextran sulfate, 2x SSC, 0.05 mg/ml labeled probe, and 0.2 mg/ml single-stranded salmon sperm DNA) was then applied and slides were incubated at 10 min at 72°C. Slides were incubated for 48 h at 37°C to allow the hybridization of the probe. Slides were then washed twice for 10 min each at 42°C in 0.05x SSC and twice in BT buffer (0.15 M NaHCO₃, 0.1% Tween 20, pH 7.5) with 0.05% BSA for 30 min.

After three washes in BT buffer, slides were mounted in 1x PBS, 80% glycerol, 24 µg/ml 1,4diazabicyclo-2,2,2,octane, pH 7.5.

3.5 Microscopy and images analysis

Live-cell microscopy was carried out with a Leica imaging system (AF6000). All live-cell images were acquired at 30°C with a $\times 100$ objective lens. Eleven 0.2 μm thick z-sections were collected.

Images from IF-FISH were acquired on a confocal microscope (Leica TCS SPE) with a $\times 100$ objective lens.

Distances were measured between local maxima on single planes using ImageJ (<http://rsb.info.nih.gov/ij/>) and Microsoft Excel. In the figures of this work the images are represented as 2D maximum projections. Graphs and statistical analysis (*t*-test allowing for unequal variance) were performed with R software and Excel (Microsoft).

3.6 BrdU-IP-Seq

3.6.1 BrdU-IP

Yeast cells were synchronized in G1 phase by addition of alpha factor (5 μg /ml) for 150 min in YPDA. Cells were then released from G1 by addition of pronase (50 μg /ml). For arresting them in early S phase and incorporate BrdU, cells were resuspended in YPDA containing 0.2 M hydroxyurea and 400 g/ ml of BrdU for 60min. For immunoprecipitation of BrdU-labeled DNA, 1.5×10^6 cells were lysed five times for 2 min in NIB buffer (17% (v/v) glycerol, 50 mM

MOPS buffer, 150 mM potassium acetate, 2 mM magnesium chloride, 500 μ M spermidine and 150 μ M spermine, pH 7.2) with zirconium beads on a Vibrax shaker at 4 °C. The DNA was isolated using Qiagen genomic DNA extraction kit and fragmented by sonication to an average DNA size of 300–600 bp. For each BrdU immunoprecipitation, 50 μ l of mouse anti-BrdU IgG1 (BD Bioscience, 555627) was prebound to DynabeadsRat anti-Mouse IgG1 (Invitrogen 110.37) and added to the denatured purified DNA.

3.6.2 BrdU-IP analysis

The BrdU-immunoprecipitated DNA was sequenced on a HiSeq2000 (Illumina) at the CRG Unltrasequencing facility. Paired-end reads of 50 bp were mapped by using bowtie2 [199] on *S. cerevisiae* genome (version sacCer3) with default parameters. The resulting aligned tags were in turn fed to MACS [200] tool (version 1.4.2) for detecting the local tag enrichment comparing sample vs input.

3.7 Polymer modeling

Each yeast chromosome of wild type and fused chromosome strains was modeled using a bead-spring polymer model previously used and validated for modeling chromatin fiber [40,201]. This model consists of three different energy contributions each describing a general physical property of the chain.

Excluded volume (Purely repulsive Lennard-Jones potential)

Each particle occupies a spherical volume of diameter equal to 30nm and cannot overlap with other particle in the system. Considering the typical compaction ratio of the chromatin fiber in yeast [186], each particle contains about 3.2 kilo-bases of chromatin fiber.

Chain connectivity (Finite extensible nonlinear elastic potential)

Consecutive particle on the same chain are connected with an elastic energy, which allows a maximum bond extension of 45nm. The simultaneous action of the excluded volume and the chain connectivity prevents chain crossings.

Bending rigidity (Kratky-Porod potential)

The bending properties of a polymer chains are usually described in terms of the *persistence length*, which is the length-scale where the chain changes its behavior from rigid to flexible. According to the bending properties experimentally measured for the yeast chromatin fiber [186,202,203], the persistence length of each model chain was set to 61.7 nm for the internal region of the chromosome, and to 195.0 nm for the terminal ones. The regions of the chains corresponding to

the telomeres (the 20 kb at the chromosomes ends) have, in fact, are more compact and rigid [9].

Since the modeling aims to describe the chromosomal configuration of haploid strains, the total number of beads in the system is 4,062, resulting from the presence of one copy for each yeast chromosome. Each chromosome is initially folded in a solenoidal arrangement, where a rosette pattern is repeatedly stacked so to yield an overall linear, rod-like conformation, as described [40,204]

On top of the polymeric properties, the yeast chromosomes are also modeled taking into account the typical confining inside the nuclear volume and the attachment of specific regions to nuclear landmarks, similarly to the approach in [176]. The 2D projection on the (x,y) plane of the compartmentalization of the model nucleus is represented in **figure 3.1**.

The chromosomes are consecutively placed inside a sphere of radius $R_N = 1.0\mu m$ centered in the origin (0,0,0). The sphere describing the typical shape of yeast cells in G1, according to imaging data [205], and interact with the chromosome particles as a rigid wall. To obtain the initial chromosome nuclear locations, the position of the chromosome centers is picked in a random, uniform way inside the nucleus, and the orientation of the rod axis is chosen randomly. The iterative placement proceeds from the longest to the shortest chromosome in a way that the newly added chromosomes must not clash with previously placed ones. In case of a clash, the placement attempt is repeated.

To simulate the tethering of the centromeres to the Spindle Pole Body (SPB), the motion of the centromeres particles was restrained into a spherical compartment of radius $R_{\text{SPB}}=150\text{nm}$ centered in coordinates $c_{\text{SPB}}=(-850,0.0,0.0)$ (see **figure 3.1**).

To describe the formation of the nucleolus in the G1 nucleus the motion of the rDNA particles was restrained to a region occupying 10% of the total nuclear volume and located at the opposite side of the SPB. This region is defined by the intersection of the nuclear sphere with a sphere of radius $R_{\text{NUCL}}=640.92\text{nm}$ whose center is located at $c_{\text{NUCL}}=(1000,0.0,0.0)$. Conversely, the other no-rDNA particles of the chromosome models are restrained to stay out of the nucleolar compartment.

Finally, to represent the tendency of the telomeres to stay anchored to the nuclear envelope (NE), the periphery of the sphere (a shell within $R_{\text{PER}}=126\text{nm}$ from the nuclear envelope which accounts for one third of the nuclear volume) is attracting for the terminal particles of the chromosome chains. This effect, previously unexplored, was obtained using a Lennard-Jones attraction.

In the FC strains, the chromosomes involved in the fusion are attached to each other using additional bonds between the telomeres involved in the fusion process [190,191]. These telomeres, which are attracted to the periphery in the wild type strain models, behave as internal chromosomal sequences in the FCs strains, and lost the attraction to the nuclear envelope.

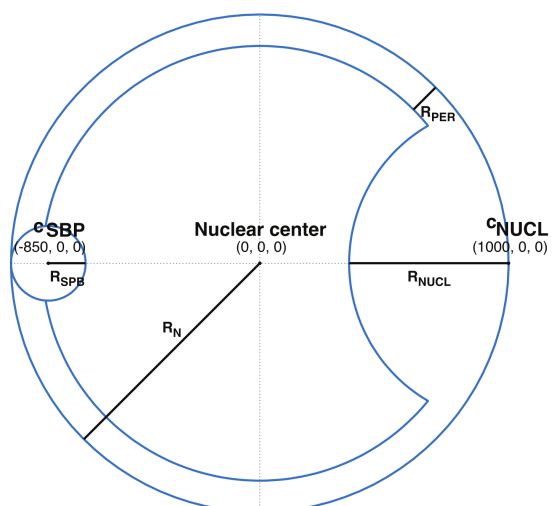


Figure 3.1 2D representation of the model nucleus compartments.

4. Results

4.1 Fused chromosome strains

4.1.1 Generation of fused chromosome strains

The spatial organization of the genome in the nuclear space is linked to important nuclear functions such as the regulation of gene expression and replication timing. A crucial question is whether nuclear organization is a cause or a consequence of nuclear functions.

To study the effect of genome organization in nuclear processes I took advantage of strains carrying fused chromosomes generated in the Manuel Mendoza laboratory [190,191]. A total of 10 fused chromosome strains were generated by end-to-end fusion of chromosomes arms. Fusion was achieved by homologous recombination of a PCR DNA fragment containing a resistant cassette flanking sequence homologous to the subtelomeric regions of the two chromosomes being fused. This led to the joining of two chromosomes and to the loss of the telomeres and several subtelomeric genes (listed in **table 4.1**).

To avoid the formation of dicentric chromosomes, which would lead to chromosomal bridges during mitosis, a *pGAL1* promoter was inserted in front of one of the centromeres. By growing the cells in

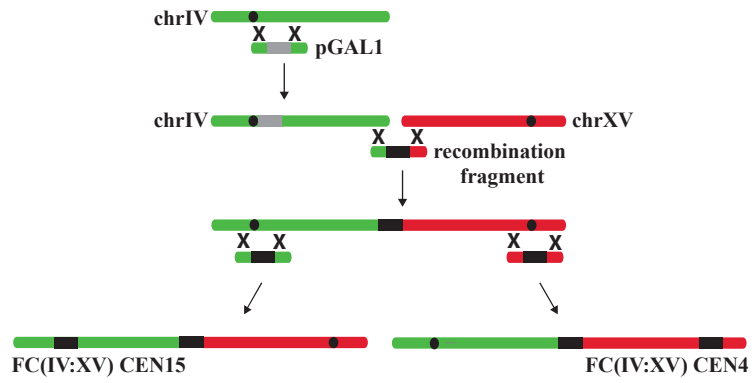
medium containing galactose, the centromere was inactivated by the transcriptional machinery recruited to the *pGALI* promoter. Finally, the deletion of the conditional centromere or its replacement with a wild-type copy generated two stable strains carrying monocentric chromosomes with different centromeres active.

FUSIONS	DELETED GENES
FC(IV:XII) CEN4 FC(IV:XII) CEN12	IRC4, YDR541C, PAU10, YLR460C, PAU4
FC(IV:XV) CEN4 FC(IV:XV) CEN15	IRC4, YDR541C, PAU10, PHR1, YOR385W, FRE5, FIT3, FIT2, YOR381W-A
FC(IV:XV:V) CEN4 FC(IV:XV:V) CEN5	IRC4, YDR541C, PAU10, PHR1, YOR385W, FRE5, FIT3, FIT2, YOR381W-A, YOL164W-A, YOLWtau1, YOLCdelta1, YOL166C, YOL166C, YOL16, PUG1, YER184C, SLO1, YERCdelta26, YER181C, FMP10, YERWdelta25, FAU1 /YER183C
FC(IV:XV:XVI) CEN4 FC(IV:XV:XVI) CEN16	IRC4, YDR541C, PAU10, PHR1, YOR385W, FRE5, FIT3, FIT2, YOR381W-A, YOL164W-A, YOLWtau1, YOLCdelta1, YOL166C, YOL166C, YOL16
FC(IV:XV:V:VII) CEN4 FC(IV:XV:V:VII) CEN7	IRC4, YDR541C, PAU10, YOL164W-A, YOLWtau1, YOLCdelta1, YOL166C, YOL166C, YOL16, PUG1, YER184C, SLO1, YERCdelta26, YER181C, FMP10, YERWdelta25, FAU1 /YER183C

Table 4.1: List of genes lost upon generation of chromosome fusions

Strains carrying more than two fused chromosomes were obtained by successive rounds of homologous recombination between subtelomeric regions, always using *CEN4* as conditional centromere (figure 4.1 A).

A



B

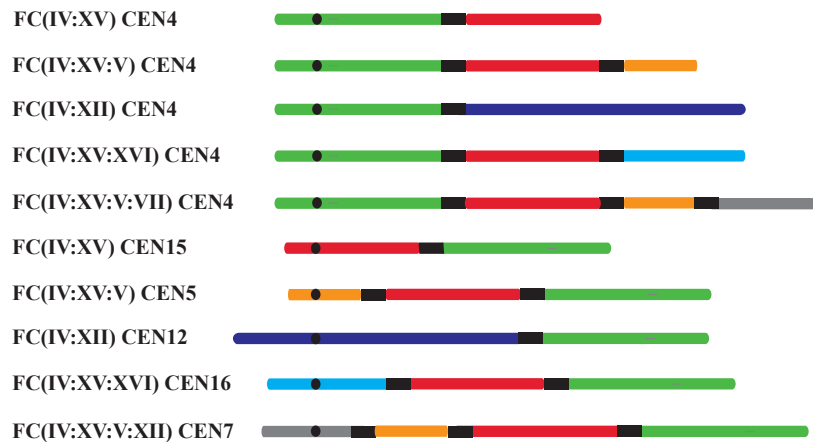


Figure 4.1 (A) Example of generation of fused chromosome. The first step consists in the integration of pGAL1 upstream of CEN4. Then a fused chromosome is generated by homologous recombination between a bridging PCR fragment and chromosomes IV and XV, followed by deletion of CEN4 or CEN15. **(B) Scheme of all fused chromosomes used in this work.**

In this study, I describe experiments performed using 10 strains carrying chromosomal translocations, which were derived from 5 different fusions involving 2, 3 or 4 different chromosomes joint together. Per each fusion, 2 different chromosomes arrangements were generated, depending on the active centromere. Strains carrying fused chromosomes were termed FC (fused chromosomes) followed by the names of the chromosomes which have been joint together, and the active centromere (**figure 4.1 B**).

The generation of strains carrying fused chromosomes was expected to lead to important changes in chromosome configuration in comparison to the wild type strain. Since the centromeric sequences are required for the attachment of the chromosome to the SPB, we expected a large nuclear displacement of the chromosomes with deleted centromeres. Therefore, the two strains with different active centromeres per each fusion were expected to assume highly different arrangement in the nucleus, both compared to wild type and also between themselves. Moreover, since the fusion involved the loss of telomeric regions, the chromosomal arms affected by the fusion were expected to be detached from the inner nuclear membrane.

Finally, by fusing up to 4 chromosomes together, corresponding up to 4.3 Mb of chromosome length, we expected to alter the global 3D organization of the genome in the nuclear space and the inter-chromosomal contacts.

In summary, chromosomes fusion is expected to dramatically change the chromosomes arrangement in the nucleus. Therefore, they are a good tool to study the effect chromosome position in untouched aspects such as transcription or cell growth.

4.1.2 Growth analysis of fused chromosome strains

To test if strains carrying fusions have defects in growth, an automated assay for cell growth was conducted using micro-cultivation in liquid media of wild type cells and fused chromosome strains. The concentration of yeast cells in a growing population was recorded every 10 minutes by automatic optical density (OD) reading in a microplate-spectrophotometer. This method allows even minor changes in growth phenotype to be detected. Two variables were extrapolated from the growth curves: the rate of growth and the stationary-phase OD (reflected by the cell density at stationary phase). The growth was carried in a rich medium containing glucose (YPDA) in triplicates (**figure 4.2**).

Fused chromosome strains grew at the same speed and reached the same yield when compared with the wild type strain (**figure 4.2**). The doubling time was around 2 hours and the maximum OD around 0.9 (**table 4.2**).

Chromosomal rearrangement derived from chromosomes fusion does not affect then cell growth in optimal growth condition.

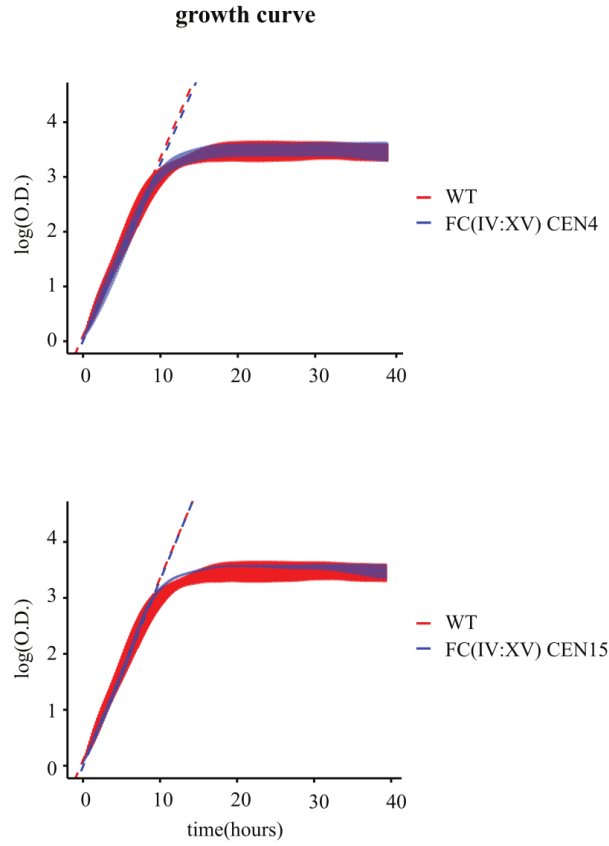


Figure 4.2 Example of growth curves for calculation of growth parameters. Cell concentration is measured by OD660 nm every 10 min over a period of 48 hours in triplicates. The growth curves correspond to the natural logarithmic curve of wild type (red) and fused chromosomes (in blue), with standard deviations of the three experiments performed. The maximal growth rate corresponds to the maximal slope (dashed lines of wild type in red and fused chromosomes in blue) of the Ln curve. The doubling time of the cells is defined by $\ln(2)/\text{maximal slope}$.

	Doubling time (hours)	maximum yield (OD)
wt	2.14 ± 0.21	1.03 ± 0.09
FC(IV:XII) CEN4	2.01 ± 0.11	1.00 ± 0.14
FC(IV:XII) CEN12	2.19 ± 0.03	1.02 ± 0.20
FC(IV:XV) CEN4	2.14 ± 0.15	1.02 ± 0.01
FC(IV:XV) CEN15	2.08 ± 0.16	1.02 ± 0.08
FC(IV:XV:V) CEN4	2.35 ± 0.16	0.98 ± 0.06
FC(IV:XV:V) CEN5	2.09 ± 0.05	1.13 ± 0.05
FC(IV:XV:XVI) CEN4	2.34 ± 0.05	1.02 ± 0.07
FC(IV:XV:XVI) CEN16	2.28 ± 0.01	1.15 ± 0.09

***Table 4.2** List of doubling time and maximum yield parameters for wild type and all the fused chromosome strains tested.*

4.2 Genome organization analysis of fused chromosomes strains

4.2.1 Polymer modeling to predict chromosomal rearrangements

To predict how fused chromosomes alter genome organization, in collaboration with Dr. Marco Di Stefano in the Structural Genomics Group at the CNAG-CRG, we generated polymer models of the wild type and fused chromosomes. The models were based on both physical assumptions [40,201] and known biological features [176](**figure 4.3**).

The 16 budding yeast chromosomes were represented as self-avoiding bead-spring chains, already used and validated for modeling chromatin fibers [40,204]. Each bead had a diameter of 30 nm equal to the nominal chromatin fiber thickness, and with a DNA content equal to 3.2 kb [186]. The beads had excluded volume interactions and consecutive beads were connected. The persistence length of the chains was 61.7 nm, according to the bending properties experimentally measured for the yeast chromatin fiber [186,202,203]. The regions of the chains corresponding to the telomeres (the 20 kb at the chromosomes ends), had a larger persistence length, 195.0 nm, to account for the increased rigidity of these regions [9]. Each of the 16 chains corresponded to one copy for each yeast chromosome and was located within a 1 μ m radius sphere, equal to the average radius of yeast nucleus in G1 [205].

Additionally, three spatial restraints were applied to the models according to known interactions between chromosomal regions and nuclear landmarks:

1. All beads corresponding to centromeres were constrained in a sphere of radius 150 nm attached to the nuclear sphere, mimicking the size of the microtubules anchoring the centromeres to the SPB, measured in G1 in Electron microscopy [206].
2. The rDNA, represented as 101 repeats of 9.1 kb in the chain corresponding to chromosome XII, was restrained in a region occupying 10% of the nuclear volume at the opposite site of the nucleus [107,133].
3. The telomeres were restrained using a Lennard-Jones potential to have higher probability to occupy the nuclear periphery, which was defined as the spherical shell closest to the nuclear envelope with a volume equal to a third of the nucleus [134,135,156,207-209].

The ensemble of chromosomal polymer models, representing the wild type and the fused chromosome strains genomic arrangement, were generated using Brownian motion dynamics [210]. Only the configurations satisfying all the imposed restraints were kept for further analysis. A total of 10,000 models were then randomly selected to be analyzed for the likelihood of particular loci and chromosomes to be positioned in the cell. The analysis compared the wild type and fused chromosome strains.

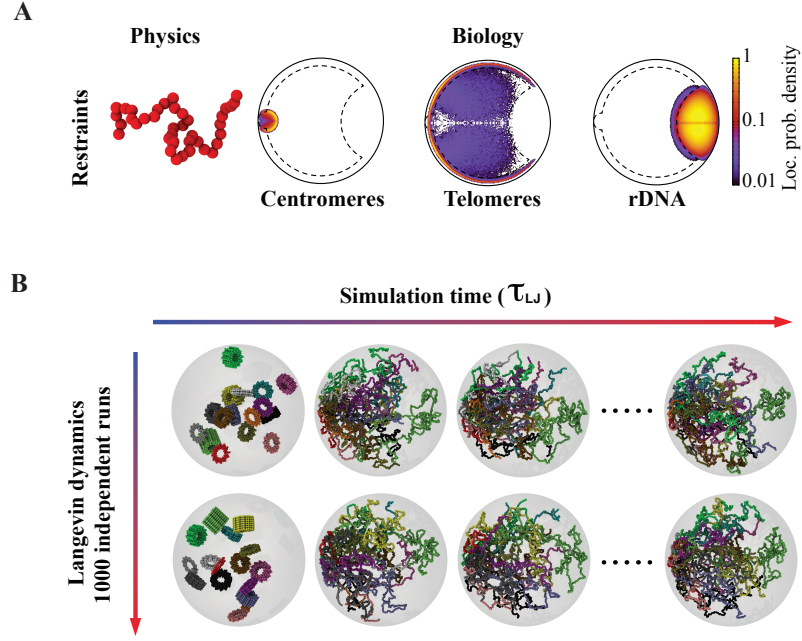


Figure 4.3 Representation of modelling procedure. (A) Restraints applied to the models. (B) Snapshots of polymers representing the 16 budding yeast chromosomes during the simulation.

By comparing the chromosomes distances in wild type and fused chromosomes strains from SPB and NE, it appeared clear that the chromosomes displaced in fused chromosome strains were those involved in the fusion (**Figure 4.4**). The rest of the chromosomes showed in fact minimal displacements ranging from 0 to about 20nm.

For example, for the FC(IV:XII) CEN12, where *CEN4* was deleted, the probability of chromosome IV to be close to the SPB was lower compared to wild type, and the same happened to chromosome XII when its centromere was deleted. The rest of the chromosomes, such as for example chromosome 7, instead did not change their

positioning compared to wild type (**figure 4.5**). This was also true for all the fusions tested. These models were later validated by microscopy (next subsection).

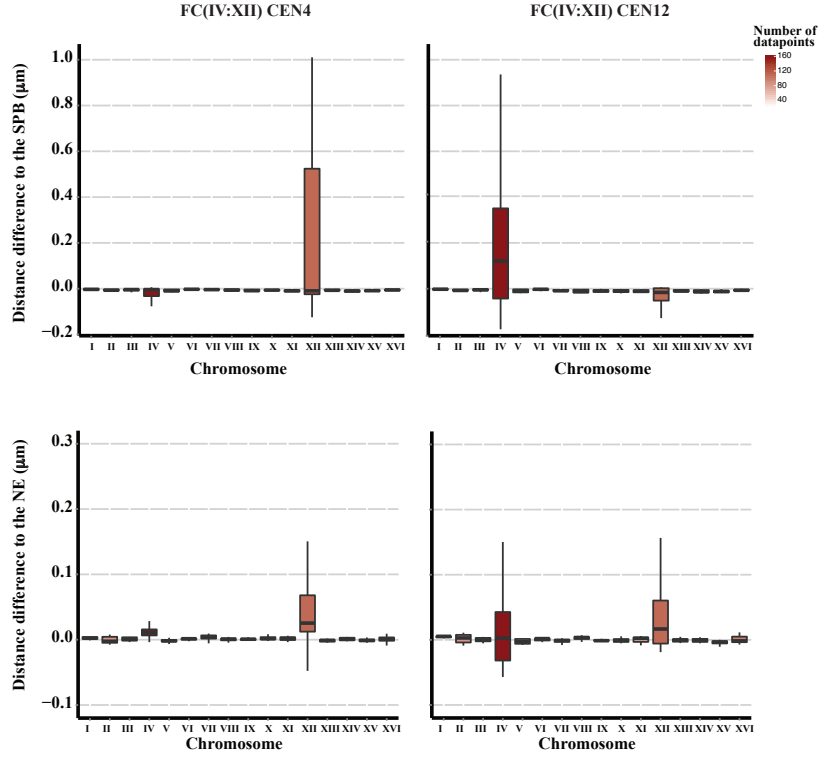


Figure 4.4: Displacement from SPB and NE in FC(IV:XII) CEN4 and FC(IV:XII) CEN12. The boxplots represent the distributions of the difference in distance from the SPB (top) and from the NE(bottom) between the fused chromosomes and wild type loci grouped by chromosome. The loci correspond to 3 particles (10 kb). A positive value indicates that the locus is farther apart from the SPB or from the NE in fused chromosomes compared to wild type.

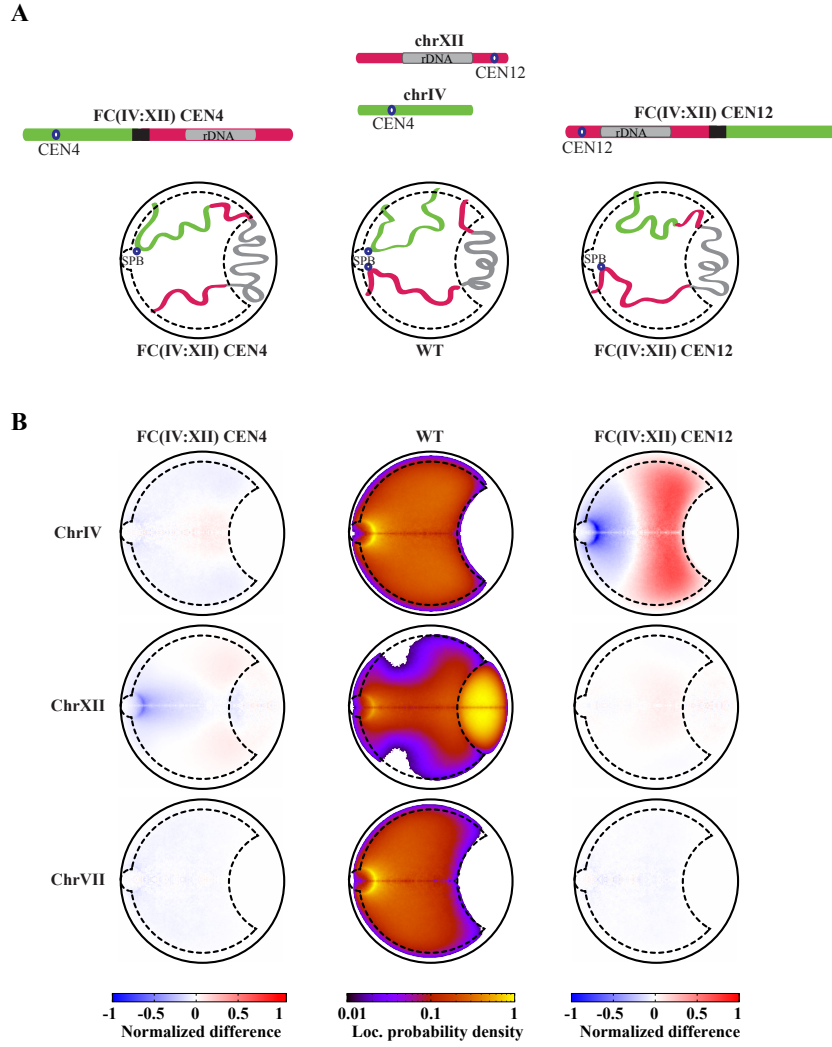


Figure 4.5: Heatmaps of chromosomes displacement in *FC(IV:XII) CEN4* and *FC(IV:XII) CEN12*. An example of the occupancy probability heatmap of 3 chromosomes, IV, XII and VII, in wild type and the relative difference to wild type in the two fused chromosome strains analyzed, *FC(IV:XII) CEN4* and *FC(IV:XII) CEN12*.

4.2.2 Microscopy analysis of loci positioning and validations of modeling

To validate the polymer models predictions, several distances inside the nucleus (listed below) were experimentally measured and then compared to the ones observed in the models. To achieve that, I used budding yeast strains in which two chromosome loci in the right arm of chromosome IV can be visualized thanks to an array-reporter system. In particular, the locus *TRP1*, 12 kb far from the centromere 4, and *LYS4*, at the middle of the right arm of chromosome. The two loci were visualized as red and green dots by RFP-TetR and GFP-LacI fusion proteins bound to the LacO and TetO arrays, respectively. The nuclear envelope and a protein component of the SPB (spc42) were also visualized in red and green, respectively. In this way I could measure for each cell, the distance between: *TRP1* locus and *LYS4* locus, the two chromosome loci and the nuclear envelope, and the two chromosome loci and the SPB (**figure 4.6**).

These distances were measured in G1 cells selected in a log-phase growing cell population in wild type, FC(IV:XII) *CEN4*, and FC(IV:XII) *CEN12*. Comparing wild type and fused chromosome strains, two main differences were found in the strain were the *CEN4* was deleted: the locus *TRP1* was in average further from SPB than in wild type (p-value < 2.2e-16), and the distance between the two loci *TRP1* and *LYS4* was shorter (p-value = 1.92e-06). Conversely, in the fused chromosome strain in which the *CEN12* was deleted, these measurements were not significantly different from the wild type (p-values = 0.19 ; 0.14).

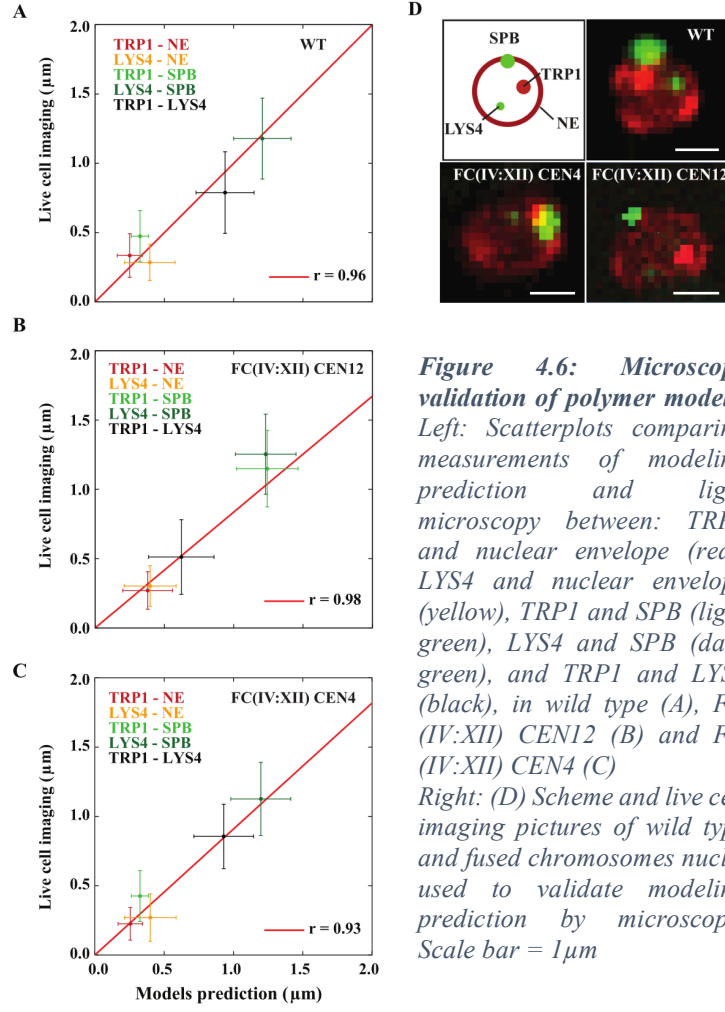


Figure 4.6: Microscopy validation of polymer models. Left: Scatterplots comparing measurements of modeling prediction and light microscopy between: TRP1 and nuclear envelope (red), LYS4 and nuclear envelope (yellow), TRP1 and SPB (light green), LYS4 and SPB (dark green), and TRP1 and LYS4 (black), in wild type (A), FC (IV:XII) CEN12 (B) and FC (IV:XII) CEN4 (C) Right: (D) Scheme and live cell imaging pictures of wild type and fused chromosomes nuclei used to validate modeling prediction by microscopy. Scale bar = $1\mu\text{m}$

Previously to this work, Neurohr et al., already noticed that the distance between these two loci in FC(IV:XII) CEN12 was shorter in mitosis compared to wild type [190]. Moreover, the increase in compaction was not found to be dependent on active hyper compaction, which is responsible for the increase in the loci proximity of the FC(IV:XII) CEN4 in mitosis [190]. Our polymer model predictions suggest in fact that the increased compaction of chromosome IV in FC(IV:XII) CEN12 can be simply explained by physical properties of the polymer.

All the experimental measurements were consistent with measures from the models, suggesting that the models accurately represent the cell nucleus and thus are a good tool to study chromosome arrangement in budding yeast.

4.3 Transcriptional analysis of fused chromosomes strains

4.3.1 Subtelomeric and peripheral genes are less expressed both in wild type and fused chromosomes strains

In budding yeast gene expression is linked to chromosome and loci positioning. In fact, heterochromatic domains are localized either at the nuclear periphery (*HML*, *HMR*, and telomeres) or in the nucleolus (rDNA). Moreover, there are numerous evidences that budding yeast genes are repositioned from nuclear interior to the periphery upon either activation or repression [163,164,166,167,172,211].

To study the effect of genome organization in gene expression, four biological replicates of RNA-Seq experiments were performed in the all 10 fused chromosomes strains. The RNA coverage per nucleotide was used to compute the average coverage per region of 3.2kb, which correspond to the size of a single particle of the produced 3D polymer models. The differentially expression analysis was carried out using DESeq2 to test whether particles had a Log2 fold-change significantly higher than 0.58 in absolute value ($p\text{-value} < 0.05$), which corresponds to an expression fold-change of 1.5.

The RNA coverage in individual biological replicates were highly correlated. ($r > 0.9$, **figure 4.7**).

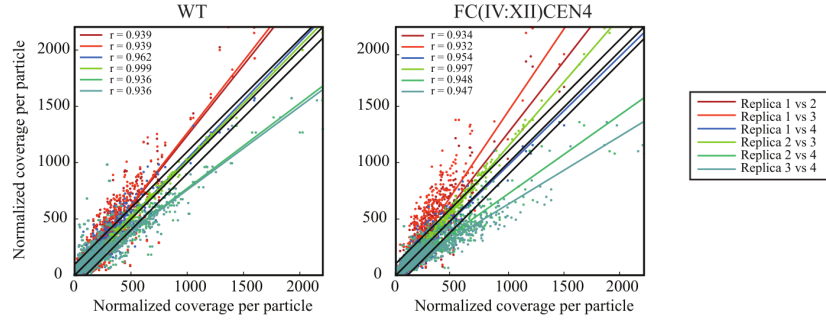


Figure 4.7 Scatter plots representing the correlation between the replicates of the RNA seq experiments in two of the strain tested.

The mapping of RNA transcript into the corresponding beads of the polymer models generated for each specific fusion, allowed to study how transcription level is distributed both along the chromosome fiber and in the nuclear space. Subtelomeric regions were less expressed compared to the rest of the chromosomes (**figure 4.8**). Furthermore, when we analyzed the RNA expression respect to different zones of the nucleus, it appeared that the more peripheral regions were less expressed compared to the interior. This might be due to the fact that the subtelomeric regions, which are less expressed, were likely to be at the periphery as a result of the restrain applied to the models.

This observation is true for the wild type and also all the fused chromosomes strains tested (example in **figure 4.9**)

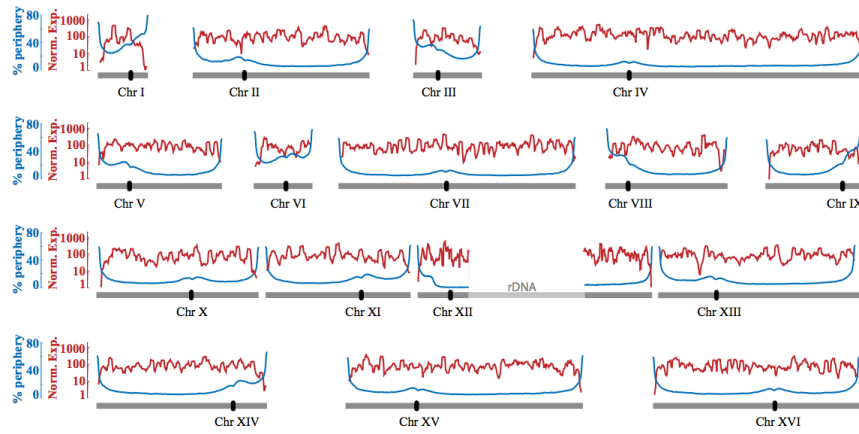


Figure 4.8 *Distribution of RNA expression along the chromosomes fiber and in the nuclear space* Representation of the normalized RNA expression (red) of the wild type strain along the chromosomes (grey) and percentage of the chromosome at the nuclear periphery (blue).

By comparing wild type and fused chromosome strains, we found that the chromosomal regions at the level of the fusion between chromosomes were lower in expression compared to wild type. This is expected because the chromosomal ends were deleted during the generation of the fusion. Moreover, and also expected, the gene *ADE2*, which was used as selection marker during the generation of the fused chromosome strains, resulted in a significantly higher expression in the fusion chromosome strains. Interestingly, no other expression differences were significant when comparing wild type with fused chromosomes strains (**figure 4.10, 4.11**). Therefore, our results suggest that large chromosomes rearrangements do not influence gene expression in log phase growing cells.

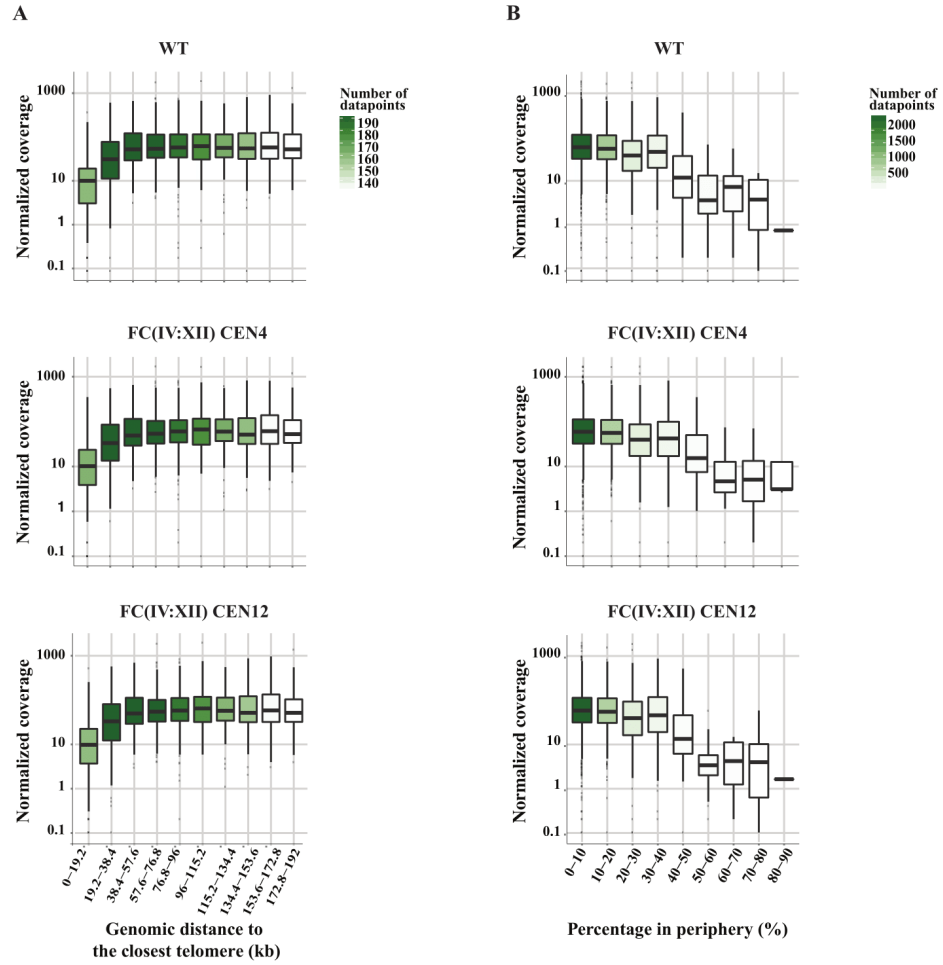


Figure 4.9: Example of RNA transcription relative to telomeres and nuclear periphery (A) Histograms representing the normalized coverage of RNA relative to the distance of the beads to the telomeres in wild type and fused chromosomes strains. (B) Histograms show normalized coverage of RNA relative to the percentage of the beads in the periphery of the nucleus for wild type and fused chromosomes strains.

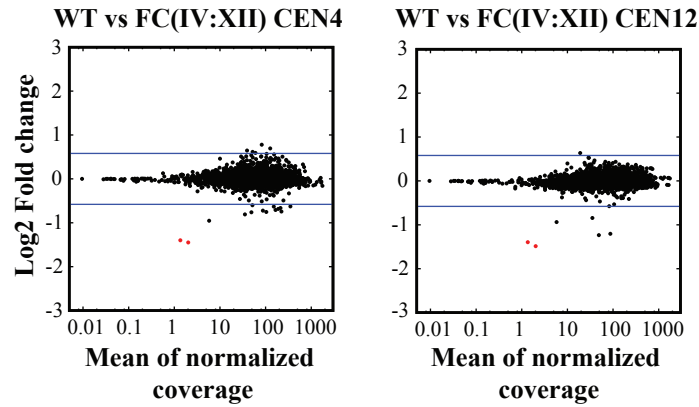


Figure 4.10 Log2 fold change of normalized RNA expression coverage between wild type and fused chromosome strains analyzed. Particles significantly changing expression compared to wild type (according to the DeSeq software) are shown in red otherwise are shown in black.

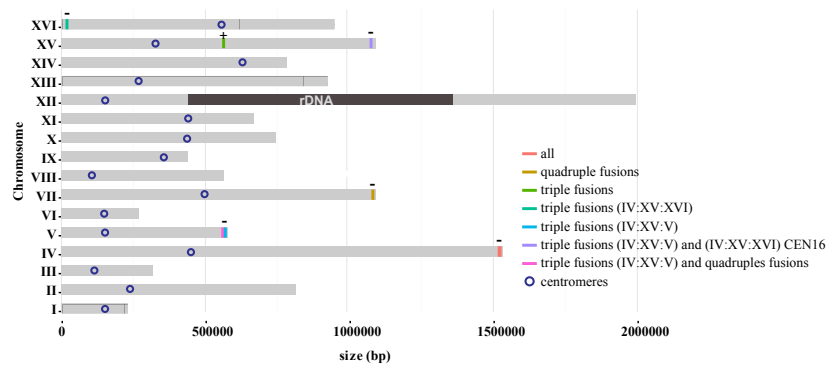


Figure 4.11 Representation of genomic position of particles significantly lower expressed (-) or higher expressed (+) in different fused chromosomes strains compared to wild type. The lower expressed regions are the ones deleted during the generation of the fusion. The ADE2 gene, in chromosome XV is a selection marker used to the generation of the fusions.

4.3.2 No differences in expression at loci displaced from their original position

Since the locus position relative to the periphery appeared to influence gene expression, we looked for chromosome regions which were predicted to be delocalized from the periphery in the strains when the chromosomes were fused. Using the 3D models, we identified chromosomal regions predicted to have an average higher displacement from the nuclear periphery by measuring the mean of the distances of all chromosomes loci (polymer particles) from the sphere periphery in the models ensemble. The end of the right arm chromosome IV suffered the largest displacement in all the fusion tested compared to wild type (example in **figure 4.12**). The average displacement was around 200 nm.

To validate the models, we performed IF-DNA FISH experiments in wild type, FC(IV:XII) CEN4 and FC(IV:XII) CEN12. A fluorescently labeled DNA probe complementary to the chromosomal region predicted to be displaced from the periphery in the fused chromosomes strains was hybridized to the DNA in the intact nuclei of previously fixed cells. By labeling in the same cells also the nuclear envelope, we were able to measure the distance between the end of the chromosome IV and the nuclear periphery (**figure 4.13**).

Although the displacement observed by IF-DNA FISH (*i.e.*, ~100nm) was smaller than the displacement predicted by the 3D models (*i.e.*, ~200nm) the imaging confirmed that the region is further located from the periphery in the fused chromosome strains compared to the

wild-type. Interestingly, that displacement did not affect at all the expression levels of the region, which were comparable to those in the wild-type strain (**Figure 4.14**).

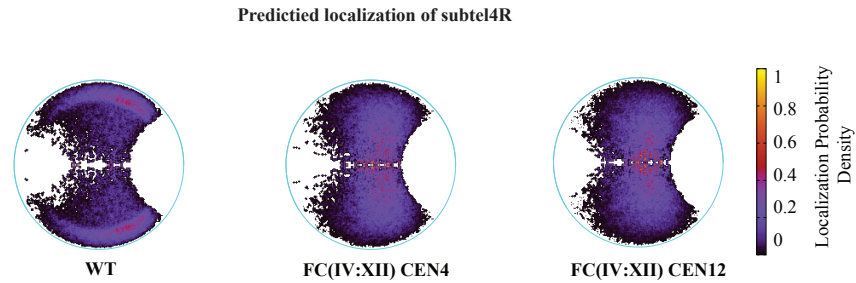


Figure 4.12 Heatmaps of the localization probability of subtelomere 4R in the nucleus predicted by polymer modeling in wild type and fused chromosome strains.

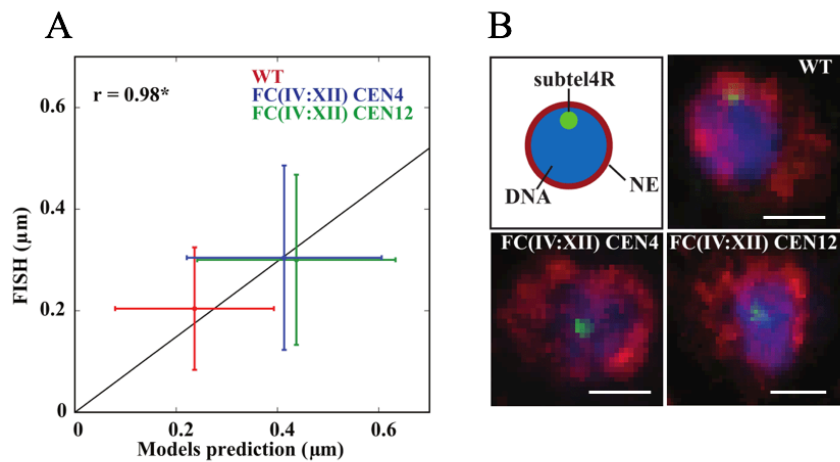


Figure 4.13 Microscopy validation of subtel4R displacement predicted by polymer models in fused chromosomes strains. (A) Scheme and IF-FISH pictures of wild type and fused chromosomes FC4:12 CEN4 and FC4:12 CEN12 nuclei used to validate modeling prediction by microscopy. (B) Scatterplot comparing

measurements of modeling prediction and light microscopy between: *TRP1* and nuclear envelope and *LYS4* and nuclear envelope in wild type (red), *FC IV:XII* *CEN4* (blue) and *FC IV:XII* *CEN12* (green). $R=0.98$ $p\text{-value} = 0.001$. Scale bar= $1\mu\text{m}$.

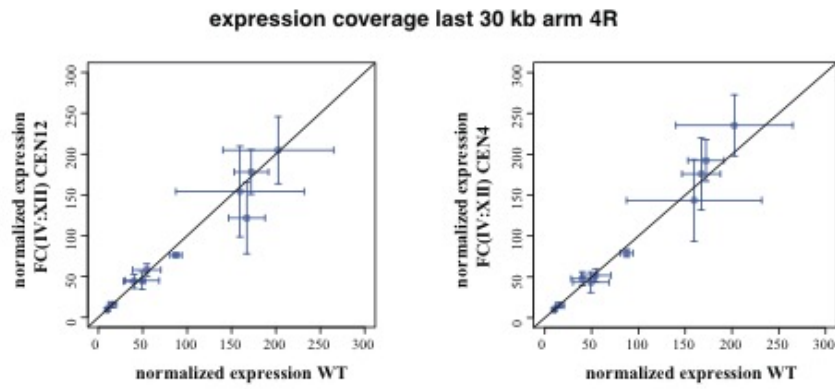


Figure 4.14 Expression coverage of the last 10 beads corresponding to the subtelomeric region long arm of chromosome IV (30 kb), between wild type and fused chromosome strains.

4.4 Analysis of replication timing in fused chromosomes

4.4.1 Analysis of early origins in wild type and fused chromosome strains

Genome organization has a role also in replication timing. Early firing origins tend in fact to cluster together, while the late firing ones are far apart from each other in the nuclear space [180]. Since fused chromosome strains carry big genome rearrangements, we tested whether this affected their replication timing.

To address the role of chromosome positioning in replication timing, the incorporation of the thymidine analog 5-bromo-20-deoxyuridine (BrdU) was monitored by chromatin immunoprecipitation followed by sequencing (BrdU-ChIP). The experiments were done in the presence of the ribonucleotide reductase inhibitor hydroxyurea (HU) to precipitate only the early origins. BrdU-ChIP experiments were performed in wild type and 4 different fused chromosomes strains, with either 2 or 3 chromosome fused together: FC(IV:XII) CEN4, FC(IV:XII) CEN12, FC(IV:XV:V) CEN4 and FC(IV:XV:V) CEN5.

Genome-wide BrdU profiles revealed that the pattern of early origin firing of the wild type was consistent with previous analysis [212]. A total of 178 peaks corresponding to early origins were detected (**figure 4.15**, example for BrdU peaks along 4 chromosomes). The pattern and efficiency of early origin in wild type and fused chromosome strains were qualitatively the same with few exceptions mentioned below.

First, in strains carrying fusions in which the *CEN4* was deleted (FC(IV:XII) *CEN12* and FC(IV:XV:V) *CEN5*), the BrdU peaks corresponding to the ARS surrounding the deleted centromere were lower compared to the wild type (**figure 4.15**), while the rest of the peaks showed the same pattern as the wild type. Second, the origins close to *CEN12* were firing later in the fused chromosomes in which the centromere 12 had been deleted (FC IV:XII *CEN4*). These results were expected because centromeric sequences induce early firing of origins within a 20 kb window [179].

Surprisingly, FC(IV:XV:V) *CEN4*, where the *CEN5* was deleted, did not show the same trend: In fact the early origins in proximity of *CEN5* and *CEN15* fire still early, as in the wild type.

Moreover, there were not new early origins in the subtelomeric regions of fused chromosomes strains. Hence, the delocalization of chromatin from the nuclear periphery did not lead to an earlier firing timing of subtelomeric origins (**figure 4.15**).

Results

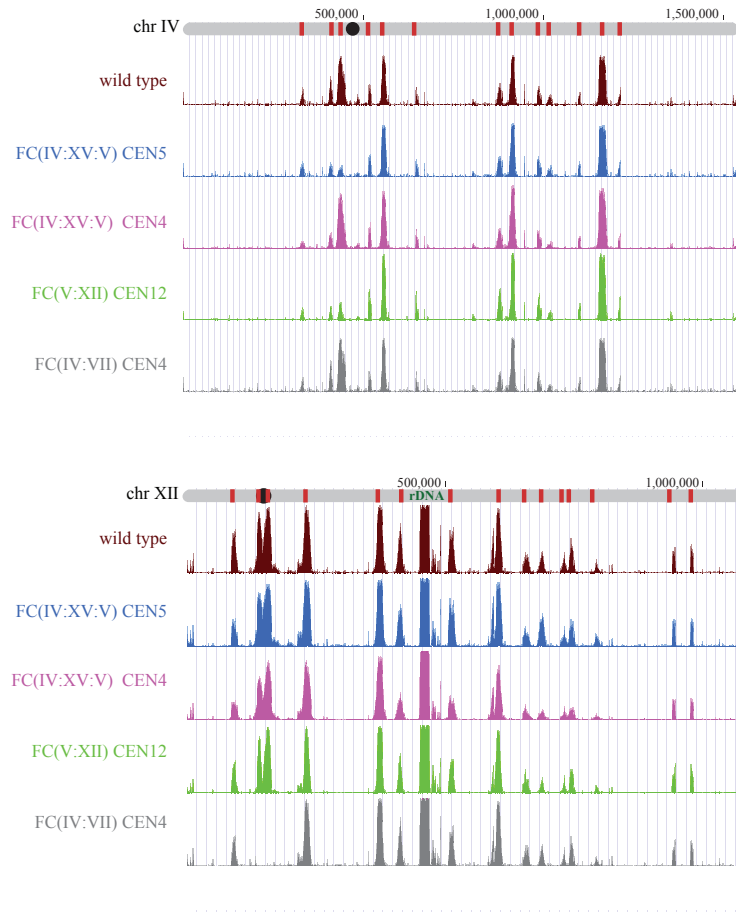


Figure 4.15 Early origins in wild type and fused chromosome strains. Each peak corresponds to BrdU incorporation in presence of HU in the 4 different chromosomes involved in the fusion. The strains tested are: wild type, FC(IV:XII) CEN4, FC (IV:XII) CEN12, FC(IV:XV:V) CEN4, and FC(IV:XV:V) CEN5. (It continues in the next page)

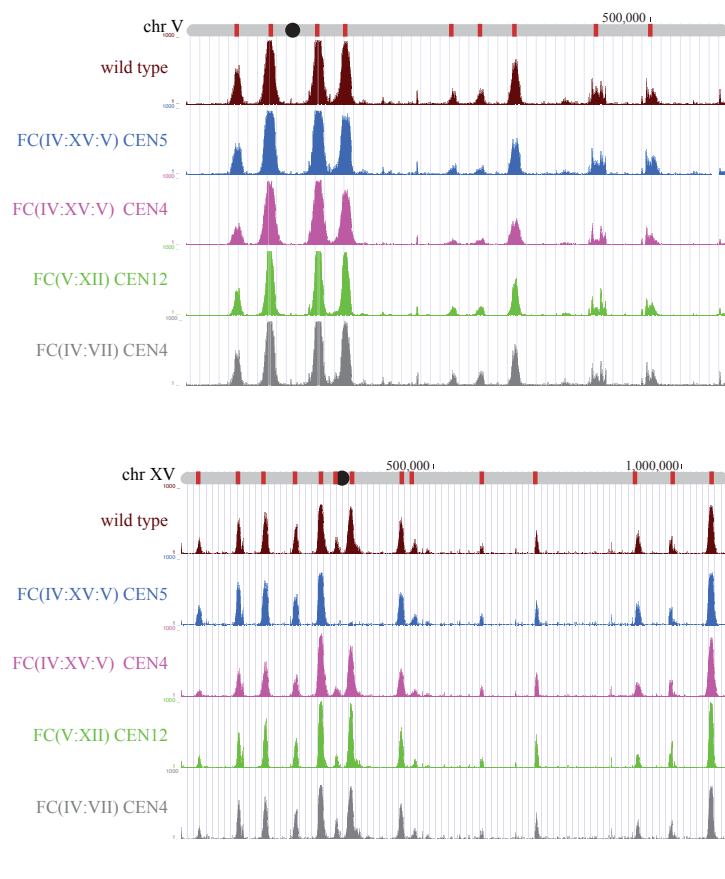


Figure 4.15 Early origins in wild type and fused chromosome strains. Each peak corresponds to BrdU incorporation in presence of HU in the 4 different chromosomes involved in the fusion. The strains tested are: wild type, FC(IV:XII) CEN4, FC (IV:XII) CEN12, FC(IV:XV:V) CEN4, and FC(IV:XV:V) CEN5.

4.4.2 Modeling reproduces clustering of early replicating origins

To assess whether the 3D models could explain the localization of early and late firing origins, we mapped in the ensembles of the polymer models all early origins detected by BrdU-ChIP. Modeling predicts that the localization of the early origins spatially is clustered around the SPB (**Figure 4.16**). This is consistent to the fact that the peri-centromeric origins, which fire always early, represent almost the 25% of all early origins and lie close to the SPB. The late origins, which were identified as the ARS not detected by the BrdU-ChIP, tended to be localized more at the periphery of the nucleus.

Moreover, we observed in the models that the sites corresponding to the early origins were closer to each other compared to the entire sample of sites with the same linear distance (**figure 4.17**). In agreement, late origins were instead farther apart. This result agrees with previous studies [72,176,177] and, interestingly, are true both for wild type and fused chromosome strains.

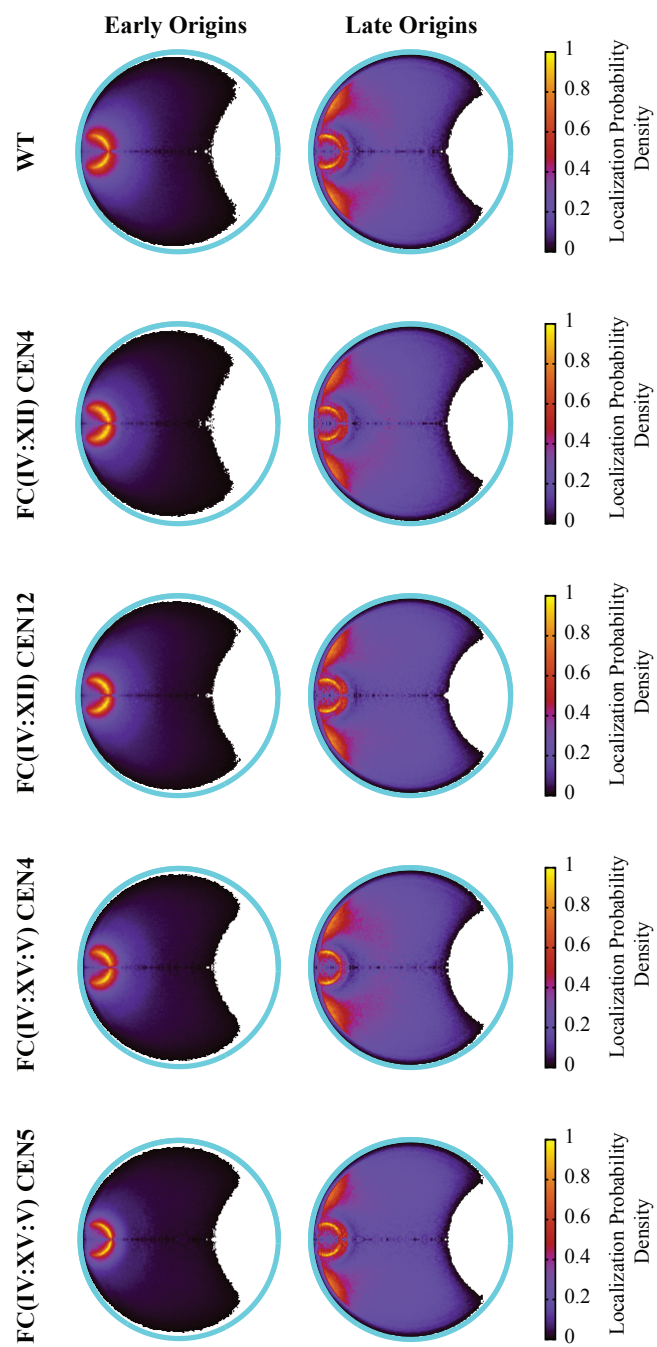


Figure 4.16 Study of early and late origins localization. Heatmaps representing the localization probability density of early (left) and late origins (right).

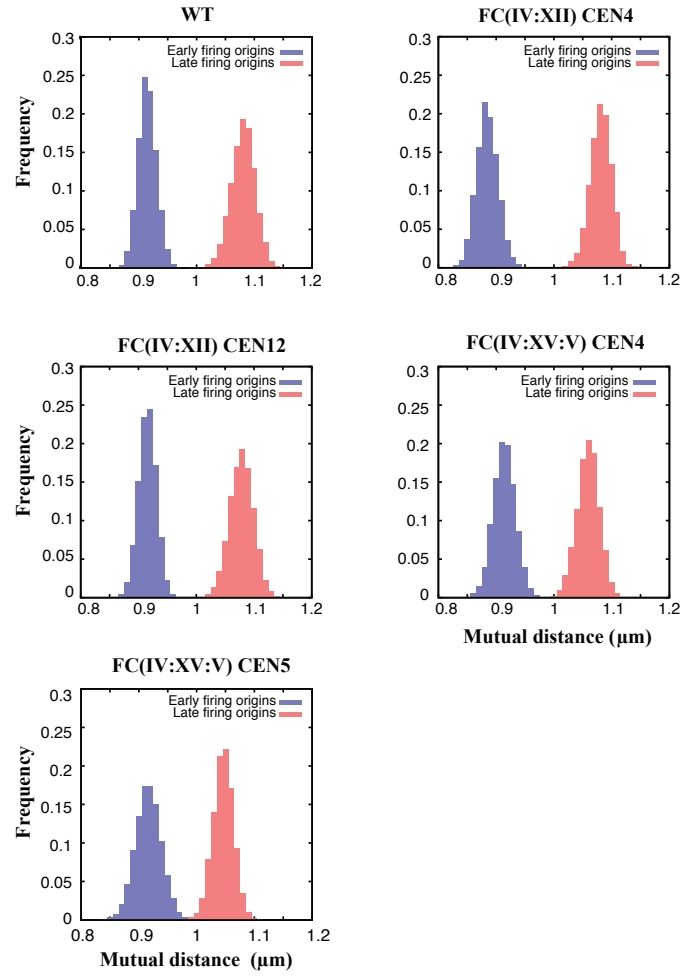


Figure 4.17 Spatial clustering of replication origins. In blue, histograms representing the distribution of the mean pair distance ratio between early replication sites and all sites in the structures of the population. In red, histograms representing the distribution of the mean pair distance ratio between late replication sites and all sites in the structures of the population.

4.5 Analysis of stress response in strains carrying translocations

Our results indicate that big genome rearrangement do not lead to important changes in nuclear processes in optimal growth condition. However, those rearrangements could have an effect in the way cells respond to external conditions. To address whether genome rearrangements have an effect in the response to stress conditions, we performed growth test experiments in triplicates of wild type and 10 different strains carrying fused chromosomes in 20 different stress conditions (**Table 4.3**). Next, we calculated the two parameters, yield and doubling time, (similar to the experiments in chapter 4.1), and compared them between wild type and fused chromosome strains (**Table 4.3**). We noticed that fused chromosome strains react differently compared to wild type in some conditions. In particular, the FC(IV:XV:XVI) CEN4 and FC(IV:XV:XVI) CEN16 did not grow at pH3 (**figure 4.18, 4.19**). And the triple fusions reached a higher yield in H₂O₂, Benomyl, Cycloheximide and MMS, as shown as example for the fusions IV:XV:XVI in **figures 4.18, 4.19**.

In order to test if these differential responses were due to changes in the position of the chromosomes within the nucleus, we tested if the same parameters (growth rate, yield) were changed between strains carrying the same chromosome fusions but with different orientations. The rationale was that chromosome position should be different in these two cases, whereas DNA sequences would be equivalent. In this case the differences did not further hold (**figure 4.20**). The differences observed might thus be due to common

features between the fused chromosomes, other than their nuclear position, such as gene deletions introduced during the generation of chromosome fusions. This result suggests that the genome rearrangements caused by chromosome fusions in our work have no major impact in growth in response to environmental stresses.

	WT	FC(IV:XI D) CEN4	FC(IV:XI D) CEN12	FC(IV:X V) CEN4	FC(IV:X V) CEN15	FC(IV:X V:V) CEN4	FC(IV:X V:V) CEN5	FC(IV:X V:XVI) CEN4	FC(IV:X V:XVI) CEN16
Glucose	2.14 ± 0.21	2.01 ± 0.11	2.19 ± 0.03	2.14 ± 0.15	2.08 ± 0.16	2.35 ± 0.16	2.09 ± 0.05	2.35 ± 0.05	2.09 ± 0.01
Galactose	3.35 ± 0.16	3.10 ± 0.12	3.21 ± 0.06	2.89 ± 0.12	3.07 ± 0.20	3.02 ± 0.20	3.09 ± 0.15	3.15 ± 0.19	3.37 ± 0.13
pH 7.5	2.95 ± 0.34	2.06 ± 0.60	2.17 ± 0.33	1.97 ± 0.06	2.68 ± 0.11	2.20 ± 0.10	2.22 ± 0.05	2.22 ± 0.04	2.37 ± 0.14
pH 3	5.05 ± 0.06	3.57 ± 0.94	3.35 ± 0.81	2.81 ± 0.35	3.88 ± 0.37	4.98 ± 0.08	132.20 ± 0.11	4.31 ± 0.20	137.72 ± 0.37
heat	5.47 ± 1.12	4.85 ± 0.12	4.96 ± 0.18	5.06 ± 0.21	5.19 ± 0.22	5.69 ± 0.31	5.18 ± 0.25	5.20 ± 0.23	5.65 ± 0.24
NaCl	2.67 ± 0.01	2.51 ± 0.08	2.44 ± 0.07	2.40 ± 0.09	2.46 ± 0.10	2.36 ± 0.03	2.41 ± 0.04	2.35 ± 0.05	2.45 ± 0.02
Doxorubicin	2.06 ± 0.03	1.96 ± 0.04	2.05 ± 0.03	1.91 ± 0.04	2.02 ± 0.07	2.03 ± 0.10	1.98 ± 0.05	1.92 ± 0.09	2.02 ± 0.04
Glucose	5.57 ± 0.07	5.37 ± 0.08	6.06 ± 0.16	5.38 ± 0.60	5.37 ± 0.57	5.42 ± 0.50	5.08 ± 0.29	4.89 ± 0.31	5.88 ± 0.29
MMS	1.72 ± 0.04	1.71 ± 0.05	1.76 ± 0.05	1.70 ± 0.04	1.79 ± 0.02	1.83 ± 0.02	1.79 ± 0.04	1.82 ± 0.08	1.80 ± 0.08
Hydroxyurea	7.67 ± 0.03	8.03 ± 0.55	6.95 ± 0.55	7.57 ± 0.51	7.13 ± 0.28	7.31 ± 0.82	8.53 ± 0.83	8.87 ± 0.72	7.66 ± 0.54

Table 4.3: List of the mean and standard deviation of doubling time, representing the speed of growth for wild type and fused chromosome strains in 20 different growth conditions in triplicate. The table continues in the next page.

	WT	FC(IV:XII) CEN4	FC(IV:XII) CEN12	FC(IV:XV) CEN4	FC(IV:XV) CEN15	FC(IV:XV: V) CEN4	FC(IV:XV: V) CEN5	FC(IV:XV: XV1) CEN4	FC(IV:XV: XV1) CEN16
Tunicamycin	6.27 ± 0.80	6.54 ± 0.40	6.34 ± 0.74	6.57 ± 0.55	6.13 ± 2.13	6.12 ± 1.94	6.11 ± 0.96	6.09 ± 1.12	6.38 ± 1.1
CaCl₂	6.71 ± 0.32	6.20 ± 0.65	6.48 ± 0.58	6.21 ± 0.55	7.16 ± 0.83	6.35 ± 0.83	6.56 ± 0.37	6.86 ± 0.35	6.64 ± 0.41
Benomyl	1.46 ± 0.19	1.37 ± 0.41	1.47 ± 0.23	1.39 ± 0.13	1.41 ± 0.15	1.40 ± 0.19	1.37 ± 0.09	1.39 ± 0.18	1.37 ± 0.12
Cycloheximide	1.80 ± 0.05	1.65 ± 0.08	1.85 ± 0.04	1.86 ± 0.03	1.89 ± 0.04	2.11 ± 0.06	2.10 ± 0.04	2.09 ± 0.08	2.01 ± 0.07
Paraquat	6.97 ± 0.14	7.53 ± 0.27	7.06 ± 0.26	7.13 ± 0.27	7.91 ± 0.17	7.79 ± 0.18	7.40 ± 0.09	8.41 ± 0.17	7.99 ± 0.17
Methanol	2.09 ± 0.08	2.02 ± 0.08	2.50 ± 0.50	1.93 ± 0.53	2.12 ± 0.09	1.93 ± 0.30	1.93 ± 0.42	1.93 ± 0.75	1.91 ± 0.82
Glycerol	2.09 ± 0.14	1.97 ± 0.12	2.05 ± 0.08	1.92 ± 0.08	2.01 ± 0.14	2.06 ± 0.14	2.00 ± 0.57	1.95 ± 0.65	2.12 ± 0.68
DTT	1.79 ± 0.03	1.82 ± 0.04	1.84 ± 0.03	1.77 ± 0.04	1.83 ± 0.07	1.85 ± 0.10	1.84 ± 0.05	1.77 ± 0.09	1.86 ± 0.04
LiCl	1.57 ± 0.04	1.59 ± 0.05	1.45 ± 0.05	1.45 ± 0.03	1.45 ± 0.04	1.45 ± 0.04	1.51 ± 0.03	1.36 ± 0.03	1.34 ± 0.02
H₂O₂	6.08 ± 0.07	5.97 ± 0.03	6.24 ± 0.03	6.20 ± 0.06	5.85 ± 0.14	3.98 ± 0.14	3.75 ± 0.11	3.94 ± 0.11	3.70 ± 0.05

Table 4.3: List of the mean and standard deviation of doubling time, representing the speed of growth for wild type and fused chromosome strains in 20 different growth conditions in triplicate.

	WT	FC(IV:XII) CEN4	FC(IV:XII) CEN12	FC(IV:XV) CEN4	FC(IV:XV) CEN15	FC(IV:XV; V) CEN4	FC(IV:XV; V) CEN5	FC(IV:XV; XVI) CEN4	FC(IV:XV; XVI) CEN16
Glucose	1.03 ± 09	1.00 ± 0.14	1.02 ± 0.20	1.02 ± 0.01	1.02 ± 0.08	0.98 ± 0.06	1.13 ± 0.05	1.02 ± 0.07	1.15 ± 0.09
Galactose	1.21 ± 0.03	1.21 ± 0.02	1.20 ± 0.07	1.24 ± 0.02	1.24 ± 0.01	1.26 ± 0.02	1.21 ± 0.07	1.25 ± 0.02	1.21 ± 0.03
pH 7.5	1.12 ± 0.04	1.09 ± 0.02	1.08 ± 0.01	1.08 ± 0.03	1.06 ± 0.03	1.19 ± 0.01	1.17 ± 0.02	1.14 ± 0.02	1.13 ± 0.02
pH 3	0.38 ± 0.02	0.40 ± 0.03	0.41 ± 0.01	0.45 ± 0.06	0.38 ± 0.01	0.39 ± 0.08	0.07 ± 0.01	0.36 ± 0.04	0.07 ± 0.18
heat	0.60 ± 0.20	0.66 ± 0.11	0.70 ± 0.05	0.76 ± 0.06	0.65 ± 0.02	0.62 ± 0.05	0.78 ± 0.29	0.66 ± 0.02	0.63 ± 0.10
NaCl	0.49 ± 0.01	0.51 ± 0.01	0.50 ± 0.01	0.50 ± 0.01	0.50 ± 0.01	0.49 ± 0.01	0.49 ± 0.01	0.50 ± 0.01	0.50 ± 0.01
Doxorubicin	0.96 ± 0.01	1.00 ± 0.03	0.96 ± 0.02	0.96 ± 0.02	0.93 ± 0.01	0.97 ± 0.04	0.95 ± 0.04	0.96 ± 0.03	0.97 ± 0.02
5 FU	0.45 ± 0.01	0.45 ± 0.03	0.44 ± 0.02	0.60 ± 0.02	0.65 ± 0.01	0.63 ± 0.04	0.58 ± 0.04	0.62 ± 0.03	0.61 ± 0.02
MMS	0.62 ± 0.01	0.60 ± 0.01	0.61 ± 0.01	0.59 ± 0.01	0.60 ± 0.01	1.46 ± 0.11	1.31 ± 0.14	1.25 ± 0.14	1.28 ± 0.12
Hydroxyurea	0.30 ± 0.01	0.36 ± 0.01	0.23 ± 0.05	0.30 ± 0.03	0.26 ± 0.03	0.29 ± 0.05	0.25 ± 0.04	0.30 ± 0.03	0.29 ± 0.02

Table 4.4: List of the mean and standard deviation of maximum O.D., representing the yield for wild type and fused chromosome strains in 20 different growth conditions in triplicate. The table continues in the next page.

	WT	FC(IV:XII) CEN4	FC(IV:XII) CEN12	FC(IV:XV) CEN4	FC(IV:XV) CEN5	FC(IV:XV: V) CEN4	FC(IV:XV: V) CEN5	FC(IV:XV: XVI) CEN4	FC(IV:XV: XVI) CEN6
Tunicamycin	0.48 ± 0.04	0.57 ± 0.04	0.61 ± 0.05	0.72 ± 0.06	0.55 ± 0.06	0.62 ± 0.10	0.61 ± 0.09	0.59 ± 0.13	0.54 ± 0.15
CaCl₂	0.59 ± 0.04	0.60 ± 0.08	0.63 ± 0.05	0.62 ± 0.11	0.49 ± 0.05	0.56 ± 0.07	0.61 ± 0.07	0.68 ± 0.05	0.58 ± 0.15
Benomyl	0.70 ± 0.02	0.73 ± 0.02	0.68 ± 0.03	0.67 ± 0.01	0.71 ± 0.04	0.92 ± 0.05	0.89 ± 0.04	0.87 ± 0.05	0.96 ± 0.09
Cycloheximide	0.53 ± 0.02	0.51 ± 0.02	0.53 ± 0.02	0.58 ± 0.02	0.56 ± 0.02	0.86 ± 0.08	0.81 ± 0.03	1.09 ± 0.12	0.83 ± 0.11
Paraquat	0.84 ± 0.03	0.83 ± 0.05	0.82 ± 0.01	0.80 ± 0.05	0.81 ± 0.01	0.77 ± 0.06	0.79 ± 0.04	0.76 ± 0.05	0.76 ± 0.01
Methanol	0.77 ± 0.04	0.77 ± 0.15	0.59 ± 0.12	0.76 ± 0.15	0.72 ± 0.08	0.76 ± 0.09	0.74 ± 0.11	0.73 ± 0.14	0.61 ± 0.17
Glycerol	0.96 ± 0.01	1.00 ± 0.03	0.96 ± 0.02	0.96 ± 0.02	0.93 ± 0.01	0.97 ± 0.04	0.95 ± 0.04	0.96 ± 0.03	0.97 ± 0.02
DTT	0.86 ± 0.01	0.95 ± 0.01	0.92 ± 0.01	0.93 ± 0.01	0.92 ± 0.02	0.85 ± 0.01	0.86 ± 0.02	0.87 ± 0.03	0.93 ± 0.03
LiCl	1.18 ± 0.10	1.10 ± 0.04	1.02 ± 0.03	1.09 ± 0.05	1.08 ± 0.05	1.39 ± 0.05	1.27 ± 0.04	1.30 ± 0.01	1.33 ± 0.01
H₂O₂	0.86 ± 0.04	0.84 ± 0.04	0.84 ± 0.04	0.88 ± 0.03	0.88 ± 0.02	1.11 ± 0.03	1.08 ± 0.03	1.16 ± 0.03	1.06 ± 0.03

Table 4.4: List of the mean and standard deviation of maximum O.D., representing the yield for wild type and fused chromosome strains in 20 different growth conditions in triplicate.

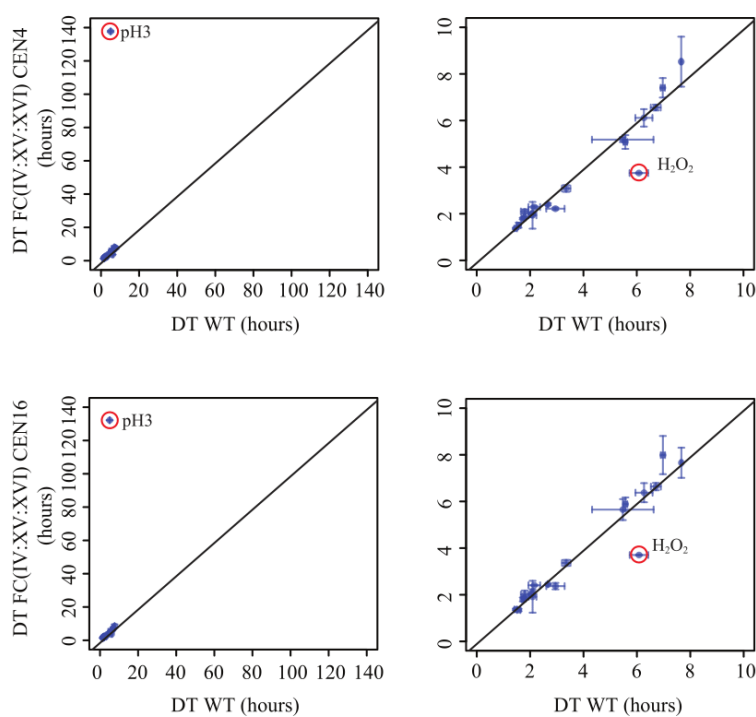


Figure 4.18 Example of comparison of doubling time between fused chromosomes and wild type. Scatterplot comparing the doubling time of wild type and fused chromosomes strains FC(IV:XV:XVI) CEN4, FC(IV:XV:XVI) CEN16, in 20 different conditions (listed in table 4.3). Left, including pH3. Right: excluding pH3.

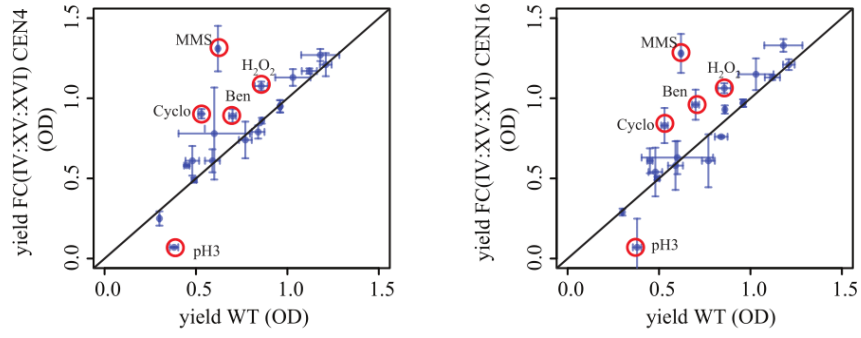


Figure 4.19 Example of comparison of yield between fused chromosomes and wild type. Scatterplot comparing the maximum OD of wild type and FC(IV:XV:XVI) CEN4, FC(IV:XV:XVI) CEN16 in 20 different conditions (listed in table 4.4)

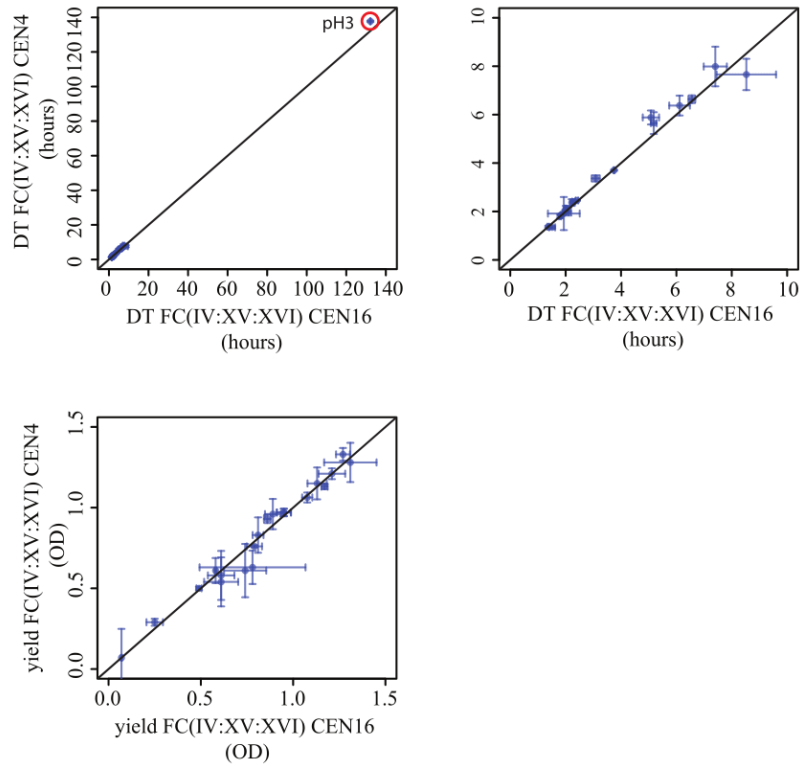


Figure 4.20 Example of comparison of yield between fused chromosomes strains with same fusion and different orientation. Scatterplot comparing the doubling time (top left: including pH3, top right: excluding pH3), and the yield of

FC(IV:XV:XVI) CEN4, FC(IV:XV:XVI) CEN16 in 20 different conditions (listed in table 4.3, 4,4)

5. Discussion

Chromatin structure and its organization within the nuclear space has been of high interest of cellular and developmental biologists for the last century. Although numerous studies have been conducted to search for a link between nuclear structure and function, it remains still controversial the role of chromosome positioning and structural feature of the chromatin in nuclear processes.

In this work we used as model system budding yeast strains carrying chromosomes translocations, in order to study how these chromosomal rearrangements affect important nuclear functions like transcription and replication timing.

To address this question we coupled biological experimental procedures with polymer modeling predictions.

5.1 The yeast genome arrangement is mostly governed by simple physical rules

To study the biological implications of genome rearrangement we took advantage of budding yeast strain carrying chromosome translocations, which are expected to bear big changes in chromosomal distribution.

The generation of chromosome translocations has been done by end-to-end chromosome joining, fusing up to 4 chromosomes together.

Growth test analysis showed that although up to a quarter of the chromosomes has been fused, cells grow at the same speed of the wild type reaching the same yield. This result indicates that budding yeast cells are a very robust system to changes in chromosomes organization.

To predict how chromosomes have changed their position in the nucleus upon fusion, in collaboration with Dr. Marco Di Stefano in Marc A. Marti-Renom laboratory, we have generated polymer models that represent the different chromosome arrangements in the strains carrying fused chromosomes.

The chromosomes models generated in the present study, are only based on few biological constrains: the bead-spring polymer chains are confined in a 1 μ m spherical space mimicking the interphase nuclear volume; centromeres are all cluster together in a pole of the sphere; telomeres stay preferentially at the periphery; and the nucleolus lies on the opposite pole of the centromere cluster [109,176].

The models predict that only the chromosomes that have been fused are affected by a displacement in the nuclear space compared to wild type.

In particular, the models predict three major changes:

- The subtelomeric regions surrounding the joints between the chromosome fused are displaced away from the nuclear periphery into the nuclear interior
- The chromosomes in which the centromere has been deleted are displaced away from the region surrounding the SPB, into regions more distant from the SPB

- Chromosome IV is interested by a change in folding in chromosome fusions where *CEN4* is inactive

Regarding this last point, the distance between loci *TRP1* (12 kb downstream from the centromere) and *LYS4* (in the middle of the long arm) is predicted to be significantly smaller in fused chromosomes strains compared to wild type. These models agree with previous observations in Manuel Mendoza's laboratory where it was observed by imaging an increase in compaction in this region both in FC(IV:XII) *CEN4* and FC(IV:XII) *CEN12* in mitosis [191]. Such increased compaction was found to be dependent on an active mechanism involving Aurora B when *CEN4* was active, but independent of that mechanism when *CEN12* was active. Our study elucidates how this change in folding persists also in interphase. It could be explained by the fact that when the centromere 4 is not active, the region close to the centromere is not being attached anymore to the SPB and therefore not stretched.

Our study elucidates how this change in folding persists also in interphase. It could be explained by the fact that when the centromere 4 is not active, the region close to the centromere is not being attached anymore to the SPB and therefore not stretched.

Importantly, all the modeling predictions mentioned above have been experimentally validated in this study. Therefore, we can conclude then that general features of yeast nuclear organization can be well explained by the physical properties of confined and constrained polymers, combined with the tethering of centromeres, telomeres and nucleolus. It is obviously not possible to rule out the presence of specific interactions of chromatin loci to each other or to nuclear

landmarks, which have not been tested in this study. The picture that polymer modeling gives, is an ensemble of interphase configurations, which does not take into account the biological processes occurring inside the nucleus. More specific factors can in fact shape chromatin, or determine the position and the dynamics of only a subset of loci, such as the relocalization of inducible genes at the nuclear periphery [164,211] and the formation of transcription factories [213].

To study these specific changes in organization and folding, experimental analysis such as high resolution imaging or chromosome conformation capture techniques are needed.

5.2 The impact of chromosome fusion in transcription

Scientists have focused on studying the link between gene transcription and chromatin localization since the two different types of chromatin, euchromatin and heterochromatin, were first observed at the beginning of the 20th century. These two chromatin types indeed correlate with different transcription levels. Euchromatin, is in fact generally more transcribed than heterochromatin, which occupies peripheral regions of the nucleus and is more compacted [15]. Also global expression of chromosome territories correlates with their localization in the nuclear space. In fact, gene-rich CTs, containing more active genes are located preferentially to the nuclear interior, while gene poor CTs and enriched in silent genes are mostly located at the nuclear periphery, similarly to heterochromatin [214]. However, it is unclear if it is transcription that shapes the chromatin, creating domains and territories, or if the chromosome arrangement

is important to regulate transcription, or if there is a contribution from both sides.

To address this question, we studied the transcriptional state of yeast strains carrying a highly altered chromosome distribution compared to wild type.

We performed 4 replicas of RNA-Seq experiments in wildtype and in 10 different fused chromosomes strains. By mapping transcript levels obtained by RNA-Seq in the polymer chains, we could detect the differences in gene expression level along the chromosome and map the position of the corresponding genes in the nuclear space. In particular, the level of RNA expression decreases in proximity of the chromosomes ends and at the nuclear periphery it is significantly lower compared to the interior of the nucleus.

These two evidences are connected to each other since the chromosome telomeres are confined at the nuclear periphery. Their anchorage to the nuclear envelope is mediated by yKu and Sirs proteins and was already known to favor transcriptional repression [156]. Such repression is mediated by the same Sir proteins and was found to be highly dependent on the distance of the reporter genes from telomeres end [153,158,215,216].

Also in metazoans, the role of nuclear periphery in the gene silencing is fully studied. Peripheral CTs, anchored to the inner nuclear envelope have been mapped by DamID, a technique which allowed to map chromatin associated to proteins of the nuclear lamina [58]. These genomic sites, correspond to large domains of chromatin, called LADs, which are characterized by a low transcriptional activity and enriched in repressive chromatin marks. However,

studies done in *Drosophila* in which different reporter genes were artificially anchored to the nuclear periphery showed that in some cases, the reporter was repressed and in others remained active [217-220]. These results suggest that even if perinuclear targeting can lead to gene silencing in some cases, the property of the promoter can also have a strong influence on the transcriptional state of a perinuclear gene.

Chromosome fusions are a good tool to test the impact of telomere detachment from the NE in gene expression, because subtelomeric regions surrounding the joints between the fused chromosomes are displaced away from the nuclear periphery. We could study then the expression level of subtelomeric genes, without interfering with Sir proteins level or telomere anchoring mediated by yKu proteins.

Our transcriptional analysis did not show any significant difference in expression level in fused chromosomes strains compared to wild type.

This discovery is in contraction with the finding that deletion of YKU70 and ESC1, which impaired the attachment of telomeres to the nuclear envelope, causes a derepression of telomere-proximal genes [156].

One explanation for this observation could be that only a subset of subtelomeric genes are actually affected in expression by their proximity to the periphery. The work of Taddei et al. in fact shows that only 3.6 percent of the subtelomeric genes are significantly more expressed compared to wild type condition when the telomere anchoring is disrupted. Moreover, another study described how the association of subtelomeric loci with peripheral telomere clusters

(visualized as Rap1-GFP foci) did not always correlate with their transcriptional state [157].

An alternative explanation is that transcriptional repression does not depend on position per se, but instead on the accessibility to local high concentrations of SIRs [157]. Hence, the delocalization of subtelomeric regions caused by chromosome fusion might still make subtelomeric regions accessible to the pool of Sir proteins. This hypothesis can be tested by performing chromatin immunoprecipitation of histone modifications, to question whether epigenetic state of the subtelomeric regions delocalized from the periphery in fused strains changes compared to wild type.

Moreover, RNA-Seq experiments have been conducted in log phase cell populations, and maybe this could have led to a lack of sensitivity for small changes in interphase gene expression. To address this question, it could be useful to compare the expression levels in wild type and fused chromosomes strains synchronized in specific cell cycle stages. Overall, however, our results suggest that perinuclear association is dispensable for silencing of genes near telomeres in yeast.

Our findings are based on transcriptional analysis of budding yeast strains in optimal growth conditions. Since it is known that specific localization of genes in the nucleus can dramatically change in response to stimuli [164,172,211], we tested the phenotypic effect of genome repositioning in stress conditions.

We showed that in presence of low pH two particular strains in which chromosomes IV, XV and XVI have been fused are not able to

growth, on the contrary of the wild type and other fused chromosomes strains tested. Since the position of the chromosomes in the two fusion is highly different both from wild type and from each other, we cannot conclude that the changing in chromosomes positioning is the cause for the difference response. The chromosome fusion itself implies the deletion of subtelomeric genes whose expression could play a role in stress response the low pH. A control experiment could be the deletion of those genes from a wild type strain and testing its growth in low pH. Unfortunately, the highly repetitive regions close to telomeres make difficult the deletion of those genes.

The change in stress response could also be due to the dislocation from the nuclear periphery of specific loci close to the chromosomes joints. To test this possibility, it should be possible to insert the loci that get delocalized in the fused chromosomes in a chromosome region that is known to be mostly in the nuclear interior and analyze cell growth in low pH.

In four stress conditions (H_2O_2 , Benomyl, Cycloheximide and MMS) strains carrying three chromosomes fused together reached a higher yield compared to wild type. Since there is not significant difference between strains carrying the same fusion and different centromere active, we again hypothesize that the different response can be due to the lack of genes close to the joining.

5.3 Chromosome positioning and replication timing

Replication timing is also correlated with nuclear organization.

Early replication origins are in fact placed in the interior of the eukaryotic nucleus, while late replicating DNA is more peripheral. This difference in positioning is conserved during development. During stem cell differentiation, has been observed using FISH that chromatin domains move toward the periphery have been detected when replication timing becomes late, while toward the interior when it becomes early [88,221].

Another example of correlation between replication timing and chromatin position is represented by X-chromosome inactivation. In this process, the entire chromosome gets displaced to the nuclear periphery and increases its compaction. All those conformational changes are also accompanied by a chromosome switch to late replication [222].

The compartmentalization of late origins in the periphery appears to be the results of the anchorage of chromatin to nuclear periphery and nucleolus [223,224] or nucleolus [225]. But whether or not this compartmentalization is important for replication timing is still unclear.

We wonder whether chromosomal rearrangements have an impact on replication timing. By mapping the loci corresponding to the early origins in the chromosomes models we show that they tend to cluster together, unlike the late ones, as already reported by several works [175-177].

Functional centromeres have been shown to promote the early activation of proximal origins in *S. cerevisiae*. This effect could either be sequence dependent or due to the clustering of centromere proximal origins close to the SPB. In FC(IV:XII) CEN4 and FC(IV:XII) CEN4 the origins close to the centromere which have been deleted, suffered from a delay in replication firing, confirming that an active centromere is responsible for early firing ARS in a 20 kb window. Surprisingly, analyzing the BrdU profiles of the strains in which three chromosomes are fused together (IV, XV and V) we could not appreciate a delay in firing due to the lack of centromeric sequences in chromosomes V and XV. A possible explanation to this observation could be that in the strains FC(IV:XV:V) the ARSs proximal to *CEN15* and *CEN5*, fall in a nuclear region where other origins fire early with a non-centromeric dependent mechanism. In fact, non-centromeric early origins tend also to cluster together, but with a different mechanism which is dependent of Fkh proteins. This hypothesis could then be then tested by studying the firing timing of those origins in a strain depleted from Fhks. Moreover, chromosome conformation capture techniques and Chromatin-IP, can help to test the eventual proximity of specific ARS loci among each other, or their binding to Fkh proteins, respectively.

It has been proposed that the late firing of ARSs close to telomeres, is dependent on the localization of subtelomeric chromatin at the nuclear periphery. In fact, a previous study showed that the insertion of an early origin (ARS1) into a subtelomeric region, caused its delay in firing in a SIR-dependent manner [182]. In addition, the deletion

of YKU70, responsible of telomeric anchoring to the NE was shown to advanced replication timing of subtelomeric origins. [181].

The BrdU experiments described in this study show that the proximity to periphery does not affect the origin firing timing. In fact, in chromosomes predicted and confirmed to be delocalized from the periphery do not appear additional BrdU peaks, which would have corresponded to an advanced firing of telomere proximal ARS. But the significance of compartmentalization to the replication timing program remains however unclear. In fact, it has been seen that tethering of budding yeast ARS305 and ARS607 to nuclear envelope does not delay in their firing timing [226,227].

Moreover, another experiment done in yeast cells demonstrated that telomeres detached from the nuclear periphery still replicate late, suggesting that peripheral positioning in interphase is not necessary for late DNA replication of chromosome ends [228].

Genome wide experiments performed in this work provide evidence that chromosome positioning does not play an essential role in the regulation of important nuclear processes in budding yeast. However, it has still an open question whether an altered chromosomal configuration, such the one generated by chromosome fusion, could affect gene repositioning upon transcriptional activation.

6. Conclusions

The presented work led to the following major conclusions:

- Chromosome fusion leads to changes in chromosome organization in budding yeast.
- Budding yeast chromosome configuration reproduced by polymer models is sufficient to describe specific changes in chromosome organization caused by chromosome fusion.
- Chromosomal rearrangements derived from chromosome fusion do not lead to changes in transcription in budding yeast.
- Chromosomes fusions are affected by changes in firing of some origins, but not dependent on chromosome positioning.
- Responses to stress conditions are not affected by chromosomal rearrangement in budding yeast.

7. Future directions

The results provided by this work open up new questions in the field:

- We showed how polymer modelling can predict specific changes in chromosome positioning upon chromosome fusions. It is important to note that although models used in this work are remarkably accurate in predicting large-scale chromosome positioning, they do not intend to reproduce detailed aspects of chromosome behaviour. Models do, however, reproduce previous observations for which no mechanism had been proposed. Specifically, it is known that the centromere-proximal region of FC(IV:XII) CEN4 undergoes hypercompaction in mitosis in order to segregate during mitosis. This mechanism is dependent on Aurora B activity and Condensin (Neurohr ref). The same region in FC(IV:XII) CEN12 is also hypercompacted but this change in folding is not specific to mitosis, and does not depend on Aurora-B. Our models reproduce this hypercompaction, raising the possibility that this stems not from specific regulation but from the physical properties of the confined chromosomes. It would be interesting to study how these two chromosomes differ in folding by using polymer modelling coupled with molecular biology techniques, like Hi-C which allows to study in high resolution specific changes in folding.

- Genome rearrangements carried by fused chromosome strains do not lead to changes in transcription in log phase growing cells. It remains still possible that in specific cell cycle stages chromosomes rearrangements cause differences in expression of genes in loci that are displaced from a wild type condition. This question can be addressed by performing a transcriptional analysis of cells synchronized in specific cell cycle stages.
- Gene expression might be affected by larger changes in chromosome arrangement, which can be tested by studying transcription levels in strains carrying more or different chromosomes fused together.
- The lack of transcriptional response to genome rearrangement could be explained by the fact that the chromatin, which gets displaced in fused chromosome strains, keeps the same epigenetic state. This hypothesis can be tested by comparing the epigenetic changes of histones and DNA markers of wild type and fused chromosome strains using chromatin immunoprecipitation.
- Replication origins close to deleted centromeres in FC(IV:XV:V) CEN4 and FC(IV:XV:V) CEN5 fire still early although they are expected to delay their replication, because

they are far from an active centromere. The hypothesis that they can fall in Fkhs-dependent early replicating cluster can be tested by performing BrdU-IP experiments in Fhk deleted cells. Their clustering can be tested by microscopy or by Hi-C.

- The reported difference in stress response is dependent on the fusion but not on the orientation of the fusion. Hence, it can be due either to the loss of genes during the generation of the fused chromosome strains or to the fact that the regions surrounding the joint-ends of the fused chromosomes are displaced from the nuclear periphery. This question can be addressed by performing growth tests in a wild type strain in which regions known to be displaced in fused chromosome strains are translocated in chromosomal domains known to be in the interior of the nucleus.

8. Bibliography

- [1] J. Watson and F. Crick, "Molecular structure of nucleic acid" *Nature*, vol. 171, pp. 737–738, 1953
- [2] R. E. Franklin and R. G. Gosling, "Molecular configuration in sodium thymonucleate," *Nature*, vol. 171, pp. 741,740, 1953
- [3] R. D. Kornberg, "Chromatin Structure: A Repeating Unit of Histones and DNA," *Science*, vol. 184, pp. 3–6, 1974.
- [4] J. Bednar, R. A. Horowitz, J. Dubochet, and C. L. Woodcock, "Chromatin Conformation and Salt-induced Compaction: Three-dimensional Structural Information from Cryoelectron Microscopy," *Journal of Cell Biology*, vol. 131, no. 6, pp. 1365–1376, 1995.
- [5] J. T. Finch and A. Klug, "Solenoidal model for superstructure in chromatin," *Proceedings of the National Academy of Sciences of the United States of America*, vol. 73, no. 6, pp. 1897–1901, 1976.
- [6] D. J. Tremethick, "Higher-Order Structures of Chromatin: The Elusive 30 nm Fiber," *Cell*, pp. 2005–2008, 2007.
- [7] T. Schalch, S. Duda, D. F. Sargent, and T. J. Richmond, "X-ray structure of a tetranucleosome and its implications for the chromatin fibre," vol. 436, no. July, pp. 7–10, 2005.
- [8] K. Maeshima, R. Imai, S. Tamura, and T. Nozaki, "Chromatin as dynamic 10-nm fibers," *Chromosoma*, vol. 123, pp. 225–237, 2014.
- [9] J. Dekker, "Mapping in Vivo Chromatin Interactions in Yeast Suggests an Extended Chromatin Fiber with Regional Variation in Compaction," vol. 283, no. 50, pp. 34532–34540, 2008.
- [10] M. Eltsov, K. M. Maclellan, K. Maeshima, A. S. Frangakis, and J. Dubochet, "Analysis of cryo-electron microscopy images does not support the existence of 30-nm chromatin fibers in mitotic chromosomes in situ," pp. 1–6, 2008.
- [11] M. A. Ricci, C. Manzo, M. Lakadamyali, and M. P. Cosma, "Chromatin Fibers Are Formed by Heterogeneous Groups of

Nucleosomes In Vivo Article Chromatin Fibers Are Formed by Heterogeneous Groups of Nucleosomes In Vivo,” *Cell*, pp. 1145–1158, 2015.

[12] E. Heitz, “Das heterochromatin der moose,” *I Jahrb wiss Bot*, vol. 69, pp. 762–818., 1928.

[13] J H Frenster, V. G. Allfrey, and A. E. Mirsky, “Repressed and Active Chromatin Isolated From Interphase Lymphocytes.,” *Proceedings of the National Academy of Sciences of the United States of America*, vol. 50, pp. 1026–32, 1963.

[14] K. L. Huisinga, B. Brower-Toland, and S. C. R. Elgin, “The contradictory definitions of heterochromatin: Transcription and silencing,” *Chromosoma*, vol. 115, no. 2, pp. 110–122, 2006.

[15] S. I. S. Grewal and S. Jia, “Heterochromatin revisited,” *Nature reviews. Genetics*, vol. 8, no. 1, pp. 35–46, 2007.

[16] P. Trojer and D. Reinberg, “Facultative Heterochromatin: Is There a Distinctive Molecular Signature?,” *Molecular Cell*, vol. 28, no. 1, pp. 1– 13, 2007.

[17] K. L. Jost, B. Bertulat, and M. C. Cardoso, “Heterochromatin and gene positioning: Inside, outside, any side?,” *Chromosoma*, vol. 121, no. 6, pp. 555–563, 2012.

[18] N. Sadoni, K. Sullivan, P. Weinzierl, E. Stelzer, and D. Zink, “Large-scale chromatin fibers of living cells display a discontinuous functional organization,” *Chromosoma*, vol. 110, no. 1, pp. 39–51, 2001.

[19] P. J. Verschure, I. van der Kraan, E. M. Manders, D. Hoogstraten, A. B. Houtsmuller, and R. van Driel, “Condensed chromatin domains in the mammalian nucleus are accessible to large macromolecules,” *EMBO Rep*, vol. 4, no. 9, pp. 861–866, 2003.

[20] J. A. Croft, J. M. Bridger, S. Boyle, P. Perry, P. Teague, and W. A. Bickmore, “Differences in the localization and morphology of chromosomes in the human nucleus,” *Journal of Cell Biology*, vol. 145, no. 6, pp. 1119–1131, 1999.

[21] M. Cremer, K. Küpper, B. Wagler, L. Wizelman, J. V. Hase, Y. Weiland, L. Kreja, J. Diebold, M. R. Speicher, and T. Cremer, “Inheritance of gene density-related higher order chromatin arrangements in normal and tumor cell nuclei,” *Journal of Cell Biology*, vol. 162, no. 5, pp. 809– 820, 2003.

- [22] H. Tanabe, K. Kupper, T. Ishida, M. Neusser, and H. Mizusawa, "Inter- and intra-specific gene-density-correlated radial chromosome territory arrangements are conserved in Old World monkeys," *Cytogenetic and Genome Research*, vol. 108, no. 1-3, pp. 255–261, 2005.
- [23] H. Tanabe, S. Müller, M. Neusser, J. von Hase, E. Calcagno, M. Cremer, I. Solovei, C. Cremer, and T. Cremer, "Evolutionary conservation of chromosome territory arrangements in cell nuclei from higher primates," *Proceedings of the National Academy of Sciences of the United States of America*, vol. 99, no. 7, pp. 4424–9, 2002.
- [24] F. A. Habermann, M. Cremer, J. Walter, G. Kreth, J. Von Hase, K. Bauer, J. Wienberg, C. Cremer, T. Cremer, and I. Solovei, "Arrangements of macro- and microchromosomes in chicken cells," *Chromosome Research*, vol. 9, no. 7, pp. 569–584, 2001.
- [25] H. Tanabe, F. A. Habermann, I. Solovei, M. Cremer, and T. Cremer, "Non-random radial arrangements of interphase chromosome territories: Evolutionary considerations and functional implications," *Mutation Research - Fundamental and Molecular Mechanisms of Mutagenesis*, vol. 504, no. 1-2, pp. 37–45, 2002.
- [26] D. Zink, M. D. Amaral, A. Englmann, S. Lang, L. A. Clarke, C. Rudolph, F. Alt, K. Luther, C. Braz, N. Sadoni, J. Rosenecker, and D. Schindelhauer, "Transcription-dependent spatial arrangements of CFTR and adjacent genes in human cell nuclei," *Journal of Cell Biology*, vol. 166, no. 6, pp. 815–825, 2004.
- [27] A. K. Csink and S. Henikoff, "Genetic modification of heterochromatic association and nuclear organization in *Drosophila*," *Nature* 381, 529–531 (1996).
- [28] A. F. Dernburg, K. W. Broman, J. C. Fung, W. F. Marshall, J. Philips, D. A. Agard, and J. W. Sedat, "Perturbation of Nuclear Architecture by Long-Distance Chromosome Interactions," *Cell*, vol. 85, pp. 745–759, 1996.
- [29] K. Ayyanathan, M. S. Lechner, P. Bell, G. G. Maul, D. C. Schultz, Y. Yamada, K. Tanaka, K. Torigoe, and F. J. R. Iii, "Regulated recruitment of HP1 to a euchromatic gene induces mitotically heritable, epigenetic gene silencing: a mammalian cell culture model of gene variegation," *Genes & development*, pp. 1855–1869, 2003.
- [30] K. E. Brown, J. Baxter, D. Graf, M. Merkenschlager, and A. G. Fisher, "Dynamic Repositioning of Genes in the Nucleus of Lympho-

cytes Preparing for Cell Division,” *Molecular Cell*, vol. 3, pp. 207–217, 1999.

[31] K. E. Brown, S. S. Guest, S. T. Smale, K. Hahm, M. Merken- schlager, and A. G. Fisher, “Association of Transcriptionally Silent Genes with Ikaros Complexes at Centromeric Heterochromatin,” *Cell*, vol. 91, pp. 845–854, 1997.

[32] C-H. Chuang, A. E. Carpenter, B. Fuchsova, T. Johnson, P. D. Lanerolle, and A. S. Belmont, “Long-Range Directional Movement of an Interphase Chromosome Site,” *Current Biology*, pp. 825–831, 2006.

[33] S. L. Hewitt, F. A. High, S. L. Reiner, A. G. Fisher, and M. Merken- schlager, “Nuclear repositioning marks the selective exclusion of lineage-inappropriate transcription factor loci during T helper cell dif- ferentiation,” *European Journal of Immunology*, pp. 3604–3613, 2004.

[34] C. Rabl, “Über Zellteilung,” *Morphologisches Jahrbuch*, vol. 10, pp. 214–330, 1885.

[35] T. Boveri, “Die Blastomerenkerne von *Ascaris megalocephala* und die Theorie der Chromosomenindividualität,” *t. Arch Zellforschung*, p. 3: 181, 1909.

[36] L. Manuelidis, “1985. Individual interphase chromosome domains revealed by in situ hybridization,” *Hum Genet*, vol. 71, pp. 288–293, 1985.

[37] M. Schardin, T. Cremer, H. Hager, and L. M., “Specific staining of human chromosomes in Chinese hamster x man hybrid cell lines demonstrates interphase chromosome territories,” *Hum Genet*, vol. 71, pp. 281 – 287, 1985.

[38] P. R. Langer-safer, M. Levine, and D. C. Ward, “Immunological method for mapping genes on *Drosophila* polytene chromosomes,” *vol. 79, no. July*, pp. 4381–4385, 1982.

[39] M. R. Speicher and N. P. Carter, “The new cytogenetics: blurring the boundaries with molecular biology,” *Nature reviews. Genetics*, vol. 6, pp. 782–792, 2005.

[40] A. Rosa and R. Everaers, “Structure and Dynamics of Interphase Chromosomes,” *PLoS Computational Biology*, vol. 4, no. 8, 2008.

[41] M. R. Branco and A. Pombo, “Intermingling of chromosome territories in interphase suggests role in translocations and

transcription-dependent associations,” *PLoS Biology*, vol. 4, no. 5, pp. 780–788, 2006.

[42] R. Mayer, A. Brero, J. von Hase, T. Schroeder, T. Cremer, and S. Dietzel, “Common themes and cell type specific variations of higher order chromatin arrangements in the mouse,” *BMC cell biology*, vol. 6, no. 1, p. 44, 2005.

[43] S. Stadler, V. Schnapp, R. Mayer, S. Stein, C. Cremer, C. Bonifer, T. Cremer, and S. Dietzel, “The architecture of chicken chromosome territories changes during differentiation,” *BMC cell biology*, vol. 5, no. 1, p. 44, 2004.

[44] J. Dekker, K. Rippe, M. Dekker, and N. Kleckner, “Capturing Chromosome Conformation,” *Science*, vol. 295, pp. 1306–1311, 2002.

[45] R. Kalhor, H. Tjong, N. Jayathilaka, F. Alber, and L. Chen, “Genome architectures revealed by tethered chromosome conformation capture and population-based modeling,” *Nature Biotechnology*, vol. 30, no. 1, pp. 90–98, 2011.

[46] E. Lieberman-aiden, N. L. V. Berkum, L. Williams, T. Ragoczy, A. Telling, I. Amit, B. R. Lajoie, J. Peter, M. O. Dorschner, R. Sandstrom, B. Bernstein, M. Groudine, A. Gnirke, J. Stamatoyannopoulos, and A. Leonid, “Comprehensive mapping of long range interactions reveals folding principles of the human genome,” *Science*, vol. 326, no. 5950, pp. 289–293, 2009.

[47] T. Sexton, E. Yaffe, E. Kenigsberg, F. Bantignies, B. Leblanc, M. Hoichman, H. Parrinello, A. Tanay, and G. Cavalli, “Three-Dimensional Folding and Functional Organization Principles of the *Drosophila* Genome,” *Cell*, vol. 148, pp. 458–472, 2012.

[48] Y. Zhang, R. P. Mccord, Y.-j. Ho, B. R. Lajoie, D. G. Hildebrand, A. C. Simon, M. S. Becker, F. W. Alt, and J. Dekker, “Spatial Organization of the Mouse Genome and Its Role in Recurrent Chromosomal Translocations,” *Cell*, vol. 148, no. 5, pp. 908–921, 2012.

[49] M. Simonis, P. Klous, E. Splinter, Y. Moshkin, R. Willemsen, E. D. Wit, B. V. Steensel, and W. D. Laat, “Nuclear organization of active and inactive chromatin domains uncovered by chromosome coformation capture-on-chip (4C),” *nature genetics*, vol. 38, no. 11, pp. 1348–1354, 2006.

[50] E. Yaffe and A. Tanay, “Probabilistic modeling of Hi-C contact

maps eliminates systematic biases to characterize global chromosomal architecture,” *Nature Genetics*, vol. 43, no. 11, pp. 1059–1065, 2011.

[51] N. L. Mahy, P. E. Perry, and W. A. Bickmore, “Gene density and transcription influence the localization of chromatin outside of chromosome territories detectable by FISH,” *Journal of Cell Biology*, vol. 159, no. 5, pp. 753–763, 2002.

[52] S. Schoenfelder, T. Sexton, L. Chakalova, N. F. Cope, A. Horton, S. Andrews, S. Kurukuti, J. A. Mitchell, D. Umlauf, D. S. Dimitrova, C. H. Eskiw, Y. Luo, C.-l. Wei, Y. Ruan, J. J. Bieker, and P. Fraser, “Preferential associations between co-regulated genes reveal a transcriptional interactome in erythroid cells,” *Nature Genetics*, vol. 42, no. 1, pp. 53–61, 2009.

[53] J. M. Brown, J. Green, R. Pires, H. A. C. Wallace, A. J. H. Smith, J. Hughes, N. Gray, S. Taylor, W. G. Wood, D. R. Higgs, F. J. Iborra, and V. J. Buckle, “Association between active genes occurs at nuclear speckles and is modulated by chromatin environment,” *Journal of Cell Biology*, vol. 182, no. 6, pp. 1083–1097, 2008.

[54] H. Sutherland and W. A. Bickmore, “Transcription factories: gene expression in unions?,” *Nature reviews. Genetics*, vol. 10, no. 7, pp. 457–466, 2009.

[55] C. Morey, C. Kress, and W. A. Bickmore, “Lack of bystander activation shows that localization exterior to chromosome territories is not sufficient to up-regulate gene expression,” *Genome Research*, pp. 1184–1194, 2009.

[56] I. I. Cisse, I. Izeddin, S. Z. Causse, L. Boudarene, A. Senecal, L. Murean, C. Dugast-Darzacq, B. Hajj, M. Dahan, and X. Darzacq, “Real-Time Dynamics of RNA Polymerase II Clustering in Live Human Cells,” *Science*, vol. 341, no. 8, pp. 664–667, 2013.

[57] B. V. Steensel and S. Henikoff, “Identification of in vivo DNA targets of chromatin proteins using tethered Dam methyltransferase,” *Nature Biotechnology*, vol. 18, no. April, 2000.

[58] L. Guelen, L. Pagie, E. Brasset, W. Meuleman, M. B. Faza, W. Talhout, and B. H. Eussen, “Domain organization of human chromosomes revealed by mapping of nuclear lamina interactions,” *Nature*, vol. 453, no. June, pp. 1–5, 2008.

[59] R. D. Goldman, Y. Gruenbaum, R. D. Moir, D. K. Shumaker, and T. P. Spann, “Nuclear lamins: building blocks of nuclear

architecture,” *Genes & development*, vol. 16, pp. 533–547, 2002.

[60] M. Prokocimer, M. Davidovich, M. Nissim-rafania, N. Wiesel-motiuk, D. Z. Bar, R. Barkan, E. Meshorer, and Y. Gruenbaum, “Nuclear lamins: key regulators of nuclear structure and activities,” *J. Cell. Mol. Med.*, vol. 13, no. 6, pp. 1059–1085, 2009.

[61] S. Belmont, Y. Zhai, and A. Thilenius, “Lamin B Distribution and Association with Peripheral Chromatin Revealed by Optical Sectioning and Electron Microscopy Tomography Sample Preparation for Electron Microscopy,” *Journal of Cell Biology*, vol. 123, no. 6, pp. 1671–1685, 1993.

[62] A. Akhtar and S. M. Gasser, “The nuclear envelope and transcriptional control,” *Nature reviews. Genetics*, vol. 8, no. July, pp. 507–517, 2007.

[63] H. Pickersgill, B. Kalverda, E. D. Wit, W. Talhout, and M. Fornerod, “Characterization of the *Drosophila melanogaster* genome at the nuclear lamina,” *Nature genetics*, vol. 38, no. 9, pp. 1005–1014, 2006.

[64] D. Peric-hupkes, W. Meuleman, L. Pagie, S. W. M. Bruggeman, I. Solovei, W. Brugman, P. Flicek, R. M. Kerkhoven, M. V. Lohuizen, M. Reinders, and L. Wessels, “Article Molecular Maps of the Reorganization of Genome-Nuclear Lamina Interactions during Differentiation,” pp. 603–613, 2010.

[65] J. Kind, L. Pagie, H. Ortazokoyun, S. Boyle, S. S. D. Vries, H. Janssen, M. Amendola, L. D. Nolen, W. A. Bickmore, and B. V. Steensel, “Single-Cell Dynamics of Genome-Nuclear Lamina Interactions,” *Cell*, vol. 153, no. 1, pp. 178–192, 2013.

[66] W. Meuleman, D. Peric-hupkes, J. Kind, J.-b. Beaudry, L. Pagie, M. Kellis, M. Reinders, L. Wessels, and B. V. Steensel, “Constitutive nuclear lamina â genome interactions are highly conserved and associated with A/T-rich sequence,” *Genome Research*, pp. 270–280, 2013.

[67] J. Kind, L. Pagie, S. S. D. Vries, J. Dekker, A. V. Oudenaarden, J. Kind, L. Pagie, S. S. D. Vries, L. Nahidiazar, S. S. Dey, M. Bienko, and Y. Zhan, “Genome-wide Maps of Nuclear Lamina Interactions in Single Human Cells Article Genome-wide Maps of Nuclear Lamina Interactions in Single Human Cells,” *Cell*, vol. 163, pp. 1–14, 2015.

[68] B. Tolhuis, R.-j. Palstra, E. Splinter, F. Grosveld, and W. D.

Laat, "Looping and Interaction between Hypersensitive Sites in the Active β -globin Locus," *Molecular Cell*, vol. 10, pp. 1453–1465, 2002.

[69] E. Crane, Q. Bian, R. P. Mccord, B. R. Lajoie, B. S. Wheeler, E. J. Ralston, S. Uzawa, J. Dekker, and B. J. Meyer, "Condensin-driven remodelling of X chromosome topology during dosage compensation," *Nature*, vol. 523, pp. 240–244, 2015.

[70] M. Guidi, M. Ruault, M. Marbouty, I. Loïdodice, A. Cournac, C. Bil-laudeau, A. Hoher, J. Mozziconacci, R. Koszul, and A. Taddei, "Spatial reorganization of telomeres in long-lived quiescent cells," *Genome Biology*, vol. 16, no. 1, p. 206, 2015.

[71] C. D. M. Rodley, F. Bertels, B. Jones, and J. M. O. Sullivan, "Global identification of yeast chromosome interactions using Genome conformation capture," *Fungal Genetics and Biology*, vol. 46, no. 11, pp. 879–886, 2009.

[72] Z. Duan, M. Andronescu, K. Schutz, S. Mcilwain, Y. J. Kim, C. Lee, J. Shendure, S. Fields, C. A. Blau, and W. S. Noble, "A three-dimensional model of the yeast genome," *Nature*, vol. 465, no. 7296, pp. 363–367, 2010.

[73] C. Hou, L. Li, Z. S. Qin, and V. G. Corces, "Resource Gene Density, Transcription, and Insulators Contribute to the Partition of the *Drosophila* Genome into Physical Domains," *Molecular Cell*, vol. 48, pp. 471–484, 2012.

[74] R. S. Grand, T. Pichugina, L. R. Gehlen, M. B. Jones, P. Tsai, J. R. Allison, R. Martienssen, and J. M. O. Sullivan, "Chromosome conformation maps in fission yeast reveal cell cycle dependent sub nuclear structure," *Nucleic Acids Research*, vol. 42, no. 20, pp. 12585–12599, 2014.

[75] T. Mizuguchi, J. Barrowman, and S. I. S. Grewal, "Chromosome domain architecture and dynamic organization of the fission yeast genome," *FEBS LETTERS*, vol. 589, pp. 2975–2986, 2015.

[76] E. Splinter, E. De Wit, P. Nora, P. Klous, H. J. G. Van De Werken, Y. Zhu, L. J. T. Kaaij, W. Van Ijcken, J. Gribnau, E. Heard, and W. De Laat, "The inactive X chromosome adopts a unique three-dimensional conformation that is dependent on Xist RNA," *Genes & development*, pp. 1371–1383, 2011.

[77] T. Nagano, Y. Lubling, T. J. Stevens, S. Schoenfelder, E. Yaffe, W. Dean, E. D. Laue, A. Tanay, and P. Fraser, "Single-cell Hi-C

reveals cell-to-cell variability in chromosome structure,” *Nature*, vol. 502, pp. 59–64, 2013.

[78] J. R. Dixon, S. Selvaraj, F. Yue, A. Kim, Y. Li, Y. Shen, M. Hu, J. S. Liu, and B. Ren, “Topological domains in mammalian genomes identified by analysis of chromatin interactions,” *Nature*, vol. 485, no. 7398, pp. 376–380, 2012.

[79] E. P. Nora, B. R. Lajoie, E. G. Schulz, L. Giorgetti, I. Okamoto, S. Nicolas, T. Piolot, N. L. Van Berkum, J. Meisig, J. Sedat, J. Gribnau, E. Barillot, N. Bluthgen, J. Dekker, and E. Heard, “Spatial partitioning of the regulatory landscape of the X-inactivation centre,” *Nature*, vol. 485, pp. 381–385, 2012.

[80] T. B. K. Le, M. V. Imakaev, L. A. Mirny, and M. T. Laub, “High-Resolution Mapping of the Spatial Organization of a Bacterial Chromosome,” *Science*, vol. 342, pp. 731–734, 2013.

[81] S. Sofueva, E. Yaffe, W.-c. Chan, D. Georgopoulou, M. V. Rudan, S. M. Pollard, G. P. Schroth, A. Tanay, and S. Hadjur, “Cohesin-mediated interactions organize chromosomal domain architecture,” *The EMBO Journal*, vol. 32, no. 24, pp. 3119–3129, 2013.

[82] J. Zuin, J. R. Dixon, M. I. J. A. V. D. Reijden, Z. Ye, P. Kolovos, R. W. W. Brouwerf, M. P. C. van de Corput, H. J. G. van de Werken, T. A. Knoch, W. F. J. van IJcken, F. G. Grosveld, B. Ren, and K. S. Wendt, “Cohesin and CTCF differentially affect chromatin architecture and gene expression in human cells,” *Proceedings of the National Academy of Sciences*, vol. 111, no. 3, pp. 996–1001, 2014.

[83] F. Jin, Y. Li, J. R. Dixon, S. Selvaraj, Z. Ye, A. Y. Lee, C.-a. Yen, A. D. Schmitt, C. A. Espinoza, and B. Ren, “A high-resolution map of the three-dimensional chromatin interactome in human cells,” *Nature*, vol. 503, pp. 290–294, 2013.

[84] F. Le Dily, F. Le Dily, D. Bau, A. Pohl, G. P. Vicent, F. Serra, D. Soronellas, G. Castellano, R. H. Wright, C. Ballare, G. Filion, M. A. Marti-Renom, Beato M., “Distinct structural transitions of chromatin topological domains correlate with coordinated hormone-induced gene regulation,” *Genes & development*, pp. 2151–2162, 2014.

[85] D. U. Gorkin, D. Leung, and B. Ren, “The 3D genome in transcriptional regulation and pluripotency,” *Cell Stem Cell*, vol. 14, no. 6, pp. 771–775, 2014.

- [86] K. Ahmed, H. Dehghani, P. Rugg-gunn, E. Fussner, J. Rossant, and P. David, "Global Chromatin Architecture Reflects Pluripotency and Lineage Commitment in the Early Mouse Embryo," *Plos one*, vol. 5, no. 5, p. e10531, 2010.
- [87] E. Fussner, U. Djuric, M. Strauss, A. Hotta, C. Perez-iratzeta, F. Lanner, F. J. Dilworth, J. Ellis, and D. P. Bazett-jones, "Constitutive heterochromatin reorganization during somatic cell reprogramming," *The EMBO Journal*, vol. 30, no. 9, pp. 1778–1789, 2011.
- [88] R. R. E. Williams, V. Azuara, P. Perry, S. Sauer, M. Dvorkina, H. Jør-gensen, J. Roix, P. Mcqueen, T. Misteli, M. Merckenschlager, and A. G. Fisher, "Neural induction promotes large-scale chromatin reorganisation of the *Mash1* locus," *Journal of Cell Science*, vol. 119, pp. 132–140, 2006.
- [89] S. T. Kosak, D. Scalzo, S. V. Alworth, F. Li, S. Palmer, T. Enver, J. S. J. Lee, and M. Groudine, "Coordinate Gene Regulation during Hematopoiesis Is Related to Genomic Organization," *PLoS Biology*, vol. 5, no. 11, p. e309, 2007.
- [90] T. Takizawa, K. J. Meaburn, and T. Misteli, "Essay The Meaning of Gene Positioning," *Cell*, vol. 135, pp. 9–13, 2008.
- [91] P. Meister, B. D. Towbin, B. L. Pike, A. Ponti, and S. M. Gasser, "The spatial dynamics of tissue-specific promoters during *C. elegans* development," *Genes & development*, vol. 24, pp. 766–782, 2010.
- [92] E. V. Volpi, E. Chevret, T. Jones, R. Vatcheva, J. Williamson, S. Beck, R. D. Campbell, M. Goldsworthy, S. H. Powis, J. Ragoussis, and J. Trowsdale, "Large-scale chromatin organization of the major histo-compatibility complex and other regions of human chromosome 6 and its response to interferon in interphase nuclei," *J Cell Sci*, vol. 1576, pp. 1565–1576, 2000.
- [93] R. R. E. Williams, S. Broad, D. Sheer, and J. Ragoussis, "Subchromosomal Positioning of the Epidermal Differentiation Complex (EDC) in Keratinocyte and Lymphoblast Interphase Nuclei," *Exp Cell Res*, vol. 175, pp. 163–175, 2002.
- [94] S. Chambeyron, N. R. D. Silva, K. A. Lawson, and W. A. Bickmore, "Nuclear re-organisation of the *Hoxb* complex during mouse embryonic development," *Development*, pp. 2215–2223, 2005.
- [95] K. Küpper, A. Kölbl, D. Biener, S. Dittrich, J. von Hase, T. Thormeyer, H. Fiegler, N. P. Carter, M. R. Speicher, T. Cremer, and

- M. Cremer, "Radial chromatin positioning is shaped by local gene density, not by gene expression," *Chromosoma*, pp. 285–306, 2007.
- [96] T. Tumber, G. Sudlow, and A. S. Belmont, "Large-Scale Chromatin Unfolding and Remodeling Induced by VP16 Acidic Activation Domain," *Journal of Cell Biology*, vol. 145, no. 7, pp. 1341–1354, 1999.
- [97] T. Tumber and A. S. Belmont, "Interphase movements of a DNA chromosome region modulated by VP16 transcriptional activator," *Nature cell biology*, vol. 3, pp. 134–139, 2001.
- [98] P. Therizols, R. S. Illingworth, C. Courilleau, S. Boyle, A. J. Wood, and W. A. Bickmore, "Chromatin decondensation is sufficient to alter nuclear organization in embryonic stem cells," *Science*, vol. 346, no. 6214, pp. 1238–1242, 2014.
- [99] J. C. Harr, T. R. Luperchio, X. Wong, E. Cohen, S. J. Wheelan, and K. L. Reddy, "Directed targeting of chromatin to the nuclear lamina is mediated by chromatin state and A-type lamins," *vol. 208*, no. 1, pp. 33–52, 2015.
- [100] J. M. Zullo, I. A. Demarco, R. Pique, D. J. Gaffney, C. B. Epstein, C. J. Spooner, T. R. Luperchio, B. E. Bernstein, J. K. Pritchard, K. L. Reddy, and H. Singh, "DNA Sequence-Dependent Compartmentalization and Silencing of Chromatin at the Nuclear Lamina," *Cell*, vol. 149, pp. 1474–1487, 2012.
- [101] B. D. Towbin, C. Gonzalez-Aguilera, R. Sack, D. Gaidatzis, V. Kalck, P. Meister, P. Askjaer, and S. M. Gasser, "Step-Wise Methylation of Histone H3K9 Positions Heterochromatin at the Nuclear Periphery," *vol. 150*, pp. 934–947, 2012.
- [102] A. Gonzalez-sandoval, B. D. Towbin, V. Kalck, D. S. Cabianca, D. Gaidatzis, M. H. Hauer, L. Geng, L. Wang, T. Yang, X. Wang, K. Zhao, and S. M. Gasser, "Perinuclear Anchoring of H3K9-Methylated Article Perinuclear Anchoring of H3K9-Methylated Chromatin Stabilizes Induced Cell Fate in *C. elegans* Embryos," *Cell*, vol. 163, pp. 1–15, 2015.
- [103] Y. Ghavi-helm, F. A. Klein, T. Pakozdi, L. Ciglar, D. Noordermeer, W. Huber, and E. E. M. Furlong, "Enhancer loops appear stable during development and are associated with paused polymerase," *Nature*, vol. 512, pp. 96–100, 2014.
- [104] S. S. P. Rao, M. H. Huntley, N. C. Durand, E. K. Stamenova, I. D. Bochkov, J. T. Robinson, A. L. Sanborn, I. Machol, A. D. Omer,

- E. S. Lander, and E. Lieberman Aiden, “Article A 3D Map of the Human Genome at Kilobase Resolution Reveals Principles of Chromatin Looping,” *Cell*, vol. 159, no. 7, pp. 1665–1680, 2014.
- [105] J. R. Dixon, I. Jung, S. Selvaraj, Y. Shen, J. E. Antosiewicz-bourget, A. Y. Lee, Z. Ye, A. Kim, N. Rajagopal, W. Xie, Y. Diao, J. Liang, H. Zhao, V. V. Lobanenko, and J. R. Ecker, “Chromatin architecture reorganization during stem cell differentiation,” *Nature*, vol. 518, no. 7539, pp. 331–336, 2015.
- [106] A. Berr, A. Pecinka, A. Meister, G. Kreth, F. R. Blattner, and M. A. Lysak, “Chromosome arrangement and nuclear architecture but not centromeric sequences are conserved between *Arabidopsis thaliana* and *Arabidopsis lyrata*,” *The plant Journal*, vol. 48, pp. 771–783, 2006.
- [107] K. Bystricky, T. Laroche, G. V. Houwe, M. Blaszczyk, and S. M. Gasser, “Chromosome looping in yeast: telomere pairing and coordinated movement reflect anchoring efficiency and territorial organization,” *Journal of Cell Biology*, vol. 168, no. 3, pp. 375–387, 2005.
- [108] T. Cremer and C. Cremer, “chromosome territories, nuclear architecture and gene regulation in mammalian cells,” *Nature reviews. Genetics*, vol. 2, no. April, pp. 292–301, 2001.
- [109] C. Zimmer and E. Fabre, “Principles of chromosomal organization: Lessons from yeast,” *Journal of Cell Biology*, vol. 192, no. 5, pp. 723–733, 2011.
- [110] H. A. Foster and J. M. Bridger, “The genome and the nucleus: A marriage made by evolution. Genome organisation and nuclear architecture,” *Chromosoma*, vol. 114, no. 4, pp. 212–229, 2005.
- [111] C. Gómez-Marín, J. J. Tena, R. D. Acemel, M. López-Mayorga, S. Naranjo, E. de la Calle-Mustienes, I. Maeso, L. Beccari, I. Aneas, E. Vielmas, P. Bovolenta, M. a. Nobrega, J. Carvajal, and J. L. Gómez-Skarmeta, “Evolutionary comparison reveals that diverging CTCF sites are signatures of ancestral topological associating domains borders,” *Proc Natl Acad Sci U S A*, vol. 112, no. 24, p. 201505463, 2015.
- [112] O. Alexandrova, I. Solovei, T. Cremer, and C. N. David, “Replication labeling patterns and chromosome territories typical of mammalian nuclei are conserved in the early metazoan *Hydra*,” pp. 190–200, 2003.

- [113] N. Sadoni, S. Langer, C. Fauth, G. Bernardi, T. Cremer, B. M. Turner, D. Zink, L. M. U. München, S. Zoologica, and A. Dohrn, “Nuclear Organization of Mammalian Genomes : Polar Chromosome Territories Build Up Functionally Distinct Higher Order Compartments,” vol. 146, no. 6, pp. 1211–1226, 1999.
- [114] W. Rens, P. C. M. O’Brien, J. A. M. Graves, and M. A. Ferguson-Smith, “Localization of chromosome regions in potoroo nuclei (*Potorous tridactylus* Marsupialia: Potoroinae),” vol. 112, pp. 66–76, 2003.
- [115] A. Bolzer, G. Kreth, I. Solovei, D. Koehler, K. Saracoglu, C. Fauth, S. Mu, R. Eils, C. Cremer, M. R. Speicher, and T. Cremer, “Three-Dimensional Maps of All Chromosomes in Human Male Fibroblast Nuclei and Prometaphase Rosettes,” vol. 3, no. 5, 2005.
- [116] J. M. Engreitz, V. Agarwala, and L. A. Mirny, “Three-Dimensional Genome Architecture Influences Partner Selection for Chromosomal Translocations in Human Disease,” *Plos one*, vol. 7, no. 9, pp. 1–9, 2012.
- [117] E. Lukášová, S. Kozubek, M. Kozubek, J. Kjeronská, L. Rýznar, J. Horáková, E. Krahulcová, and G. Horneck, “Localisation and distance between ABL and BCR genes in interphase nuclei of bone marrow cells of control donors and patients with chronic myeloid leukaemia,” pp. 525–535, 1997.
- [118] H. Neves, C. Ramos, M. Gomes da Silva, A. Parreira, and L. Parreira, “The Nuclear Topography of ABL, BCR, PML, and RAR ã Genes: Evidence for Gene Proximity in Specific Phases of the Cell Cycle and Stages of Hematopoietic Differentiation,” pp. 1197–1208, 1999.
- [119] E. Bartova, K. Stanislav, M. Kozubek, P. Jirsova, E. Lukasova, and M. Skalnikova, “The influence of the cell cycle, differentiation and irradiation on the nuclear location of the abl, bcr and c-myc genes in human leukemic cells,” vol. 24, pp. 233–241, 2000.
- [120] H. Lans and J. H. J. Hoeijmakers, “Ageing nucleus gets out of shape Hannes,” *Nature*, vol. 440, no. March, pp. 1–3, 2006.
- [121] C. L. Ramírez, J. Cadiñanos, I. Varela, and J. M. P. Freije, “Human progeroid syndromes , aging and cancer: new genetic and epigenetic insights into old questions,” *Cellular and molecular life science*, vol. 64, pp. 155–170, 2007.
- [122] M. S. Lawrence, P. Stojanov, C. H. Mermel, J. T. Robinson, L.

A. Garraway, T. R. Golub, M. Meyerson, S. B. Gabriel, E. S. Lander, and G. Getz, "Discovery and saturation analysis of cancer genes across 21 tumour types," *Nature*, vol. 505, no. 7484, pp. 495–501, 2014.

[123] M. D'Angelo and M. W. Hetzer, "Structure, dynamics and function of nuclear pore complexes," *Trends in Cell Biology* Vol.18, vol. 18, pp. 456–466, 2008.

[124] S. L. Jaspersen, T. H. Giddings, and M. Winey, "Mps3p is a novel component of the yeast spindle pole body that interacts with the yeast centrin homologue Cdc31p," vol. 159, no. 6, pp. 945–956, 2002.

[125] M. C. King, C. P. Lusk, and G. Blobel, "Karyopherin-mediated import of integral inner nuclear membrane proteins," vol. 442, no. August, pp. 1003–1007, 2006.

[126] A. Taddei and S. M. Gasser, "Multiple pathways for telomere tethering: Functional implications of subnuclear position for heterochromatin formation," *Biochimica et Biophysica Acta*, vol. 1677, no. 1-3, pp. 120–128, 2004.

[127] A. Taddei, H. Schober, and S. M. Gasser, "The budding yeast nucleus," *Mechanisms Of Ageing And Development*, vol. 120, pp. 1– 22, 2011.

[128] K. L. Mckinley and I. M. Cheeseman, "The molecular basis for cen- tromere identity and function," *Nature Reviews. Molecular Cell Biology*, vol. 17, pp. 16–29, 2015.

[129] J. Shampay, J. W. Szostak, and E. H. Blackburn, "DNA sequences of telomeres maintained in yeast," *Nature*, vol. 310, pp. 154–157, 1984.

[130] M. Larrivee, C. Lebel, and R. J. Wellinger, "The generation of proper constitutive G-tails on yeast telomeres is dependent on the MRX complex," *Genes & development*, vol. 18, pp. 1391–1396, 2004.

[131] Q-W. Jin, J. Fuchs, and J. Loidl, "Centromere clustering is a major determinant of yeast interphase nuclear organization," *Journal of Cell Science*, vol. 1912, pp. 1903–1912, 2000.

[132] H. Schober, V. Kalck, M. A. Vega-Palas, G. Van Houwe, D. Sage, M. Unser, M. R. Gartenberg, and S. M. Gasser, "Controlled exchange of chromosomal arms reveals principles driving telomere

interactions in yeast,” *Genome Research*, vol. 18, no. 2, pp. 261–271, 2008.

[133] C. H. Yang, E. J. Lambie, J. Hardin, J. Craft, and M. Snyder, “Higher order structure is present in the yeast nucleus: autoantibody probes demonstrate that the nucleolus lies opposite the spindle pole body,” *Chromosoma*, vol. 98, pp. 123–128, 1989.

[134] F. Hediger, F. R. Neumann, G. V. Houwe, K. Dubrana, and S. M. Gasser, “Live Imaging of Telomeres : yKu and Sir Proteins Define Redundant Telomere-Anchoring Pathways in Yeast,” *Current Biology*, vol. 12, pp. 2076–2089, 2002.

[135] A. Taddei, F. Hediger, F. R. Neumann, C. Bauer, and S. M. Gasser, “Separation of silencing from perinuclear anchoring functions in yeast Ku80, Sir4 and Esc1 proteins,” *The EMBO journal*, vol. 23, no. 6, pp. 1301–12, 2004.

[136] D. Shore and K. Nasmyth, “Purification and Cloning of a DNA Binding Protein from Yeast That Binds to Both Silencer and Activator Elements,” *Cell*, vol. 51, pp. 721–732, 1987.

[137] P. Moretti, K. Freeman, L. Coodly, and D. Shore, “Evidence that a complex of SIR proteins interacts with the silencer and telomere-binding protein RAP1,” *Genes & development*, vol. 8, pp. 2257–2269, 1994.

[138] S. Marcand, E. Gilson, and D. Shore, “A Protein-Counting Mechanism for Telomere Length Regulation in Yeast,” *Science*, vol. 275, pp. 986–990, 1997.

[139] D. Wotton and D. Shore, “A novel Raplp-interacting factor, Rif2p, cooperates with Rif1p to regulate telomere length in *Saccharomyces cerevisiae*,” *Genes & development*, vol. 11, pp. 748–760, 1997.

[140] O. M. Aparicio, B. L. Billington, and D. E. Gottschling, “Modifiers of Position Effect Are Shared between Telomeric and Silent Mating-Type Loci in *S. cerevisiae*,” *Cell*, vol. 66, pp. 1279–1287, 1991.

[141] F. Martino, S. Kueng, P. Robinson, M. Tsai-pflugfelder, F. V. Leeuwen, M. Ziegler, F. Cubizolles, M. M. Cockell, D. Rhodes, and S. M. Gasser, “Article Reconstitution of Yeast Silent Chromatin : Multiple Contact Sites and O-AADPR Binding Load SIR Complexes onto Nucleosomes In Vitro,” *Molecular Cell*, vol. 33, no. 3, pp. 323–334, 2009.

- [142] E. D. Andrulis, D. C. Zappulla, A. Ansari, S. Perrod, C. V. Laiosa, M. R. Gartenberg, and R. Sternglanz, "Esc1, a Nuclear Periphery Protein Required for Sir4-Based Plasmid Anchoring and Partitioning," *molecular and cellular biology*, vol. 22, no. 23, pp. 8292–8301, 2002.
- [143] M. R. Gartenberg, F. R. Neumann, T. Laroche, M. Blaszczyk, and S. M. Gasser, "Sir-Mediated Repression Can Occur Independently of Chromosomal and Subnuclear Contexts," *Cell*, vol. 119, pp. 955–967, 2004.
- [144] R. Roy, B. Meier, A. D. Mcainsh, H. M. Feldmann, and S. P. Jackson, "Separation-of-function Mutants of Yeast Ku80 Reveal a Yku80p-Sir4p Interaction Involved in Telomeric Silencing *," *The Journal of Biological Chemistry*, vol. 279, no. 1, pp. 86–94, 2004.
- [145] H. Schober, H. Ferreira, L. R. Gehlen, and S. M. Gasser, "Yeast telomerase and the SUN domain protein Mps3 anchor telomeres and repress subtelomeric recombination," *Genes & development*, vol. 23, pp. 928–938, 2009.
- [146] L. M. Antoniaci, M. Kenna, R. V. Skibbens, L. M. Antoniaci, M. Kenna, R. V. S. The, M. A. Kenna, and R. V. Skibbens, "The Nuclear Envelope and Spindle Pole Body-Associated Mps3 Protein Bind Telomere Regulators and Function in Telomere Clustering," *Cell Cycle*, vol. 6, no. 1, pp. 75–79, 2007.
- [147] J. M. Bupp, A. E. Martin, E. S. Stensrud, and S. L. Jaspersen, "Telomere anchoring at the nuclear periphery requires the budding yeast Sad1-UNC-84 domain protein Mps3," *Journal of Cell Biology*, vol. 179, no. 5, pp. 845–854, 2007.
- [148] J. Torres-rosell, I. Sunjevaric, G. D. Piccoli, M. Sacher, N. Eckert-boulet, R. Reid, S. Jentsch, R. Rothstein, L. Aragón, and M. Lisby, "The Smc5 & Smc6 complex and SUMO modification of Rad52 regulates recombinational repair at the ribosomal gene locus," *Nature cell biology*, vol. 9, no. 8, pp. 923–931, 2007.
- [149] D. E. Gottschling, O. M. Aparicio, B. L. Billington, and V. A. Zakiant, "Position Effect at *S. cerevisiae* Telomeres Reversible Repression of Pol II Transcription," *Cell*, vol. 63, pp. 751–762, 1990.
- [150] A. Hecht, T. Laroche, S. Strahl-bolsinger, S. M. Gasser, and M. Grunstein, "Histone H3 and H4 N-Termini Interact with SIR3 and SIR4 Proteins: A Molecular Model for the Formation of Heterochromatin in Yeast," *Cell*, vol. 80, pp. 583–592, 1995.
- [151] S. Strahl-bolsinger, A. Hecht, K. Luo, and M. Grunstein, "SIR2

and SIR4 interactions differ in core and extended telomeric heterochromatin in yeast,” *Genes & development*, vol. 11, pp. 83–93, 1997.

[152] R. K. Mann and M. Grunstein, “Histone H3 N-terminal mutations allow hyperactivation of the yeast GAL1 gene in vivo,” *The EMBO Journal*, vol. 11, no. 9, pp. 3297–3306, 1992.

[153] J. S. Thompson, X. Ling, and M. Grunstein, “Histone H3 amino terminus is required for telomeric and silent mating locus repression in yeast,” *Nature*, vol. 369, pp. 245–247, 1994.

[154] G. J. Hoppe, J. C. Tanny, A. D. Rudner, S. A. Gerber, S. Danaie, S. P. Gygi, and D. Moazed, “Steps in Assembly of Silent Chromatin in Yeast: Sir3-Independent Binding of a Sir2/Sir4 Complex to Silencers and Role for Sir2-Dependent Deacetylation,” *molecular and cellular biology*, pp. 4167–4180, 2002.

[155] L. Maillet, F. Gaden, V. Brevet, G. Fourel, S. G. Martin, K. Dubrana, S. M. Gasser, and E. Gilson, “Ku-deficient yeast strains exhibit alternative states of silencing competence,” *EMBO Rep*, vol. 2, no. 3, pp. 203–210, 2001.

[156] A. Taddei, G. V. Houwe, S. Nagai, I. Erb, E. V. Nimwegen, and S. M. Gasser, “The functional importance of telomere clustering: Global changes in gene expression result from SIR factor dispersion The functional importance of telomere clustering: Global changes in gene expression result from SIR factor dispersion,” *Genome Research*, pp. 611–625, 2009.

[157] M. A. Mondoux, J. G. Scaife, and V. A. Zakian, “Differential nuclear localization does not determine the silencing status of *Saccharomyces cerevisiae* telomeres,” *Genetics*, vol. 177, no. 4, pp. 2019–2029, 2007.

[158] J. B. Stavenhagen and V. A. Zakian, “Internal tracts of telomeric DNA act as silencers in *Saccharomyces cerevisiae*,” *Genes & development*, vol. 8, pp. 1411–1422, 1994.

[159] J. J. Wyrick, F. C. P. Holstege, E. G. Jennings, H. C. Causton, D. Shore, M. Grunstein, E. S. Lander, and R. A. Young, “Chromosomal landscape of nucleosome-dependent gene expression and silencing in yeast,” *Nature*, vol. 402, no. November, pp. 25–28, 1999.

[160] D. Robyr, Y. Suka, I. Xenarios, S. K. Kurdistani, A. Wang, N. Suka, and M. Grunstein, “Determine Genome-Wide Functions for Yeast Histone Deacetylases,” *Cell*, vol. 109, pp. 437–446, 2002.

- [161] W. Ai, P. G. Bertram, C. K. Tsang, T.-f. Chan, X. F. S. Zheng, et al., "Regulation of Subtelomeric Silencing during Stress Response," *Molecular Cell*, vol. 10, pp. 1295–1305, 2002.
- [162] K. Ishii, G. Arib, C. Lin, G. V. Houwe, and U. K. Laemmli, "Chromatin Boundaries in Budding Yeast: The Nuclear Pore Connection," *Cell*, vol. 109, pp. 551–562, 2002.
- [163] A. Taddei, "Active genes at the nuclear pore complex," *Current Opinion in Cell Biology*, vol. 19, pp. 305–310, 2007.
- [164] J. M. Casolari, C. R. Brown, S. Komili, J. West, H. Hieronymus, and P. A. Silver, "Genome-Wide Localization of the Nuclear Transport Machinery Couples Transcriptional Status and Nuclear Organization," *Cell*, vol. 117, pp. 427–439, 2004.
- [165] R. Luthra, S. C. Kerr, M. T. Harreman, L. H. Apponi, M. B. Fasken, S. Ramineni, S. Chaurasia, S. R. Valentini, and A. H. Corbett, "Actively Transcribed GAL Genes Can Be Physically Linked to the Nuclear Pore by the SAGA Chromatin Modifying Complex," *Journal of biological chemistry*, vol. 282, no. 5, pp. 3042–3049, 2007.
- [166] G. G. Cabal, A. Genovesio, S. Rodriguez-navarro, C. Zimmer, O. Gadgil, A. Lesne, H. Buc, F. Feuerbach-fournier, E. C. Hurt, and U. Nehrbass, "SAGA interacting factors confine sub-diffusion of transcribed genes to the nuclear envelope," *Nature*, vol. 441, pp. 770–773, 2006.
- [167] M. Schmid, G. Arib, C. Laemmli, J. Nishikawa, T. Durussel, and U. K. Laemmli, "Nup-PI: The Nucleopore-Promoter Interaction of Genes in Yeast," *Molecular Cell*, vol. 21, pp. 379–391, 2006.
- [168] D. G. Brickner, I. Cajigas, Y. Fondufe-mittendorf, S. Ahmed, P.-c. Lee, J. Widom, and J. H. Brickner, "H2A.Z-Mediated Localization of Genes at the Nuclear Periphery Confers Epigenetic Memory of Previous Transcriptional State," *PLoS Biology*, vol. 5, no. 4, pp. 704–716, 2007.
- [169] G. Diepkins, N. Iglesias, and F. Stutz, "Cotranscriptional Recruitment to the mRNA Export Receptor Mex67p Contributes to Nuclear Pore Anchoring of Activated Genes," *Molecular and Cellular Biology*, vol. 26, no. 21, pp. 7858–7870, 2006.
- [170] B. B. Menon, N. J. Sarma, S. Pasula, S. J. Deminoff, K. A. Willis, K. E. Barbara, B. Andrews, and G. M. Santangelo, "Reverse recruitment: The Nup84 nuclear pore subcomplex mediates

Rap1/Gcr1/Gcr2 transcriptional activation,” *Proceedings of the National Academy of Sciences*, vol. 102, no. 16, pp. 5749–5754, 2005.

[171] E. Fabre, H. Muller, P. Therizols, I. Lafontaine, B. Dujon, and C. Fairhead, “Comparative Genomics in Hemiascomycete Yeasts: Evolution of Sex, Silencing, and Subtelomeres,” *Molecular Biology and Evolution*, vol. 22, no. 4, pp. 856–873, 2005.

[172] A. Taddei, G. Van Houwe, F. Hediger, V. Kalck, F. Cubizolles, H. Schober, and S. M. Gasser, “Nuclear pore association confers optimal expression levels for an inducible yeast gene,” *Nature*, vol. 441, no. 7094, pp. 774–778, 2006.

[173] C. S. Newlon, I. Collins, A. Dershowitz, A. M. Deshpande, S. A. Greenfeder, L. Y. Ong, and J. F. Theis, “Analysis of Replication Origin Function on Chromosome III of *Saccharomyces cerevisiae*,” *Cold Spring Harb Symp Quant Biol*, vol. 58, pp. 415–423, 1993.

[174] K. Yoshida, A. Poveda, and P. Pasero, “Time to be versatile: Regulation of the replication timing program in budding yeast,” *Journal of Molecular Biology*, vol. 425, no. 23, pp. 4696–4705, 2013.

[175] D. M. Witten and W. S. Noble, “On the assessment of statistical significance of three-dimensional colocalization of sets of genomic elements,” *Nucleic Acids Research*, vol. 40, no. 9, pp. 3849–3855, 2012.

[176] H. Tjong, K. Gong, L. Chen, and F. Alber, “Physical tethering and volume exclusion determine higher-order genome organization in budding yeast,” *Genome Research*, vol. 22, pp. 1295–1305, 2012.

[177] S. R. V. Knott, J. M. Peace, A. Z. Ostrow, Y. Gan, A. E. Rex, C. J. Viggiani, and S. Tavare, “Forkhead Transcription Factors Establish Origin Timing and Long-Range Clustering in *S. cerevisiae*,” *Cell*, no. 148, pp. 99–111, 2012.

[178] M. Looke and K. Kristjuhan, “Chromatin-dependent and -independent regulation of DNA replication origin activation in budding yeast,” *EMBO Rep*, vol. 14, no. 2, pp. 1–8, 2013.

[179] T. J. Pohl, B. J. Brewer, and M. K. Raghuraman, “Functional Centromeres Determine the Activation Time of Pericentric Origins of DNA Replication in *Saccharomyces cerevisiae*,” *plos genetics*, vol. 8, no. 5, 2012.

- [180] O. M. Aparicio, "Location, location, location: it's all in the timing for replication origins," *Genes & development*, vol. 27, pp. 117–128, 2013.
- [181] A. J. Cosgrove, C. A. Nieduszynski, and A. D. Donaldson, "Ku complex controls the replication time of DNA in telomere regions," *Genes & development*, pp. 2485–2490, 2002.
- [182] J. B. Stevenson and D. E. Gottschling, "Telomeric chromatin modulates replication timing near chromosome ends," *Genes & development*, no. 206, pp. 146–151, 1999.
- [183] S. R. V. Knott, C. J. Viggiani, and S. Tavaré, "Genome-wide replication profiles indicate an expansive role for Rpd3L in regulating replication initiation timing or efficiency , and reveal genomic loci of Rpd3 function in *Saccharomyces cerevisiae*," *Genes & development*, pp. 1077–1090, 2009.
- [184] J. G. Aparicio, C. J. Viggiani, D. G. Gibson, and O. M. Aparicio, "The Rpd3-Sin3 Histone Deacetylase Regulates Replication Timing and Enables Intra-S Origin Control in *Saccharomyces cerevisiae*," *molecular and cellular biology*, vol. 24, no. 11, pp. 4769–4780, 2004.
- [185] H. Wong, H. Marie-Nelly, S. Herbert, P. Carrivain, H. Blanc, R. Koszul, E. Fabre, and C. Zimmer, "A predictive computational model of the dynamic 3D interphase yeast nucleus," *Current Biology*, vol. 22, no. 20, pp. 1881–1890, 2012.
- [186] K. Bystricky, P. Heun, L. Gehlen, J. Langowski, and S. M. Gasser, "Long-range compaction and flexibility of interphase chromatin in bud- ding yeast analyzed by high-resolution imaging techniques.," *Proceedings of the National Academy of Sciences of the United States of America*, vol. 101, no. 47, pp. 16495–500, 2004.
- [187] M. Toussaint and A. Conconi, "High-throughput and sensitive assay to measure yeast cell growth: a bench protocol for testing genotoxic agents," *Nature protocols*, vol. 1, no. 4, pp. 1922–1928, 2006.
- [188] A. C. J. Vas, C. A. Andrews, K. K. Matesky, and D. J. Clarke, "In Vivo Analysis of Chromosome Condensation in *Saccharomyces cerevisiae*," *Molecular Biology of the Cell*, vol. 18, pp. 557–568, 2007.
- [189] S. I. Reed, J. A. Hadwiger, and A. T. Lorincz, "Protein kinase activity associated with the product of the yeast cell division cycle

- gene CDC28,” Proceedings of the National Academy of Sciences of the United States of America, vol. 82, pp. 4055–4059, 1985.
- [190] G. Neurohr, A. Naegeli, I. Titos, D. Theler, B. Greber, J. Díez, T. Gabaldón, M. Mendoza, and Y. Barral, “A Midzone-Based Ruler Adjusts Chromosome Compaction to Anaphase Spindle Length,” *Science*, vol. 332, pp. 465–468, 2011.
- [191] I. Titos, T. Ivanova, and M. Mendoza, “Chromosome length and perinuclear attachment constrain resolution of DNA intertwinings,” *Journal of Cell Biology*, vol. 206, no. 6, pp. 719–733, 2014.
- [192] C. J. Viggiani and O. M. Aparicio, “New vectors for simplified construction of BrdU-Incorporating strains of *Saccharomyces cerevisiae*,” *Yeast*, vol. 23, pp. 1045–1051, 2006.
- [193] C. Janke, M. M. Magiera, N. Rathfelder, C. Taxis, S. Reber, H. Maekawa, E. Schwob, E. Schiebel, M. Knop, A. Moreno-Borchart, and G. Doenges, “A versatile toolbox for PCR-based tagging of yeast genes: new fluorescent proteins, more markers and promoter substitution cassettes,” *Yeast*, vol. 21, pp. 947–962, 2004.
- [194] S. Harju, H. Fedosyuk, and K. R. Peterson, “Rapid isolation of yeast genomic DNA: Bust n’ Grab,” *BMC Biotechnology*, vol. 4, p. 8, 2004.
- [195] A. Dobin, C. A. Davis, F. Schlesinger, J. Drenkow, C. Zaleski, S. Jha, P. Batut, M. Chaisson, and T. R. Gingeras, “Sequence analysis,” *Bioinformatics*, vol. 29, no. 1, pp. 15–21, 2013.
- [196] A. R. Quinlan and I. M. Hall, “BEDTools: a flexible suite of utilities for comparing genomic features,” *Bioinformatics*, vol. 26, no. 6, pp. 841–842, 2010.
- [197] M. Hanna and W. Xiao, “Isolation of Nucleic Acids,” *Methods in Molecular Biology*, vol. 313, pp. 15–20, 2006.
- [198] M. Gotta, T. Laroche, and S. M. Gasser, “Analysis of Nuclear Organization in *Saccharomyces cerevisiae*,” *Methods in Enzymology*, vol. 304, no. 1993, 1999.
- [199] B. Langmead and S. L. Salzberg, “Fast gapped-read alignment with Bowtie 2,” *Nature Methods*, vol. 9, no. 4, pp. 357–360, 2012.
- [200] Y. Zhang, T. Liu, C. A. Meyer, J. Eeckhoute, D. S. Johnson, B. E. Bernstein, C. Nusbaum, R. M. Myers, M. Brown, W. Li, and X. S.

- Liu, “Open Access Model-based Analysis of ChIP-Seq (MACS),” *Genome Biology*, vol. 9, no. 9, p. R137, 2008.
- [201] A. Rosa, N. B. Becker, and R. Everaers, “Looping Probabilities in Model Interphase Chromosomes,” *Biophysical Journal*, vol. 98, no. 11, pp. 2410–2419, 2010.
- [202] Y. Cui and C. Bustamante, “Pulling a single chromatin fiber reveals the forces that maintain its higher-order structure,” *Proc Natl Acad Sci*, vol. 97, no. 1, pp. 127–132, 2000.
- [203] J. Langowski, “Polymer chain models of DNA and chromatin,” *The European Physical Journal*, vol. 19, pp. 241–249, 2006.
- [204] M. Di Stefano, A. Rosa, V. Belcastro, D. Bernardo, and C. Micheletti, “Colocalization of Coregulated Genes: A Steered Molecular Dynamics Study of Human Chromosome 19,” *PLoS Computational Biology*, vol. 9, no. 3, p. e1003019, 2013.
- [205] P. Meister, L. R. Gehlen, E. Varela, and S. M. Gasser, “Visualizing Yeast Chromosomes and Nuclear Architecture,” *Methods in Enzymology*, vol. 470, no. 10, pp. 535–567, 2010.
- [206] E. T. O. Toole, M. Winey, and J. R. McIntosh, “High-Voltage Electron Tomography of Spindle Pole Bodies and Early Mitotic Spindles in the Yeast,” *Molecular Biology and Evolution*, vol. 10, pp. 2017–2031, 1999.
- [207] M. Gotta, T. Laroche, A. Formenton, L. Maillet, H. Scherthan, and S. M. Gasser, “The Clustering of Telomeres and Colocalization with Rap1, Sir3, and Sir4 Proteins in Wild-Type *Saccharomyces cerevisiae*,” *Journal of Cell Biology*, vol. 134, no. 6, pp. 1349–1363, 1996.
- [208] K. Mekhail and D. Moazed, “The nuclear envelope in genome organization, expression and stability,” *Nature Reviews. Molecular Cell Biology*, vol. 11, no. 5, pp. 317–328, 2011.
- [209] C. Horigome, T. Okada, K. Shimazu, S. M. Gasser, and K. Mizuta, “Ribosome biogenesis factors bind a nuclear envelope SUN domain protein to cluster yeast telomeres,” *The EMBO Journal*, vol. 30, no. 18, pp. 3799–3811, 2011.
- [210] P. Langevin, “Sur la théorie du mouvement brownien,” *C. R. Acad. Sci. (Paris)*, vol. 146, pp. 530–533, 1908.
- [211] J. H. Brickner and P. Walter, “Gene recruitment of the activated

INO1 locus to the nuclear membrane,” *PLoS Biology*, vol. 2, no. 11, 2004.

[212] L. Crabbé, A. Thomas, V. Pantesco, J. D. Vos, P. Pasero, and A. Lengronne, “Analysis of replication profiles reveals key role of RFC- Ctf18 in yeast replication stress response,” *Nature Structural & Molecular Biology*, vol. 17, no. 11, pp. 1391–1397, 2010.

[213] S. V. Razin, A. A. Gavrillov, A. Pichugin, M. Lipinski, O. V. Iarovaia, and Y. S. Vassetzky, “Transcription factories in the context of the nuclear and genome organization,” *Nucleic Acids Research*, vol. 39, no. 21, pp. 9085–9092, 2011.

[214] S. Boyle, S. Gilchrist, J. M. Bridger, N. L. Mahy, J. A. Ellis, and W. A. Bickmore, “The spatial organization of human chromosomes within the nuclei of normal and emerin-mutant cells,” *Human Molecular Genetics*, vol. 10, no. 3, pp. 211–220, 2001.

[215] H. Renauld, O. M. Aparicio, P. D. Zierath, B. L. Billington, S. K. Chhablani, and D. E. Gottschling, “Silent domains are assembled continuously from the telomere and are defined by promoter distance and strength , and by SIR3 dosage,” *Genes & development*, 1993.

[216] L. Maillet, C. Boscheron, M. Gotta, S. Marcand, E. Gilson, and S. M. Gasser, “Evidence for silencing compartments within the yeast nucleus: A role for telomere proximity and Sir protein concentration in silencer-mediated repression,” *Genes and Development*, vol. 10, no. 14, pp. 1796–1811, 1996.

[217] G. Dialynas, S. Speese, V. Budnik, P. K. Geyer, and L. L. Wallrath, “The role of *Drosophila* Lamin C in muscle function and gene expression,” *Development*, vol. 137, pp. 3067–3077, 2010.

[218] L. E. Finlan, D. Sproul, I. Thomson, S. Boyle, E. Kerr, P. Perry, J. R. Chubb, B. Ylstra, and W. A. Bickmore, “Recruitment to the Nuclear Periphery Can Alter Expression of Genes in Human Cells,” *Plos genetics*, vol. 4, no. 3, p. e1000039, 2008.

[219] R. I. Kumaran and D. L. Spector, “A genetic locus targeted to the nuclear periphery in living cells maintains its transcriptional competence,” *Journal of Cell Biology*, vol. 180, no. 1, pp. 51–65, 2008.

[220] K. L. Reddy, J. M. Zullo, E. Bertolino, and H. Singh, “Transcriptional repression mediated by repositioning of genes to the nuclear lamina,” *Nature*, vol. 452, pp. 243–247, 2008.

- [221] I. Hiratani, T. Ryba, M. Itoh, T. Yokochi, M. Schwaiger, C.-w. Chang, Y. Lyou, T. M. Townes, D. Schu, and D. M. Gilbert, “Global Reorganization of Replication Domains During Embryonic Stem Cell Differentiation,” *PLoS Biology*, vol. 6, no. 10, p. e245, 2008.
- [222] I. Hiratani, D.M. Gilbert, “Autosomal lyonization of replication domains during early mammalian development,” *Adv Exp Med Biol*, vol. 695, pp. 41–58, 2010.
- [223] D.M. Gilbert, S.M. Gasser. “Nuclear structure and DNA replication”. In *DNA replication and human disease* (ed. DePamphilis ML), pp. 175–196 Cold Spring Harbor Laboratory Press, Cold Spring Harbor, NY, 2006
- [224] B. Steglich, G. J. Filion, B. V. Steensel, and K. Ekwall, “The inner nuclear membrane proteins Man1 and Imal link to two different types of chromatin at the nuclear periphery in *S. pombe*,” *Nucleus*, vol. 3, no. 1, pp. 77–87, 2012.
- [225] A. Nemeth and G. Langst, “Genome organization in and around the nucleolus,” *Trends in Genetics*, vol. 27, no. 4, pp. 149–156, 2011.
- [226] D. C. Zappulla, R. Sternglanz, and J. Leatherwood, “Control of Replication Timing by a Transcriptional Silencer,” *Current Biology*, vol. 12, pp. 869–875, 2002.
- [227] H. Ebrahimi, E. D. Robertson, A. Taddei, S. M. Gasser, A. D. Donaldson, and S.-I. Hiraga, “Early initiation of a replication origin tethered at the nuclear periphery,” *Journal of Cell Science*, vol. 123, no. 7, pp. 1015–1019, 2010.
- [228] S. Hiraga, E. D. Robertson, and A. D. Donaldson, “The Ctf18 RFC-like complex positions yeast telomeres but does not specify their replication time,” *The EMBO journal*, vol. 25, no. 7, pp. 1505–1514, 2006.